

# The LHC String Hunter’s Companion

Dieter Lüst<sup>a,b</sup>, Stephan Stieberger<sup>a</sup>, Tomasz R. Taylor<sup>a,c</sup>

<sup>a</sup> *Max-Planck-Institut für Physik, Werner-Heisenberg-Institut,  
80805 München, Germany*

<sup>b</sup> *Arnold-Sommerfeld-Center for Theoretical Physics,  
Ludwig-Maximilians-Universität München, 80333 München, Germany*

<sup>c</sup> *Department of Physics, Northeastern University, Boston, MA 02115, USA*

## Abstract

The mass scale of fundamental strings can be as low as few  $\text{TeV}/c^2$  provided that spacetime extends into large extra dimensions. We discuss the phenomenological aspects of weakly coupled low mass string theory related to experimental searches for physics beyond the Standard Model at the Large Hadron Collider (LHC). We consider the extensions of the Standard Model based on open strings ending on D-branes, with gauge bosons due to strings attached to stacks of D-branes and chiral matter due to strings stretching between intersecting D-branes. We focus on the model-independent, universal features of low mass string theory. We compute, collect and tabulate the full-fledged string amplitudes describing all  $2 \rightarrow 2$  parton scattering subprocesses at the leading order of string perturbation theory. We cast our results in a form suitable for the implementation of stringy partonic cross sections in the LHC data analysis. The amplitudes involving four gluons as well as those with two gluons plus two quarks do not depend on the compactification details and are completely model-independent. They exhibit resonant behavior at the parton center of mass energies equal to the masses of Regge resonances. The existence of these resonances is the primary signal of string physics and should be easy to detect. On the other hand, the four-fermion processes like quark-antiquark scattering include also the exchanges of heavy Kaluza-Klein and winding states, whose details depend on the form of internal geometry. They could be used as “precision tests” in order to distinguish between various compactification scenarios.

## Contents

1. <i>Introduction</i> . . . . .	2
2. <i>Physics of large extra dimensions and low string scale</i> . . . . .	5
2.1. Planck mass and gauge couplings in D-brane compactifications . . . . .	5
2.2. Large extra dimensions and low string scale . . . . .	7
2.3. Exchanges of string Regge excitations and string contact interactions . . . . .	9
3. <i>Standard Model from D-branes</i> . . . . .	10
3.1. Generalities . . . . .	10
3.2. Three stack D-brane models . . . . .	12
3.3. Four stack D-brane models . . . . .	13
4. <i>Embedding of SM D-branes into large volume Calabi–Yau spaces</i> . . . . .	14
4.1. Type IIB large volume compactifications with wrapped D7-branes . . . . .	16
4.2. Type IIA large volume compactifications with wrapped D6-branes . . . . .	19
5. <i>Four-point string amplitudes of gauge and matter Standard Model fields</i> . . . . .	20
5.1. Notation and Conventions . . . . .	21
5.2. Four-point string amplitudes and open string vertex operators . . . . .	23
5.3. Four gluon amplitudes . . . . .	27
5.4. Two gauge bosons and two fermions . . . . .	28
5.5. Four chiral fermions . . . . .	30
6. <i>From Amplitudes to Parton Cross Sections</i> . . . . .	46
6.1. $gg \rightarrow gg, gg \rightarrow gA, gg \rightarrow AA$ . . . . .	47
6.2. $gg \rightarrow q\bar{q}, gq \rightarrow gq, gq \rightarrow qA, gq \rightarrow qB, q\bar{q} \rightarrow gg, q\bar{q} \rightarrow gA, q\bar{q} \rightarrow gB$ . . . . .	49
6.3. $qq \rightarrow qq, q\bar{q} \rightarrow q\bar{q}$ . . . . .	50
6.4. $q\bar{q} \rightarrow l\bar{l}$ . . . . .	54
6.5. Tables . . . . .	55
7. <i>Summary</i> . . . . .	58

## 1. Introduction

The Standard Model (SM) of particle physics is a well established quantum field theory that describes the spectrum and the interactions of elementary particles to high accuracy and in excellent agreement with almost all experiments. Only astrophysical observations provide indirect experimental evidence for new physics beyond the SM in the form of not yet directly observed dark matter particles. However at the conceptual level, there exist several unsolved problems, which strongly hint at new physics beyond the SM. Probably the most mysterious puzzle is the hierarchy problem, namely the question why the Planck mass  $M_{\text{Planck}} \simeq 10^{19}$  GeV is huge compared to the electroweak scale  $M_{EW}$ :

$$M_{\text{Planck}} \gg M_{EW} ? \tag{1.1}$$

In fact, there are some good reasons to believe that the resolution of the hierarchy problem lies in new physics around the TeV mass scale. The LHC collider at CERN is designed to discover new physics precisely in this energy range, hopefully giving important clues about the nature of dark matter and perhaps at the same time about the solution of the hierarchy problem. In fact, there are at least three, not necessarily mutually exclusive scenarios, offered as solutions of the hierarchy problem:

- Low energy supersymmetry at around 1 TeV.
- New strong dynamics at around 1 TeV (technicolor, little Higgs models, etc).
- Low energy scale for (quantum) gravity and large extra dimensions at few TeVs.

In the latter scenario, the observed weakness of gravity at energies below few TeVs is due to the existence of large extra dimensions [1,2]. In string theory, extra dimensions appear naturally, therefore it is an obvious question to ask whether they can be large enough to accommodate such new physics at few TeVs. This is possible only if the intrinsic scale of string excitations, called the string mass  $M_{\text{string}}$  is also of order few TeVs. In this case a whole tower of infinite string excitations will open up at the string mass threshold, and new particles follow the well known Regge trajectories of vibrating strings,

$$j = j_0 + \alpha' M^2 , \tag{1.2}$$

with the spin  $j$  and  $\alpha'$  the Regge slope parameter that determines the fundamental string mass scale  $M_{\text{string}}^2 = \alpha'^{-1}$ . In this work, we discuss the phenomenological aspects of low mass string theory related to experimental searches for physics beyond the SM at the LHC. We focus on its model-independent, universal features that can be observed and tested at the LHC.

Let us list what kind of string signatures from a low string scale and from large extra dimensions can be possibly expected at the LHC:

- The discovery of new exotic particles around  $M_{\text{string}}$ . For example, many string models predict the existence of new, massive  $Z'$  gauge bosons from additional  $U(1)$  gauge symmetries (see e.g. [3]). They can also have an interesting effect, since they mix with the standard photon by their kinetic energies (see e.g. [4]).
- The discovery of quantum gravity effects in the form of mini black holes (see e.g. [5,6]).
- The discovery of string Regge excitations with masses of order  $M_{\text{string}}$ . These stringy states will lead to new contributions to SM scattering processes, which can be measurable at LHC in case of low string scale. Furthermore, there are the Kaluza–Klein (KK) and winding excitations along the small internal dimensions, i.e. KK and winding excitations of the SM fields. Their masses depend on the internal volumes<sup>1</sup>, and they should be also near the string scale  $M_{\text{string}}$ .

It is precisely this last item, which we want to discuss in this work. So let us be more specific with what we mean by new contributions to SM processes from a low string scale  $M_{\text{string}}$ . Namely these are the  $\alpha'$ -contributions to ordinary SM processes like the scattering of quarks and gluons into SM fields. As already mentioned, at tree-level the  $\alpha'$ -corrections to SM processes are due to the exchanges of massive string excitations encompassing all Regge recurrences. In addition, there are contributions of KK states and winding modes with their spectrum depending on the form of extra-dimensional geometry. However a class of amplitudes, e.g. the N-gluon amplitudes of QCD, receive universal  $\alpha'$ -corrections only, which are insensitive to the details of specific compactifications and to the extent of supersymmetry preserved in four dimensions [8–11]. Similarly, also other SM processes that involve quarks, leptons and other gauge bosons receive  $\alpha'$ -corrections, leading to characteristic deviations from the SM predictions and hence can be tested at the LHC. An important step in this direction has already been undertaken in [7], where the effects of string resonances have been pointed out as an important signal of string physics. Other string four-point amplitudes that involve four SM fermions, relevant to Yukawa couplings and possibly leading to proton decay and FCNC in specific models, have been computed and analyzed in [12–20]. More recently, in [21] and [22] the string effects in the process  $gg \rightarrow$

---

<sup>1</sup> In fact, there may be another kind of KK excitations, namely along the large extra dimensions, i.e. KK excitations in the gravitational (bulk) sector of the theory. Their masses can be as low as  $10^{-3}$  eV. However, KK modes from the bulk couple only at one-loop (annulus) to SM fields resulting in a suppression by a factor of  $g_{\text{string}}$  compared to tree-level processes on the brane. Hence contributions from KK modes of the bulk are less relevant than those from string Regge excitations, cf. also the discussion in [7].

$g\gamma$  have been considered. In the present work we systematically investigate all possible string tree-level  $\alpha'$ -corrections to SM processes that involve quarks, leptons and SM gauge bosons, as they arise in intersecting D-brane compactifications of orientifold models<sup>2</sup>. We work in a model-independent way and essentially only need the local information about how the SM is realized on type IIA/IIB intersecting D-branes. Some of the processes exist already at tree level in the SM, and hence the tree level SM background must be subtracted from the string corrections. Other processes like  $gg \rightarrow g\gamma$  or  $gg \rightarrow \gamma\gamma$  do not at all exist in the SM at tree-level and can be viewed as the “smoking guns” for D-brane string compactifications with a low string scale and large extra dimensions. However let us remind that it requires much fortune to see these string effects at the LHC along the lines discussed in this work. In particular we need a low string scale, large extra dimensions and also weak string coupling in order for our calculations to be reliable and testable at the LHC.

The present work is organized as follows. In the next Section we discuss some general aspects and the basic setting of string compactifications with a low string scale and large extra dimensions. Then, in Section three, we recall how the SM can be constructed from type IIA/IIB D-branes on orientifolds. We do not discuss fully consistent global orientifold models, which lead to the SM, but we rather focus on the local, intersecting D-brane configurations that realize the SM by open strings. Eventually the local D-brane systems have to be included into a compact manifold in order to obtain a fully consistent orientifold compactifications. However, as we shall argue, the local D-brane systems are sufficient to compute all relevant tree level scattering amplitudes among the SM open string excitations. In Section four we discuss how large extra dimensions can be realized in Calabi–Yau (CY) orientifolds and how the local, SM D-brane system has to be embedded into a large volume CY space. To some extent we follow the recent constructions for large volume compactifications by [23] using the “Swiss cheese” CY spaces, however with the difference that in [23] the string scale is around an intermediate scale of  $10^{11}$  GeV and supersymmetry is broken at the TeV scale, whereas in our case  $M_{\text{string}}$  is at few TeVs and low energy supersymmetry is not needed. In Section five we present a complete calculation of all possible four-point string scattering amplitudes of gauge and SM matter fields. We analyze string corrections to scattering processes that involve quarks and gluons, since they are the most relevant processes for the LHC. The computations of the scattering of four gauge bosons and of the scattering of two gauge bosons and two matter fermions is performed in a model independent and universal way. Our results hold for all compactifications, even for those that break supersymmetry. The poles of the respective amplitudes are due to

---

<sup>2</sup> In contrast to Ref. [7] we are describing the SM fermions, which are located at D-brane intersections, by boundary changing operators in the open string CFT. This leads to different  $\alpha'$  corrections in the fermion scattering amplitudes.

the exchanges of massless gauge bosons and universal string Regge excitations only. On the other hand, the amplitudes that involve four matter fields depend on the details of the D-brane geometry, and how the D-branes are embedded into the compact CY space. Here also modes of the internal geometry can be exchanged during the four fermion scattering processes. Finally, in Section six, we compute the squared moduli of all amplitudes, sum over polarizations and colors of final particles and average over polarization and colors of incident particles, as needed for the unpolarized parton cross sections. The results are presented in Tables.

In another publication [24] written in collaboration with Luis Anchordoqui, Haim Goldberg and Satoshi Nawata, we use our results to analyze the dijet signals for low mass strings at the LHC.

## 2. Physics of large extra dimensions and low string scale

Large extra dimensions are a very appealing solution to the hierarchy problem [2]. The gravitational and gauge interactions are unified at the electroweak scale and the observed weakness of gravity at lower energies is due to the existence of large extra dimensions. Gravitons may scatter into the extra space and by this the gravitational coupling constant is decreased to its observed value. Extra dimensions arise naturally in string theory. Hence, one obvious question is how to embed the above scenario into string theory and how to compute cross sections.

### *2.1. Planck mass and gauge couplings in D-brane compactifications*

Here we discuss the gravitational and gauge couplings in orientifold compactifications. In the following we consider the type II superstring compactified on a six-dimensional compactification manifold. In addition, we consider a  $Dp$ -brane wrapped on a  $p-3$ -cycle with the remaining four dimensions extended into the uncompactified space-time. We have  $d_{\parallel} = p-3$  internal directions parallel to the  $Dp$ -brane world volume and  $d_{\perp} = 9-p$  internal directions transverse to the  $Dp$ -brane world volume. Let us denote the radii (in the string frame) of the parallel directions by  $R_i^{\parallel}$ ,  $i = 1, \dots, d_{\parallel}$  and the radii of the transverse directions by  $R_j^{\perp}$ ,  $j = 1, \dots, d_{\perp}$ . The generic setup is displayed in Figure 1.

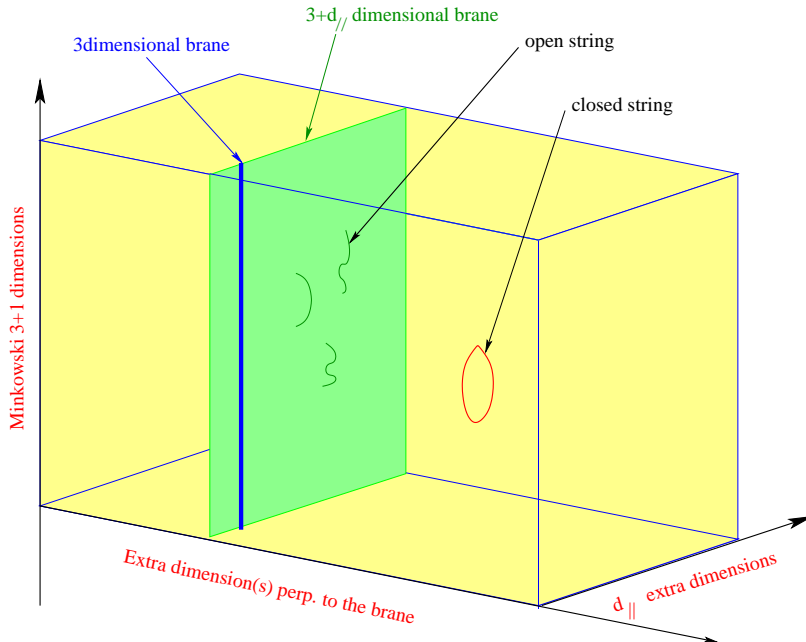


**Fig. 1** D-brane setup with  $d_{\parallel}$  parallel and  $d_{\perp}$  transverse internal directions (from Ref. [25]).

While the gauge interactions are localized on the D-brane world volume, the gravitational interactions are also spread into the transverse space. This gives qualitatively different quantities for their couplings. In  $D = 4$  we obtain for the Planck mass ( $\alpha' = M_{\text{string}}^{-2}$ ) [17]

$$M_{\text{Planck}}^2 = 8 e^{-2\phi_{10}} M_{\text{string}}^8 \frac{V_6}{(2\pi)^6}, \quad (2.1)$$

where the internal six-dimensional (string frame) volume  $V_6$  is expressed in terms of the parallel and transversal radii as

$$V_6 = (2\pi)^6 \prod_{i=1}^{d_{\parallel}} R_i^{\parallel} \prod_{j=1}^{d_{\perp}} R_j^{\perp}. \quad (2.2)$$

The dilaton field  $\phi_{10}$  is related to the  $D = 10$  type II string coupling constant through  $g_{\text{string}} = e^{\phi_{10}}$ . The gravitational coupling constant follows from (2.1) through the relation  $G_N = M_{\text{Planck}}^{-2}$ . On the other hand, in type II superstring theory the gauge theory on the D-brane world-volume has the gauge coupling:

$$g_{Dp}^{-2} = (2\pi)^{-1} \alpha'^{\frac{3-p}{2}} e^{-\phi_{10}} \prod_{i=1}^{d_{\parallel}} R_i^{\parallel}. \quad (2.3)$$

In (2.3) each factor  $i$  accounts for an 1-cycle wrapped along the  $i$ -th coordinate segment. While the size of the gauge couplings is determined by the size of the parallel dimensions, the strength of gravity is influenced by all directions.

## 2.2. Large extra dimensions and low string scale

From (2.1) and the gauge coupling (2.3) we may deduce a relation between the Planck mass  $M_{\text{Planck}}$ , the string mass  $M_{\text{string}}$  and the sizes  $R_j$  of the compactified internal directions. For type II we obtain<sup>3</sup>:

$$g_{Dp}^2 M_{\text{Planck}} = 2^{5/2} \pi M_{\text{string}}^{7-p} \left( \prod_{j=1}^{d_{\perp}} R_j^{\perp} \right)^{\frac{1}{2}} \left( \prod_{i=1}^{d_{\parallel}} R_i^{\parallel} \right)^{-1/2}. \quad (2.4)$$

Hence, by enlarging some of the transverse compactification radii  $R_j^{\perp}$  the string scale has to become lower in order to achieve the correct Planck mass ( $p < 7$ ). This is to be contrasted with a theory of closed (heterotic) strings only. In that case the relation between the Planck mass and the string scale does not depend on the volume. It is given by the relation  $M_{\text{string}} = g_{\text{string}} M_{\text{Planck}}$ , which requires a high string scale  $M_{\text{string}} \sim 10^{17} \text{GeV}$  for the correct Planck mass.

A priori, there are no compelling reasons why the string mass scale  $M_{\text{string}}$  should be much lower than the Planck mass. In the large volume compactifications of [23,27,28] it was shown that that one can indeed stabilize moduli in such a way that the string scale  $M_{\text{string}}$  is at intermediate energies of about  $10^{11-12} \text{GeV}$ . Then the internal CY volume  $V_6$  is of order  $V_6 M_{\text{string}}^6 = \mathcal{O}(10^{16})$ . The motivation for this scenario is to obtain a supersymmetry breaking scale around 1 TeV, since one derives the following relation for the gravitino mass:

$$m_{3/2} \sim \frac{M_{\text{string}}^2}{M_{\text{Planck}}}. \quad (2.5)$$

However, giving up the requirement of supersymmetry at the TeV scale, one is free to consider CY manifolds with much larger volume. In fact, if it happens for  $M_{\text{string}}$  to be within the range of LHC energies, not too far beyond 1 TeV, string theory can be tested. In this case the CY volume is as large as  $V_6 M_{\text{string}}^6 = \mathcal{O}(10^{32})$ . Of course one has to find scalar potentials with minima that lead to such big internal volumes.

Some spectacular signatures are expected near the string mass threshold. They are related to the production of virtual or real string Regge excitations of mass of order  $M_{\text{string}}$  and to the effects of strongly coupled gravity like the production and decays of microscopic

---

<sup>3</sup> The discussion takes over to type I superstring theory. The type I theory may be obtained from type IIB by an orientifold projection. The world-volume gauge theory on the D-brane sitting on the orientifold plane becomes then  $SO(2N)$  or  $USp(N)$ . In that case, all gauge couplings, derived in the following for  $U(N)$  gauge groups, have to be multiplied by a factor of 2, i.e.  $g_{Dp,SO(2N)}^2 = 2g_{Dp}^2$  [26].



black holes [29,30]. The reason why gravity is expected to become strong at energies comparable to the string mass is the inevitable presence of Kaluza Klein excitations of gravitons and other particles propagating in the bulk of large extra dimensions, with the (model-dependent) masses expected in the range from  $10^{-3}$  eV order to 1 MeV order. Although ordinary matter particles couple to these excitations very weakly, with the strength determined by the Newton's constant, the combined effect of a large number of virtual Kaluza Klein gravitons is to increase the strength of gravitational forces at high energies. In string theory, this effect may occur below or above the fundamental string mass scale, depending on the string coupling constant  $g_{\text{string}}$ . For example, black holes are expected to be produced at energies of order  $M_{\text{string}}/g_{\text{string}}^2$  [5], although some strong gravity effects may appear already at slightly lower energies [6]. Thus in weakly coupled string theory with  $g_{\text{string}} < 1$ , black hole production and in general, the onset of strong gravity effects occur above the string mass scale. In this case, the lowest energy signals of strings at the LHC would be due to virtual Regge excitations produced in parton collisions. The corresponding scattering amplitudes can be evaluated by using string perturbation theory, with the dominant contributions originating from disk diagrams. In this work, we discuss the disk amplitudes necessary for studying all  $2 \rightarrow 2$  scattering processes of gluons and quarks originating from D-brane intersections. Some results are new while other are known, nevertheless we believe that it is useful to collect all of them in one place as a resource for the LHC string hunters.

Let us now discuss the possible sizes of large extra dimensions subject to the experimental facts. Cavendish type experiments test Newton's law up to a scale of millimeters. This provides an upper bound on the large extra dimensions  $R_j^\perp$  to be in the millimeter range. On the other hand, QCD and electroweak scattering experiments give an upper bound on the small extra dimensions  $R_i^\parallel$  in the range of the electroweak scale  $M_{EW}^{-1}$ .

A first look at the relations (2.1) gives an estimate on the string scale  $M_{\text{string}}$  and the size of  $d_\perp$  extra dimensions  $R_j^\perp$ . For the  $d_\parallel$  small directions to be of the order of the string scale  $M_{\text{string}}$  and  $d_\perp$  extra dimensions of size  $R^\perp$  we obtain<sup>4</sup> the numbers listed in Table 1.

	$d_\perp = 1$	$d_\perp = 2$	$d_\perp = 3$	$d_\perp = 4$	$d_\perp = 5$	$d_\perp = 6$
$R^\perp$ [GeV <sup>-1</sup> ]	$1.6 \cdot 10^{26}$	$4 \cdot 10^{11}$	$5.4 \cdot 10^6$	$2 \cdot 10^4$	693	74
$R^\perp$ [m]	$1.6 \cdot 10^{11}$	$4 \cdot 10^{-4}$	$5.4 \cdot 10^{-9}$	$2 \cdot 10^{-11}$	$7 \cdot 10^{-13}$	$7 \cdot 10^{-14}$
$E_R$ [MeV]	$7.7 \cdot 10^{-24}$	$3 \cdot 10^{-9}$	$2 \cdot 10^{-4}$	0.06	1	16

**Table 1:** Size of  $d_\perp$  large extra dimensions for a string scale of  $M_{\text{string}} = 1$  TeV.

So, the case  $d_\perp = 1$  is ruled out experimentally.

---

<sup>4</sup> The above values are computed for  $g_{\text{string}} \simeq g^2 = \frac{1}{25}$ , i.e.  $\alpha = \frac{g^2}{4\pi} = 0.003$ . Furthermore,  $E_R = \frac{hc}{R^\perp}$  and  $1 \text{ GeV}^{-1} \sim 10^{-15} m$ .

### 2.3. Exchanges of string Regge excitations and string contact interactions

Due to the extended nature of strings, the world-sheet string amplitudes are generically non-trivial functions of  $\alpha'$  in addition to the usual dependence on the kinematic invariants and degrees of freedom of the external states. In the effective field theory description this  $\alpha'$ -dependence gives rise to a series of infinite many resonance channels<sup>5</sup> due to Regge excitations and/or new contact interactions.

Generically, as we shall see in Section 5, tree-level string amplitudes involving four gluons or amplitudes with two gluons and two fermions are described by the Euler Beta function depending on the kinematic invariants  $s = (k_1 + k_2)^2$ ,  $t = (k_1 - k_3)^2$ ,  $u = (k_1 - k_4)^2$ , with  $s + t + u = 0$  and  $k_i$  the four external momenta. The whole amplitudes  $A(k_1, k_2, k_3, k_4; \alpha')$  may be understood as an infinite sum over  $s$ -channel poles with intermediate string states  $|k; n\rangle$  exchanged, cf. Figure 2.

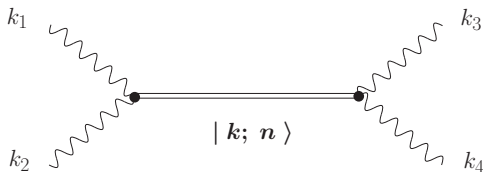


**Fig. 2** Exchange of string Regge excitations.

After neglecting kinematical factors the string amplitude  $A(k_1, k_2, k_3, k_4; \alpha')$  assumes the form

$$A(k_1, k_2, k_3, k_4; \alpha') \sim -\frac{\Gamma(-\alpha' s) \Gamma(1 - \alpha' u)}{\Gamma(-\alpha' s - \alpha' u)} = \sum_{n=0}^{\infty} \frac{\gamma(n)}{s - M_n^2} \quad (2.6)$$

as an infinite sum over  $s$ -channel poles at the masses

$$M_n^2 = M_{\text{string}}^2 n \quad (2.7)$$

of the string Regge excitations. In (2.6) the residues  $\gamma(n)$  are determined by the three-point coupling of the intermediate states  $|k; n\rangle$  to the external particles and given by

$$\gamma(n) = \frac{t}{n!} \frac{\Gamma(-u\alpha' + n)}{\Gamma(-u\alpha')} = \frac{t}{n!} \prod_{j=1}^n [-u\alpha' - 1 + j] \sim (-\alpha' u)^n \quad , \quad (2.8)$$

with  $n + 1$  being the highest possible spin of the state  $|k; n\rangle$ .

---

<sup>5</sup> In addition, there may be additional resonance channels due to the exchange of KK and winding states, as it is the case for four fermions amplitudes in four dimensions, cf. Section 5.

Another way of looking at the expression (2.6) appears when we express each term in the sum as a power series expansion in  $\alpha'$ :

$$A(k_1, k_2, k_3, k_4; \alpha') \sim \underbrace{\frac{t}{s}}_{n=0} - \underbrace{\frac{\pi^2}{6} tu \alpha'^2 + \dots}_{n \neq 0} . \quad (2.9)$$

In this form (2.9) the massless state  $n = 0$  gives rise to a field–theory contribution ( $\alpha' = 0$ ), while at the order  $\alpha'^2$  all massive states  $n \neq 0$  sum up to a finite term. The  $n = 0$  term in (2.9) describes the field–theory contribution to the diagram Figure 2, e.g. the exchange of a massless gluon. On the other hand, the term at the order  $\alpha'^2$  describes a new string contact interaction as a result of summing up all heavy string states. Expanding (2.9) to higher orders in  $\alpha'$  yields an infinite series of new string contact interactions for the effective field theory. For example, for a four gluon superstring amplitude the first string contact interaction is given by  $\alpha'^2 g_{Dp}^{-2} \text{tr}F^4$ , which represent a correction to YM theory:

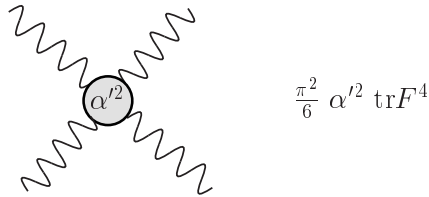


**Fig. 3** New string contact interaction.

While the first string correction for four–gluon scattering yields  $\alpha'^2$  contact terms, the scattering of four chiral fermions yields already a correction at  $\alpha'$ , cf. Section 5.

### 3. Standard Model from D-branes

#### 3.1. Generalities

We will consider type II orientifolds<sup>6</sup> with several stacks of  $Dp_a$ -branes, each being wrapped around individual compact homology  $(p-3)$ -cycles  $\pi_a$  of the internal space. Hence the effective open string gauge theories with groups  $G_a$  live in the  $(p+1)$ -dimensional subspaces  $\mathbf{R}^{1,3} \otimes \pi_a$ .

---

<sup>6</sup> Alternative GUT constructions from F-theory have recently been discussed in [31].

In order to incorporate non-Abelian gauge interactions and to obtain massless fermions in non-trivial gauge representations, one has to introduce D-branes in type II superstrings. Specifically there exist three classes of four-dimensional models:

(i) *Type I compactifications with D9/D5 branes*

This class of IIB models contain different stacks of D9-branes, which wrap the entire space  $\mathcal{M}_6$ , and which also possess open string, magnetic, Abelian gauge fields  $F_{ab}$  on their world volumes (magnetized branes). This magnetic fields are in fact required, if one wants to get chiral fermions from open strings. Because of Ramond tadpole cancellation one also needs an orientifold 9-plane (O9-plane). In addition one can also include D5-branes and corresponding O5-planes.

(ii) *Type IIB compactifications with D7/D3 branes*

Here we are dealing with different stacks of D7-branes, which wrap different internal 4-cycles, which intersect each other. The D7-branes can also carry non-vanishing open string gauge flux  $F_{ab}$ , which is needed for chiral fermions. In addition, one can also allow for D3-branes, which are located at different point of  $\mathcal{M}_6$ . In order to cancel all Ramond tadpoles one needs in general O3- and O7-planes. A specific class of chiral gauge models can be obtained by placing a stack of D3-branes at a singularity of the internal space  $\mathcal{M}_6$ .

(iii) *Type IIA compactifications with D6 branes*

This class of models contains intersecting D6-branes, which are wrapped around 3-cycles of  $\mathcal{M}_6$ . Now, orientifold O6-planes  $\pi_{O6}$  are needed for Ramond tadpole cancellation. In general, each stack of  $D6_a$ -branes, which is wrapped around the cycle  $\pi_a$ , is accompanied by the the orientifold mirror stack, wrapped around the reflected cycles  $\pi'_a$ . The chiral massless spectrum is completely fixed by the topological intersection numbers  $I$  of the 3-cycles of the configuration, cf. Table 2.

sector	representation	intersection number $I$
$a' a$	$A_a$	$\frac{1}{2} (\pi'_a \circ \pi_a + \pi_{O6} \circ \pi_a)$
$a' a$	$S_a$	$\frac{1}{2} (\pi'_a \circ \pi_a - \pi_{O6} \circ \pi_a)$
$a b$	$(\bar{N}_a, N_b)$	$\pi_a \circ \pi_b$
$a' b$	$(N_a, N_b)$	$\pi'_a \circ \pi_b$

**Table 2:** *Intersection of 3-cycles  $\pi_a, \pi_b$ , mirror cycles  $\pi'_a$  and orientifold plane  $\pi_{O6}$*

In general some of the string  $U(1)$ 's are anomalous and receive masses due to Green-Schwarz mechanism. However, for intersecting brane worlds it may also happen that via

axionic couplings some anomaly-free Abelian gauge groups become massive. The condition that a linear combination  $U(1)_Y = \sum_i c_i U(1)_i$  remains massless reads:

$$\sum_i c_i N_i (\pi_i - \pi'_i) = 0 . \quad (3.1)$$

In general, if the hypercharge is such a linear combination of  $U(1)$ 's,  $Q_Y = \sum_i c_i Q_i$ , then the gauge coupling is given by

$$\frac{1}{\alpha_Y} = \sum_i \frac{N_i c_i^2}{2} \frac{1}{\alpha_i} , \quad (3.2)$$

where we have taken into account that the  $U(1)$ 's are generically not canonically normalized (for all possible hyper charge assignments in D-brane orientifolds see [32]).

In the following we will describe some local type IIA/IIB D-brane configurations that lead to the SM in a very economic way.

### 3.2. Three stack D-brane models

Here one starts with three stacks of D-branes with initial gauge symmetries:

$$U(3) \times U(2) \times U(1) \times U(1) . \quad (3.3)$$

The (left-handed) SM spectrum is shown in Table 3.

matter	$SU(3) \times SU(2) \times U(1)^3$	$U(1)_Y$	$U(1)_{B-L}$
$q$	$(\mathbf{3}, \mathbf{2})_{(1,1,0)}$	$\frac{1}{3}$	$\frac{1}{3}$
$\bar{u}$	$(\bar{\mathbf{3}}, \mathbf{1})_{(2,0,0)}$	$-\frac{4}{3}$	$-\frac{1}{3}$
$\bar{d}$	$(\bar{\mathbf{3}}, \mathbf{1})_{(-1,0,1)}$	$\frac{2}{3}$	$-\frac{1}{3}$
$l$	$(\mathbf{1}, \mathbf{2})_{(0,-1,1)}$	$-1$	$-1$
$\bar{e}$	$(\mathbf{1}, \mathbf{1})_{(0,2,0)}$	$2$	$1$
$\bar{\nu}$	$(\mathbf{1}, \mathbf{1})_{(0,0,-2)}$	$0$	$1$

**Table 3:** *Left-handed fermions for the 3 stack model.*

The hypercharge  $Q_Y$  is given as the following linear combination of the three  $U(1)$ 's:

$$Q_Y = -\frac{2}{3} Q_a + \frac{1}{2} Q_b . \quad (3.4)$$

Here one is forced to realize the left-handed  $(\bar{u}, \bar{c}, \bar{t})$ -quarks in the antisymmetric representation of  $U(3)$ , which is the same as the anti-fundamental representation  $\bar{\mathbf{3}}$ . Note that the three stack models with antisymmetric matter are dual to the D3-brane quivers at CY singularities [33,34,35].

### 3.3. Four stack D-brane models

One of the most common ways to realize the SM is by considering four stacks of D-branes. There are several simple ways to embed the SM gauge group into products of unitary and symplectic gauge groups (see [36]). We will use as a prototype model four stacks of D-branes with gauge symmetries:

$$U(3)_a \times U(2)_b \times U(1)_c \times U(1)_d . \quad (3.5)$$

The intersection pattern of the four stacks of D6-branes can be depicted as in Figure 4.

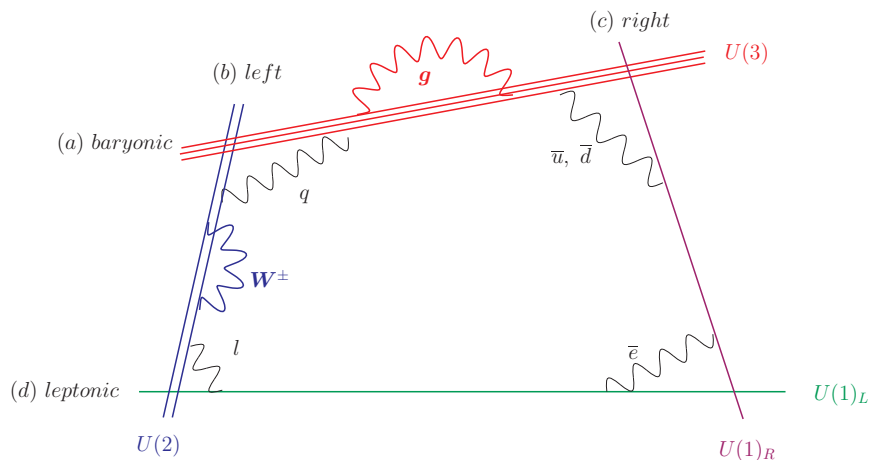


**Fig. 4** Intersection pattern of four stacks of D6-branes giving rise to the MSSM.

The chiral spectrum of the intersecting brane world model should be identical to the chiral spectrum of the SM particles. In type IIA, this fixes uniquely the intersection numbers of the 3-cycles,  $(\pi_a, \pi_b, \pi_c, \pi_d)$ , the four stacks of D6-branes are wrapped on.

There exist several ways to embed the hypercharge  $Q_Y$  into the four  $U(1)$  gauge symmetries. The standard electroweak hypercharge  $Q_Y^{(S)}$  is given as the following linear combination of three  $U(1)$ 's

$$Q_Y^{(S)} = \frac{1}{6} Q_a + \frac{1}{2} Q_c + \frac{1}{2} Q_d . \quad (3.6)$$

Therefore, in this case the gauge coupling of the hypercharge is given as

$$\frac{1}{\alpha_Y} = \frac{1}{6} \frac{1}{\alpha_a} + \frac{1}{2} \frac{1}{\alpha_c} + \frac{1}{2} \frac{1}{\alpha_d} . \quad (3.7)$$

Now we turn to the particle content of our prototype model. In compact orientifold compactifications each stack of D-branes is accompanied by a orientifold mirror stack

of D'-branes. In the next Section about the amplitudes, we will not make a difference between the the D-brane and the mirror D'-branes. Hence we will use in the following the indices  $a, b, c, d$  collectively for the D-branes as well as for their mirror branes. Then self-intersections among D-branes include intersections between D- and D'-branes. Furthermore, for simplicity, we will suppress from the spectrum those open string states which one also gets from intersections between D-branes and orientifold planes. With these restrictions the left-handed fermion spectrum for our prototype model is presented in Table 4.

particle	$U(3)_a \times U(2)_b \times U(1)_a \times U(1)_b \times U(1)_c \times U(1)_d$	mult.
$q$	$(\mathbf{3}, \mathbf{2})_{1,-1,0,0} + (\mathbf{3}, \mathbf{2})_{1,1,0,0}$	$I_{ab}$
$\bar{u}$	$(\bar{\mathbf{3}}, \mathbf{1})_{-1,0,-1,0} + (\bar{\mathbf{3}}, \mathbf{1})_{-1,0,0,-1}$	$I_{ac} + I_{ad}$
$\bar{d}$	$(\bar{\mathbf{3}}, \mathbf{1})_{-1,0,1,0} + (\bar{\mathbf{3}}, \mathbf{1})_{-1,0,0,1}$	$I_{ac} + I_{ad}$
$\bar{d}'$	$(\bar{\mathbf{3}}_A, \mathbf{1})_{2,0,0,0}$	$\frac{1}{2}I_{aa}$
$l$	$(\mathbf{1}, \mathbf{2})_{0,1,-1,0} + (\mathbf{1}, \mathbf{2})_{0,1,0,-1}$ $+ (\mathbf{1}, \mathbf{2})_{0,-1,-1,0} + (\mathbf{1}, \mathbf{2})_{0,-1,0,-1}$	$I_{bc} + I_{bd}$
$\bar{e}$	$(\mathbf{1}, \mathbf{1})_{0,0,2,0}$	$\frac{1}{2}I_{cc}$
$\bar{e}'$	$(\mathbf{1}, \mathbf{1})_{0,0,0,2}$	$\frac{1}{2}I_{dd}$
$\bar{e}''$	$(\mathbf{1}, \mathbf{1})_{0,0,1,1}$	$I_{cd}$

**Table 4:** Chiral spectrum for the four stack model with  $Q_Y^{(S)}$

To derive three generations of quark and leptons, the intersection number in Table 4 must satisfy certain phenomenological restrictions: We must have  $I_{ab} = 3$ . From the left-handed anti u-quarks, we get that  $I_{ac} = 3$ , and likewise for the two types of left-handed anti d-quarks, we infer that  $I_{ac} + I_{ad} + \frac{1}{2}I_{aa} = 3$ . In the lepton sector we require that  $I_{bc} + I_{bd} = 3$  and  $\frac{1}{2}(I_{cc} + I_{dd}) + I_{cd} = 3$ .

#### 4. Embedding of SM D-branes into large volume Calabi–Yau spaces

Let us now discuss large extra dimensions in the context of string compactifications. In fact, it is not completely straightforward to construct SM-like D-brane models on CY spaces with large transverse dimensions. In order to combine D-branes with SM particle content with the scenario of large extra dimensions, one has to consider specific types of CY compactifications. The three or four stacks of intersecting D-branes that give rise to the spectrum of the SM are just local modules that have to be embedded into a global large volume CY-manifold in order to obtain a consistent string compactification. For internal

consistency several tadpole and stability conditions have to be satisfied that depend on the details of the compactification, such as background fluxes etc. In this work we will not aim to provide fully consistent orientifold compactifications with all tadpoles cancelled, since it is enough for us to know the properties of the local SM D-brane modules for the computation of the scattering amplitudes among the SM open strings. However it is important to emphasize that in order to allow for large volume compactification, the D-branes eventually cannot be wrapped around untwisted 3- or 4-cycles of a compact torus or of toroidal orbifolds, but one has to consider twisted, blowing-up cycles of an orbifold or more general CY spaces with blowing-up cycles. The reason for this is that wrapping the three or four stacks of D-branes around internal cycles of a six-torus or untwisted orbifold cycles, the volumes of these cycles involve the toroidal radii. Therefore these volumes cannot be kept small while making the overall volume of the six-torus very big. Hence, the SM D-branes must be wrapped around small cycles inside a blown up orbifold or a CY manifold. Other cycles have to become large, in order to get a CY space with large volume and a low string scale  $M_{\text{string}}$ .

The embedding of the local SM D-brane module into a large CY manifold is depicted in Figure 5.

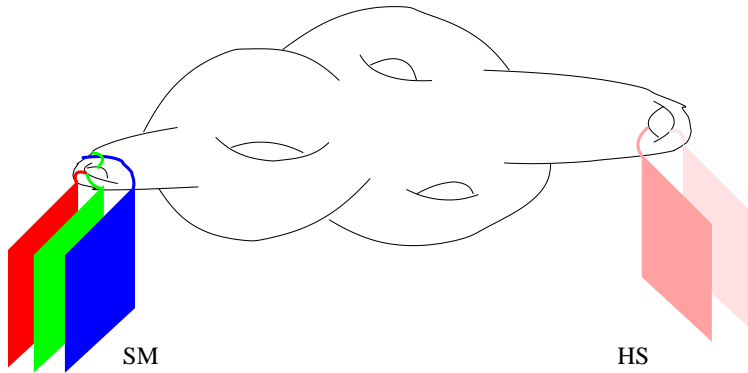


**Fig. 5** Embedding of the SM-branes into a large CY space.

At some other corner of the CY manifold there can be possibly other D-branes, which do not intersect the SM branes and build a hidden gauge sector of the theory.

In Section 5 we shall compute open string disk four-point amplitudes involving SM matter fields. For those amplitudes involving four gauge bosons or two gauge bosons and two matter fermions, the amplitudes do not depend on the geometry of the underlying CY spaces. On the other hand, the four-fermion amplitudes depend on the internal CY geometry and topology. Concretely, the four-fermion amplitudes in general depend on the CY intersection numbers, and also on the rational instanton numbers of the CY space. However, to perform the open string CFT computations for the scattering amplitudes of



matter fields we shall assume that the SM D–branes are wrapped around flat, toroidal like cycles. Therefore the four–fermion amplitudes are functions of toroidal wrapping numbers. Eventually switching from our toroidal-like results to more general CY expressions, some of the factors, which depend on the toroidal geometry, have to be replaced by geometrical or topological CY parameters. However, the kinematical structure of the matter field amplitudes is universal and not affected by the underlying CY geometry. At any rate, as we shall argue at the end of Section 5, for the case that the longitudinal brane directions are somewhat greater than the string scale  $M_{\text{string}}$  the four–fermion couplings depend only on the local structure of the brane intersections, but not on the global CY geometry.

#### 4.1. Type IIB large volume compactifications with wrapped D7-branes

In type IIB orientifolds we assume that the D7-branes are wrapped around 4-cycles inside a CY-orientifold. The relation (2.2) for the volume  $V_6$  applies only for toroidal and orbifold compactifications. Therefore we shall generalize the expressions (2.1) for  $M_{\text{Planck}}$  to the case of large volume CY compactifications. In the string frame<sup>7</sup>, the volume  $V_6$  of a CY space  $X$  is given by

$$V_6 = \frac{1}{3!} \int_X J \wedge J \wedge J = \frac{1}{6} \kappa_{ijk} t_i t_j t_k , \quad (4.1)$$

with  $t_i$  ( $i = 1, \dots, h^{1,1}$ ) the (real) Kähler moduli in the string basis and  $\kappa_{ijk}$  the triple intersection numbers of  $X$ . The Kähler form  $J$  is expanded w.r.t. a base  $\{\widehat{D}_i\}$  of the cohomology  $H^{1,1}(X, \mathbb{Z})$  as  $J = \sum_{i=1}^{h^{1,1}} t_i \widehat{D}_i$ . Without loss of generality we restrict to orientifold projections with  $h_-^{1,1} = 0$ ,  $h_+^{1,1} = h^{1,1}$ . On the other hand, the real parts of the physical Kähler moduli  $T_i$  correspond to the volumes of the CY homology four-cycles  $D_k$  and are computed from the relation:

$$T_i = \frac{1}{2} \int_{D_i} J \wedge J = \frac{\partial V_6}{\partial t_i} = \frac{1}{2} \kappa_{ijk} t_j t_k . \quad (4.2)$$

It follows that the volume  $V_6$  of  $X$  becomes a function of degree 3/2 in the Kähler moduli  $T_i$ :

$$V_6 = \frac{1}{3!} \int_X J \wedge J \wedge J = \mathcal{O}(T_i^{3/2}) . \quad (4.3)$$

For D7–branes wrapped around the four-cycle  $D_k$ , the corresponding gauge coupling constant takes the form

$$g_{D7_k}^{-2} = (2\pi)^{-1} \alpha'^{-2} T_k , \quad (4.4)$$

---

<sup>7</sup> In the Einstein frame the Kähler moduli  $t_k$  are multiplied by the factor  $e^{-\frac{1}{2}\phi_{10}}$ . Therefore, in the Einstein frame the CY volume reads  $V_6 = \frac{1}{6} e^{-\frac{3}{2}\phi_{10}} \kappa_{ijk} t_i t_j t_k$ .

in analogy<sup>8</sup> to Eq. (2.3). In the case of magnetic F-fluxes on the D7-brane world-volume the gauge couplings (4.4) receive an additional  $S$ -dependent contribution, cf. [17].

Now we consider CY manifolds which allow for large volume compactification. Here we assume that a set of four-cycles  $D_\alpha^b$  ( $\alpha = 1, \dots, h_b^{1,1}$ ) can be chosen arbitrarily large while keeping the rest of the four-cycles  $D_\beta^s$  ( $\beta = 1, \dots, h^{1,1} - h_b^{1,1}$ ) small, i.e.  $T_\alpha^b \gg T_\beta^s$ . Since we want the gauge couplings of the SM gauge groups to have finite, not too small values, we must assume that the SM gauge bosons originate from D7-branes wrapped around the small 4-cycles  $D_\beta^s$ . This splitting of the four-cycles into big and small cycles is only possible, if the CY triple intersection numbers form a specific pattern. In addition, the Euler number of the CY space must be negative, i.e.  $h^{2,1} > h^{1,1} > 1$ .

For a simple class of CY spaces with this property the overall volume  $V_6$  is controlled by one big four-cycle  $T^b$ . In this case it has been shown [27,28,37] that one may indeed find minima of the scalar potential, induced by fluxes and radiative corrections in the Kähler potential, that allow for  $T^b \gg T_\beta^s$ . For these CY-spaces, the volume has to take the form

$$V_6 \sim (T^b)^{3/2} - h(T_\beta^s) , \quad (4.6)$$

where  $h$  is a homogeneous function of the small Kähler moduli  $T_\beta^s$  of degree 3/2. E.g. one may consider the following more specific volume form:

$$V_6 \sim (T^b)^{3/2} - \sum_{\beta=1}^{h^{1,1}-1} (T_\beta^s)^{3/2} . \quad (4.7)$$

Looking from the geometrical point of view, these models have a "Swiss cheese" like structures, with holes inside the CY-space given by the small four-cycles.

The simplest example of a Swiss cheese example is the CY manifold  $\mathbf{P}_{[1,1,1,6,9]}$ [18] with  $h^{1,1} = 2$ . In terms of the 2-cycles the volume is given by

$$V_6 = 6 (t_1^3 + t_2^3) . \quad (4.8)$$

According to (4.2) the corresponding 4-cycle volumes become:

$$\begin{aligned} T^b &= \frac{\partial V_6}{\partial t_1} = 18 t_1^2 & \iff & t_1 = \frac{\sqrt{T^b}}{3\sqrt{2}} , \\ T^s &= \frac{\partial V_6}{\partial t_2} = 18 t_2^2 & \iff & t_2 = -\frac{\sqrt{T^s}}{3\sqrt{2}} . \end{aligned} \quad (4.9)$$

---

<sup>8</sup> On the other hands, for (space-time filling) D3-branes the corresponding gauge coupling constant is given by:

$$g_{D3}^{-2} = (2\pi)^{-1} e^{-\phi_{10}} \equiv S . \quad (4.5)$$

Then the volume can be written in terms of the 4-cycles as

$$V_6 = \frac{1}{9\sqrt{2}} \left[ (T^b)^{3/2} - (T^s)^{3/2} \right]. \quad (4.10)$$

Another interesting Swiss cheese example, the CY manifold  $\mathbf{P}_{[1,3,3,3,5]}$ [15] with  $h^{1,1} = 3$  has recently been discussed in [38] in the context of a phenomenologically attractive CY orientifold model where the small cycles are wrapped by D7-branes.

However, in order to accommodate the SM with at least three or four stack of wrapped D7-branes we need more small 4-cycles. Therefore we assume that there exist CY spaces which have a set of small, blowing-up four-cycles that do not intersect the big cycles, i.e. the CY volume is of the form

$$V_6 = t_1^3 + \frac{1}{6} \kappa_{\beta_i \beta_j \beta_k} t_{\beta_i} t_{\beta_j} t_{\beta_k}. \quad (4.11)$$

The SM D7-branes are wrapped around the four-cycles  $D_{\beta_i}$  with volumes  $T_{\beta_i}$  that are kept small. At the same time one is allowed to choose the four-cycle volume  $T^b$  to be large. Let us give one example of a hypothetical CY space with three distinct four-cycles  $D_\beta$  ( $\beta = 1, 2, 3$ ), who still have toroidal-like intersection numbers  $\kappa_{123} = 1$ , and whose intersections with the large four-cycles are absent. The dual two-cycles locally form a  $T^2 \times T^2 \times T^2$  torus inside the CY space. Its volume form is assumed to be

$$V_6 = t_1^3 + t_2 t_3 t_4 + \dots, \quad (4.12)$$

where the dots stand for the contribution of other possible cycles. The big four-cycle is just

$$T^b = \frac{\partial V_6}{\partial t_1} = 3t_1^2, \quad (4.13)$$

and the three small four-cycles intersect in one point and are given as

$$\begin{aligned} T_1^s &= \frac{\partial V_6}{\partial t_2} = t_3 t_4, & T_2^s &= \frac{\partial V_6}{\partial t_3} = t_2 t_4, & T_3^s &= \frac{\partial V_6}{\partial t_4} = t_2 t_3, \\ t_2 &= -\sqrt{\frac{T_2^s T_3^s}{T_1^s}}, & t_3 &= -\sqrt{\frac{T_1^s T_3^s}{T_2^s}}, & t_4 &= -\sqrt{\frac{T_1^s T_2^s}{T_3^s}}. \end{aligned} \quad (4.14)$$

In term of the four-cycle volumes,  $V$  is then given as

$$V_6 = \frac{1}{3\sqrt{3}} (T^b)^{3/2} - (T_1^s T_2^s T_3^s)^{1/2} - \dots. \quad (4.15)$$

Hence, this would-be CY has the form of a Swiss cheese with geometry, where the intersecting four-cycle holes cut themselves a local  $T^2 \times T^2 \times T^2$  space out of the entire CY manifold. However we do not know if this kind of CY does exist.

Let us comment briefly on IIB large volume orientifolds with D5-branes, which are wrapped around CY 2-cycles. Again, the two have to be kept small, whereas the overall volume of the CY-space is very large. Models of this kind are e.g. possible on toroidal orbifolds, where the D5-branes are located at a singularity in a transversal two-dimensional space, as discussed in [39].

#### 4.2. Type IIA large volume compactifications with wrapped D6-branes

Type IIA orientifolds with wrapped D6-branes can be obtained from the type IIB compactifications via T-duality resp. via mirror transformations, which basically exchange the role of the Kähler moduli with the role of the complex structure moduli and vice versa, i.e going from the type IIB CY space  $X$  to its type IIA mirror space, denoted by  $\tilde{X}$ . The volume of  $\tilde{X}$  is still given by eqs. (2.2) resp. (4.11), now expressed in terms of properly defined type IIA radii resp. IIA Kähler moduli  $T_i$ , which are the 2-cycle volumes on  $\tilde{X}$ . Moreover the orientifold O3/O7-planes in type IIB become O6-planes in type IIA, which are wrapped around certain homology 3-cycles  $\Pi_{O6}$  inside  $\tilde{X}$ . Similarly, the type IIB D3/D7-branes become D6-branes, wrapped around homology 3-cycles  $\Pi_a$ , which are suitably embedded into the large volume CY space  $\tilde{X}$ . The  $\Pi_a$  intersect each other at angles  $\theta_{ab}$ , and their intersection angles with orientifold cycles  $\Pi_{O6}$  are denoted by  $\theta_a$ .

The corresponding D6-brane gauge coupling constants are proportional to the volumes of the wrapped 3-cycles, i.e.:

$$g_{D6_a}^{-2} = (2\pi)^{-1} \alpha'^{-2} \text{Vol}(\Pi_a) . \quad (4.16)$$

The volume of the cycle  $\Pi_a$  is given in terms of the associated complex structure moduli  $U_a$  of  $\tilde{X}$ . To accommodate type IIA orientifolds with low string scale and large overall volume, the corresponding complex structure moduli  $U_\beta^s$ , around which the SM D6-branes are wrapped, must be small compared to the volume of  $\tilde{X}$  to achieve finite values for the corresponding gauge coupling constants. As in type IIB, the CY spaces  $\tilde{X}$  must satisfy certain restrictions for large volume compactifications to be possible. In principle the structure of the allowed IIA CY spaces can be inferred from type IIB via mirror symmetry. E.g. one can wrap the D6-branes around certain rigid (twisted) 3-cycles of orbifold compactifications (see e.g. [40]), which can be kept small, whereas the overall volume is made very large.

To perform the computation of the matter field scattering amplitudes, as in type IIB we assume that the 3-cycles, which are wrapped by the SM D6-branes, are flat and have a kind of toroidal like intersection pattern. Specifically, we assume that the SM sector is wrapped around 3-cycles inside a local  $T^2 \times T^2 \times T^2$ , and the D6-brane wrappings around the tree 2-tori are described by wrapping numbers  $(n_a^i, m_a^i)$  ( $i = 1, 2, 3$ ), where the lengths  $L_a^i$  of the wrapped 1-cycles in each  $T^2$  is given by the following equation:

$$L_a^i = \sqrt{(n_a^i)^2 (R_i)^2 + (m_a^i)^2 (R_{i+1})^2} . \quad (4.17)$$

Then the gauge coupling on a D6-brane which is wrapped around a 3-cycle, is [41,42,43]:

$$g_{D6_a}^{-2} = (2\pi)^{-1} \alpha'^{-3/2} e^{-\phi_{10}} \prod_{i=1}^3 L_a^i . \quad (4.18)$$

Here, the 3-cycle  $\Pi_a$  is assumed to be a direct product of three 1-cycles with wrapping numbers  $(n^i, m^i)$  w.r.t. a pair of two internal directions<sup>9</sup>. In terms of the corresponding three complex structure moduli  $U_i$  of the  $T^2$ 's this equation becomes

$$g_{D6_a}^{-2} = (2\pi)^{-1} e^{-\phi_4} \prod_{i=1}^3 \frac{|n_a^i - m_a^i U_i|}{\sqrt{\text{Im}(U_i)}}. \quad (4.20)$$

Finally, the intersection angles of the D6-branes with the O6-planes along the three  $y_i$  directions can be expressed as

$$\tan(\theta_a^i) = \frac{m_a^i R_{i+1}}{n_a^i R_i}, \quad (4.21)$$

and the D6-brane intersection angles are simply given as  $\theta_{ab}^i = \theta_b^i - \theta_a^i$ . More details about the effective gauge couplings, and also about matter field metrics of these kind of intersecting D-brane models can be found in [17,44].

## 5. Four-point string amplitudes of gauge and matter Standard Model fields

In this Section we compute the four-particle amplitudes relevant to LHC physics at the leading order of string perturbation theory, with the string disk world-sheet incorporating the propagation of virtual Regge string excitations at the tree level of effective field theory<sup>10</sup>. With the protons colliding at LHC, there are always two incident partons, gluons or quarks, while the two outgoing particles are partons fragmenting into jets, electroweak gauge bosons or leptons produced via the Drell–Yan mechanism. In all these processes, the baryonic stack of branes plays a special role. We will call it stack  $a$ . Note that in addition to gluons  $g$  in the adjoint representation of  $SU(N_a) = SU(3)$  color group, this stack gives rise to a color singlet gauge boson  $A$  coupled to the baryon number. This boson combines with gauge bosons associated to other stacks to form the vector boson coupled to electroweak hypercharge. We will not enter into details of the mixing mechanism because they are model-dependent. Thus we simply consider  $A$  as one of the particles possibly produced in parton collisions. Starting from the amplitudes involving  $A$  and gauge bosons associated to different stacks, one can easily obtain the physical amplitudes describing the

---

<sup>9</sup> In type IIB orientifolds, the gauge coupling of a D7-brane, wrapped around the 4-cycle  $T^{2,j} \times T^{2,k}$  with wrapping numbers  $m^j, m^k$  and magnetic fluxes  $f^j, f^k$  is (cf. (4.4))

$$g_{D7_i}^{-2} = (2\pi)^{-1} \alpha'^{-2} |m^j m^k| \text{Re}(T_j - f^j f^k S). \quad (4.19)$$

<sup>10</sup> The SM amplitudes reappear in the formal  $\alpha' \rightarrow 0$  ( $M_{\text{string}} \rightarrow \infty$ ) limit.

production of photons,  $Z^0$ , or hypothetical  $Z'$ 's in the framework of specific models. Since four-point disk amplitudes can involve as many as four different stacks, it is very important to establish a transparent notation. In this Section, we are still using the string (hep-th) conventions, with the metric signature  $(-+++)$  and some kinematic invariants defined in the string units. In the next Section, we will make transition to the conventions used in experimental literature (hep-ex).

### 5.1. Notation and Conventions

- $a, b, c, d$ : Dp-brane stacks. Associated gauge groups are  
 $G_a = SU(3) \times U(1)_a$ ,  $G_b = SU(2) \times U(1)_b$ ,  $G_c = U(1)_c$ ,  $G_d = U(1)_d$   
gauge couplings:  $g_{Dp_a} \equiv g$ ,  $g_{Dp_b}$ ,  $g_{Dp_c}$ ,  $g_{Dp_d}$
- Summary of index notation  
indices  $a, \alpha$  ( $\alpha = 1, 2, 3$ ) (possibly with subscripts): are associated to stack  $a$   
indices  $b, \beta$  ( $\beta = 1, 2$ ) (possibly with subscripts): are associated to stack  $b$   
indices  $c, \gamma$  ( $\gamma = 1$ ) (possibly with subscripts): are associated to stack  $c$   
indices  $d, \delta$  ( $\delta = 1$ ) (possibly with subscripts): are associated to stack  $d$
- gauge bosons:  
 $(A^a, A^0) = (g^a, A)$ : indices  $a$  labels adjoint representation of  $G_a$   
 $B^b$ : indices  $b$  labels adjoint representation of  $G_b$   
 $\vdots$
- quarks (compare with Table 4):  
 $q_\beta^\alpha$ : left-handed quarks  
 $u_\gamma^\alpha, u_\delta^\alpha, d_\gamma^\alpha, d_\delta^\alpha$ : right-handed quarks  
 $\bar{q}_\alpha^\beta$  right-handed antiquarks  
 $\bar{u}_\alpha^\gamma, \bar{u}_\alpha^\delta, \bar{d}_\alpha^\gamma, \bar{d}_\alpha^\delta$ : left-handed antiquarks  
 $G_a$ : superscripts  $\alpha$  label fundamental rep.  $\mathbf{N}_a = \mathbf{3}$ , subscripts  $\alpha$  label rep.  $\bar{\mathbf{N}}_a = \bar{\mathbf{3}}$   
 $G_b$ : superscripts  $\beta$  label rep.  $\mathbf{N}_b = \mathbf{2}$ , subscripts  $\beta$  label  $\bar{\mathbf{N}}_b = \bar{\mathbf{2}}$   
 $\vdots$
- leptons (compare with Table 4)  
 $l_\beta^\gamma, l_\beta^\delta$ : left-handed leptons  
 $e_\delta^\gamma, e_\gamma^\gamma, e_\delta^\delta$ : right-handed leptons  
 $\bar{l}_\gamma^\beta, \bar{l}_\delta^\beta$ : right-handed antileptons  
 $\bar{e}_\gamma^\delta, \bar{e}_\gamma^\gamma, \bar{e}_\delta^\delta$ : left-handed antileptons
- Chan-Paton factors (all traces in the fundamental representation): gauge bosons  
gluons  $A^a = g^a$ :  $[T^a]_{\alpha_2}^{\alpha_1}$  generators of  $SU(N_a) = SU(3)$   
 $A^0 = A$  boson:  $[T^0]_{\alpha_2}^{\alpha_1} = \frac{1}{\sqrt{2N}} \delta_{\alpha_2}^{\alpha_1}$   
 $B^b$  bosons:  $[T^b]_{\beta_2}^{\beta_1}$  generators of  $G_b$

⋮

The generators are normalized according to  $\text{Tr}(T^{a_1}T^{a_2}) = \frac{1}{2}\delta^{a_1a_2}$ .

- Chan-Paton factors: quarks and leptons

left-handed quarks:  $[T_{\beta_1}^{\alpha_1}]_{\alpha_2}^{\beta_2} = \delta_{\alpha_2}^{\alpha_1}\delta_{\beta_1}^{\beta_2}$

right-handed quarks:  $[T_{\gamma_1}^{\alpha_1}]_{\alpha_2}^{\gamma_2} = \delta_{\alpha_2}^{\alpha_1}\delta_{\gamma_1}^{\gamma_2}$

⋮

- Wave functions: fermions

left-handed helicity:  $u^{-\lambda}(k_i) \equiv u_i^\lambda$

right-handed helicity:  $\bar{u}_\lambda^+(k_i) \equiv \bar{u}_{i\lambda}$

$k_\mu\sigma_{\lambda\lambda}^\mu = u_\lambda(k)\bar{u}_\lambda(k)$

helicity notation:  $\langle ij \rangle = u_i^\lambda u_{j\lambda} \equiv u_i u_j$   $[ij] = \bar{u}_{i\lambda} \bar{u}_j^\lambda \equiv \bar{u}_i \bar{u}_j$

important property:  $|\langle ij \rangle| = |[ij]| = \sqrt{-2k_i k_j}$ ,  $\langle ij \rangle [ij] = 2k_i k_j$

- Wave functions: vector bosons (with reference momentum  $r$ )

left-handed polarization:  $\xi^{-\mu}(k_i, r) = \frac{u^\lambda(i)\sigma_{\lambda\lambda}^\mu \bar{u}^\lambda(r)}{\sqrt{2}[r i]}$

right-handed polarization:  $\xi^{+\mu}(k_i, r) = \frac{\bar{u}_\lambda(i)\bar{\sigma}^{\mu\lambda} u_\lambda(r)}{\sqrt{2}\langle i r \rangle}$

- Four-particle kinematics (all momenta incoming)

$k_1 + k_2 + k_3 + k_4 = 0$

$\hat{s} = \alpha'(k_1 + k_2)^2 = 2\alpha'k_1k_2$

$\hat{t} = \alpha'(k_1 + k_3)^2 = 2\alpha'k_1k_3$

$\hat{u} = \alpha'(k_1 + k_4)^2 = 2\alpha'k_1k_4$

$\hat{s} + \hat{t} + \hat{u} = 0$

In this Sections, carets are dropped; standard Mandelstam variables will be reintroduced in the next Section.

For the correct normalization of the various fields we recall the low-energy effective ( $N = 1$  SUSY) action of the gauge and matter sectors, which reads up to the two derivative level:

$$\mathcal{L} = -\text{Tr} \sum_{r=a,b,\dots} \frac{1}{2g_{Dp_r}^2} (F_{\mu\nu}^r F^{r\mu\nu} + 4i\bar{\lambda}^r \not{D}\lambda^r) - \text{Tr} \sum_{r\cap s} (D_\mu^{r\cap s} \bar{\phi} D_{r\cap s}^\mu \phi + i\bar{\psi} \not{D}^{r\cap s} \psi) + \dots, \quad (5.1)$$

where  $F_{\mu\nu}^r$  is the field strength of  $A_\mu^r$  and  $\lambda^r$  is its partner gaugino. The first sum runs over all stacks of D-branes, while the second over their intersections. All traces are in the fundamental representations. The gauge covariant derivatives of matter fermions  $\psi_\beta^\alpha$  associated to the intersection of  $a$  and  $b$  are given by:

$$(D_\mu^{a\cap b} \psi)_\beta^\alpha = \partial_\mu \psi_\beta^\alpha + i[T^a]_{\alpha'}^\alpha A_\mu^a \psi_\beta^{\alpha'} - i[T^b]_\beta^{\beta'} A_\mu^b \psi_\beta^{\alpha'}, \quad (5.2)$$

and similar expressions for scalars  $\phi_\beta^\alpha$ . Note that all matter fields are canonically normalized in Eq. (5.1), *i.e.* the moduli-dependent metrics have been absorbed by appropriate field redefinitions.

## 5.2. Four-point string amplitudes and open string vertex operators

Let  $\Phi^i$ ,  $i = 1, 2, 3, 4$ , represent gauge bosons, quarks or leptons of the SM realized on three or more stacks of intersecting D-branes. The corresponding string vertex operators  $V_{\Phi^i}$  are constructed from the fields of the underlying superconformal field theory (SCFT) and contain explicit (group-theoretical) Chan-Paton factors. In order to obtain the scattering amplitudes, the vertices are inserted at the boundary of a disk world-sheet, and the following SCFT correlation function is evaluated:

$$\mathcal{M}(\Phi^1, \Phi^2, \Phi^3, \Phi^4) = \sum_{\pi \in S_4/\mathbf{Z}_2} V_{CKG}^{-1} \int_{\mathcal{I}_\pi} \left( \prod_{k=1}^4 dz_k \right) \langle V_{\Phi^1}(z_1) V_{\Phi^2}(z_2) V_{\Phi^3}(z_3) V_{\Phi^4}(z_4) \rangle . \quad (5.3)$$

Here, the sum runs over all six cyclic inequivalent orderings  $\pi$  of the four vertex operators along the boundary of the disk. Each permutation  $\pi$  gives rise to an integration region  $\mathcal{I}_\pi = \{z \in \mathbf{R} \mid z_{\pi(1)} < z_{\pi(2)} < z_{\pi(3)} < z_{\pi(4)}\}$ . The group-theoretical factor is determined by the trace of the product of individual Chan-Paton factors, ordered in the same way as the vertex positions. The disk boundary contains four segments which may be associated to as many as four different stacks of D-branes, since each vertex of a field originating from a D-brane intersection connects two stacks. Thus the Chan-Paton factor may actually contain as many as four traces, all in the fundamental representations of gauge groups associated to the respective stacks. However, purely partonic amplitudes for the scattering of quarks and gluons involve no more than three stacks.

In order to cancel the total background ghost charge of  $-2$  on the disk, the vertices in the correlator (5.3) have to be chosen in the appropriate ghost picture and the picture “numbers” must add to  $-2$ . Furthermore, in Eq. (5.3), the factor  $V_{CKG}$  accounts for the volume of the conformal Killing group of the disk after choosing the conformal gauge. It will be canceled by fixing three vertex positions and introducing the respective  $c$ -ghost correlator. Because of the  $PSL(2, \mathbf{R})$  invariance on the disk, we can fix three positions of the vertex operators. Depending on the ordering  $\mathcal{I}_\pi$  of the vertex operator positions we obtain six partial amplitudes. The first set of three partial amplitudes may be obtained by the choice

$$z_1 = 0 \quad , \quad z_3 = 1 \quad , \quad z_4 = \infty \quad , \quad (5.4)$$

while for the second set we choose:

$$z_1 = 1 \quad , \quad z_3 = 0 \quad , \quad z_4 = \infty \quad . \quad (5.5)$$

The two choices imply the ghost factor  $\langle c(z_1)c(z_2)c(z_3) \rangle = z_{13}z_{14}z_{34}$ . The remaining vertex position  $z_2$  takes arbitrary values along the boundary of the disk. After performing



all Wick contractions in (5.3) the correlators become basic [45,11] and generically for each partial amplitude the integral (5.3) may be reduced to the Euler Beta function:

$$B(s, u) = \int_0^1 x^{s-1} (1-x)^{u-1} = \frac{\Gamma(s) \Gamma(u)}{\Gamma(s+u)} = \frac{1}{s} + \frac{1}{u} - \frac{\pi^2}{6} (s+u) + \mathcal{O}(\alpha'^2) . \quad (5.6)$$

Although we are mainly interested in the amplitudes involving the particles of the SM, we give below, for completeness, the vertex operators  $V_{\Phi}$  for the full  $N = 1$  SUSY multiplets.

(i) *Gauge vector multiplet:*

The gauge boson vertex operator in the  $(-1)$ -ghost picture reads

$$V_{A^a}^{(-1)}(z, \xi, k) = g_A [T^a]_{\alpha_2}^{\alpha_1} e^{-\phi(z)} \xi^\mu \psi_\mu(z) e^{ik_\rho X^\rho(z)} , \quad (5.7)$$

while in the zero-ghost picture we have:

$$V_{A^a}^{(0)}(z, \xi, k) = \frac{g_A}{(2\alpha')^{1/2}} [T^a]_{\alpha_2}^{\alpha_1} \xi_\mu [i\partial X^\mu(z) + 2\alpha' (k\psi) \psi^\mu(z)] e^{ik_\rho X^\rho(z)} . \quad (5.8)$$

where  $\xi^\mu$  is the polarization vector. The vertex must be inserted on the segment of disk boundary on stack  $a$ , with the indices  $\alpha_1$  and  $\alpha_2$  describing the two string ends.

For our purposes, the most important property of the gluon vertex operators (5.7) and (5.8) is that they do not depend on the internal (CY) part of the SCFT. They depend only on the SCFT fields describing string coordinates  $X^\mu$  in four dimensions, and on their world-sheet superpartners  $\psi^\mu$ . Although the construction of these vertices utilizes SCFT, their form is universal to all compactifications and remains unaffected by eventual SUSY breaking in the bulk or by D-brane configurations. This is the reason why the results for  $N$ -gluon disk amplitudes [9,10,45,11] are completely universal and hold even if SUSY is broken in four dimensions.

In case of  $N = 1$  supersymmetry, the gaugino vertex operators, in the  $(-1/2)$ -ghost picture, are

$$\begin{aligned} V_{\lambda^a, I}^{(-1/2)}(z, u, k) &= g_\lambda [T^a]_{\alpha_2}^{\alpha_1} e^{-\phi(z)/2} u^\lambda S_\lambda(z) \Sigma^I(z) e^{ik_\rho X^\rho(z)} , \\ V_{\bar{\lambda}^a, I}^{(-1/2)}(z, \bar{u}, k) &= g_\lambda [T^a]_{\alpha_2}^{\alpha_1} e^{-\phi(z)/2} \bar{u}_\lambda S^\lambda(z) \bar{\Sigma}^I(z) e^{ik_\rho X^\rho(z)} . \end{aligned} \quad (5.9)$$

where  $S_\lambda$  and  $S^\lambda$  are the world-sheet spin fields associated to the negative and positive helicity fermions, respectively. The index  $I$  labeling gaugino species may range from 1 to 4, depending on the amount of supersymmetries on the D-brane world-volume, while the associated world-sheet fields  $\Sigma^I$  of conformal dimension  $3/8$  belong to the Ramond sector of SCFT [46,47,48]. In the case of extended supersymmetry on the D-brane world-volume

we also have scalars  $\phi^{a,i}$  in the adjoint representation of the gauge group. Their vertex operators take the form:

$$\begin{aligned} V_{\phi^{a,i}}^{(-1)}(z, k) &= g_\phi [T^a]_{\alpha_2}^{\alpha_1} e^{-\phi(z)} \Psi^i e^{ik_\rho X^\rho(z)} , \\ V_{\bar{\phi}^{a,i}}^{(-1)}(z, k) &= g_\phi [T^a]_{\alpha_2}^{\alpha_1} e^{-\phi(z)} \bar{\Psi}^i e^{ik_\rho X^\rho(z)} . \end{aligned} \quad (5.10)$$

For this multiplet, the open string couplings are:

$$g_\lambda = (2\alpha')^{1/2} \alpha'^{1/4} g_{Dp_a} \quad , \quad g_A = (2\alpha')^{1/2} g_{Dp_a} \quad , \quad g_\phi = (2\alpha')^{1/2} g_{Dp_a} . \quad (5.11)$$

These prefactors, together with the universal factor<sup>11</sup>

$$C_{D_2} = \frac{1}{g_{Dp_a}^2 \alpha'^2} , \quad (5.12)$$

which must be inserted in all disk amplitudes with the boundary on a single stack  $a$  of D-branes, ensure agreement of the string computations with the effective action (5.1). Indeed, with these normalizations the three-gluon superstring disk amplitude is:

$$\begin{aligned} \mathcal{M}[A^{a_1}(\xi_1, k_1) A^{a_2}(\xi_2, k_2) A^{a_3}(\xi_3, k_3)] &= g_{Dp_a} \text{Tr}(T^{a_1} [T^{a_2}, T^{a_3}]) \\ &\quad \times [(\xi_1 \xi_2)(\xi_3 k_{12}) + (\xi_1 \xi_3)(\xi_2 k_{31}) + (\xi_2 \xi_3)(\xi_1 k_{23})] . \end{aligned} \quad (5.13)$$

Furthermore, the string coupling of one gauge boson (5.7) to two gauginos (5.9) is:

$$\mathcal{M}[\lambda^{a_1}(k_1, u_1) \bar{\lambda}^{a_2}(k_2, \bar{u}_2) A^{a_3}(\xi, k_3)] = g_{Dp_a} (u_1^\lambda \sigma_{\lambda\dot{\lambda}}^\mu \bar{u}_2^{\dot{\lambda}}) \xi_\mu \times \text{Tr}(T^{a_1} [T^{a_2}, T^{a_3}]) , \quad (5.14)$$

in agreement<sup>12</sup> with Eq. (5.1).

(ii) *Matter multiplet:*

The chiral fermion vertex operators of the quarks and leptons are:

$$\begin{aligned} V_{\psi_\beta^\alpha}^{(-1/2)}(z, u, k) &= g_\psi [T_\beta^\alpha]_{\alpha_1}^{\beta_1} e^{-\phi(z)/2} u^\lambda S_\lambda(z) \Xi^{a \cap b}(z) e^{ik_\rho X^\rho(z)} , \\ V_{\bar{\psi}_\alpha^\beta}^{(-1/2)}(z, \bar{u}, k) &= g_\psi [T_\alpha^\beta]_{\beta_1}^{\alpha_1} e^{-\phi(z)/2} \bar{u}_{\dot{\lambda}} S^{\dot{\lambda}}(z) \bar{\Xi}^{a \cap b}(z) e^{ik_\rho X^\rho(z)} . \end{aligned} \quad (5.15)$$

These vertices connect two segments of disk boundary, associated to stacks  $a$  and  $b$ , with the indices  $\alpha_1$  and  $\beta_1$  representing the string ends on the respective stacks. The internal

<sup>11</sup> See [26] for the derivation of this factor.

<sup>12</sup> The results (5.13) and (5.14) can be matched directly with the interaction vertices of Eq. (5.1) by an additional rescaling  $V_A \rightarrow g_{Dp_a}^{-1} V_A$  ,  $V_\lambda \rightarrow g_{Dp_a}^{-1} V_\lambda$ .

field  $\Xi^{a\cap b}$  of conformal dimension  $3/8$  is the fermionic boundary changing operator. In the intersecting D-brane models, the intersections are characterized by angles  $\theta_{ba}$ . Then  $\Xi^{a\cap b}$  can be expressed in terms of bosonic and fermionic twist fields  $\sigma$  and  $s$ :

$$\Xi^{a\cap b} = \prod_{j=1}^3 \sigma_{\theta_{ba}^j} s_{\theta_{ba}^j} \quad , \quad \bar{\Xi}^{a\cap b} = \prod_{j=1}^3 \sigma_{-\theta_{ba}^j} s_{-\theta_{ba}^j} \quad . \quad (5.16)$$

The spin fields

$$s_{\theta^j} = e^{i(\theta^j - \frac{1}{2})H^j} \quad , \quad s_{-\theta^j} = e^{-i(\theta^j - \frac{1}{2})H^j} \quad (5.17)$$

have conformal dimension  $h_s = \frac{1}{2}(\theta^j - \frac{1}{2})^2$  and twist the internal part of the Ramond ground state spinor. The field  $\sigma_\theta$  has conformal dimension  $h_\sigma = \frac{1}{2}\theta^j(1 - \theta^j)$  and produces discontinuities in the boundary conditions of the internal complex bosonic Neveu–Schwarz coordinates  $Z^j$ .

In case of  $N = 1$  supersymmetry, the vertex operators of chiral matter scalars originating from strings stretching between stacks  $a$  and  $b$  are

$$\begin{aligned} V_{\phi_\beta^\alpha}^{(-1)}(z, k) &= g_\phi [T_\beta^\alpha]_{\alpha_1}^{\beta_1} e^{-\phi(z)} \Pi^{a\cap b}(z) e^{ik_\rho X^\rho(z)} \quad , \\ V_{\bar{\phi}_\alpha^\beta}^{(-1)}(z, k) &= g_\phi [T_\alpha^\beta]_{\beta_1}^{\alpha_1} e^{-\phi(z)} \bar{\Pi}^{a\cap b}(z) e^{ik_\rho X^\rho(z)} \quad . \end{aligned} \quad (5.18)$$

where  $\Pi^{a\cap b}$  is the scalar boundary changing operator of conformal dimension  $1/2$ . Again, for the D-branes  $a$  and  $b$  intersecting at angles  $\theta_{ba}^j$ , an explicit representation can be given in terms of bosonic and fermionic twist fields

$$\Pi^{a\cap b} = \prod_{j=1}^3 \sigma_{\theta_{ba}^j} s_{\theta_{ba}^j} \quad , \quad \bar{\Pi}^{a\cap b} = \prod_{j=1}^3 \sigma_{-\theta_{ba}^j} s_{-\theta_{ba}^j} \quad (5.19)$$

The spin fields

$$s_{\theta^j} = e^{i\theta^j H^j} \quad , \quad s_{-\theta^j} = e^{-i\theta^j H^j} \quad (5.20)$$

have conformal dimension  $h_s = \frac{1}{2}(\theta^j)^2$  and twist the internal part of the Neveu–Schwarz ground state.

For the chiral multiplet, the open string couplings are:

$$g_\phi = (2\alpha')^{1/2} e^{\phi_{10}/2} \quad , \quad g_\psi = (2\alpha')^{1/2} \alpha'^{1/4} e^{\phi_{10}/2} \quad . \quad (5.21)$$

These prefactors, together with the universal factor<sup>13</sup>

$$\tilde{C}_{D_2} = \frac{e^{-\phi_{10}}}{\alpha'^2} \quad , \quad (5.22)$$

which must be inserted in the presence of operators changing disk boundary, ensure agreement of the string computations with the effective action (5.1). Indeed, the coupling of fermions (5.15) to the gauge boson (5.7) is

$$\mathcal{M}[\psi_{\beta_1}^{\alpha_1}(k_1, u_1) \bar{\psi}_{\alpha_2}^{\beta_2}(k_2, \bar{u}_2) A^a(\xi, k_3)] = g_{Dp_a} (u_1^\lambda \sigma_{\lambda\lambda}^\mu \bar{u}_2^\lambda) \xi_\mu \times [T^a]_{\alpha_2}^{\alpha_1} \delta_{\beta_1}^{\beta_2} \quad , \quad (5.23)$$

in agreement with Eq. (5.1).

<sup>13</sup> See [26] for the derivation of this factor.

### 5.3. Four gluon amplitudes

Four-gluon amplitudes have been known for many years [49]. The corresponding string disk diagram is shown in Figure 6:

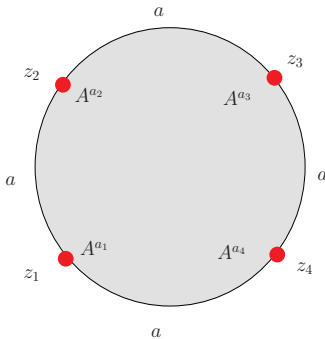


**Fig. 6** Gauge boson vertex operators along the boundary of the disk world-sheet.

The complete amplitude can be generated from the maximally helicity violating MHV amplitudes [9,10]. Usually only one amplitude is written explicitly – a *partial* amplitude associated to one specific Chan-Paton factor. The full expression is necessary, however, for collider applications. Let us start from the partial amplitude [9,10]

$$\mathcal{M}_P(g_1^-, g_2^-, g_3^+, g_4^+) = 4g^2 \text{Tr}(T^{a_1} T^{a_2} T^{a_3} T^{a_4}) \frac{\langle 12 \rangle^4}{\langle 12 \rangle \langle 23 \rangle \langle 34 \rangle \langle 41 \rangle} \widehat{V}(k_1, k_2, k_3, k_4), \quad (5.24)$$

where  $\pm$  refer to polarizations. The Veneziano formfactor is given by

$$\widehat{V}(k_1, k_2, k_3, k_4) = \widehat{V}(s, t, u) = \frac{su}{(s+u)} B(s, u), \quad (5.25)$$

Its low-energy expansion reads

$$\widehat{V}(s, t, u) \approx 1 - \frac{\pi^2}{6} s u + \zeta(3) s t u + \dots \quad (5.26)$$

It is convenient to introduce:

$$\widehat{V}_t = \widehat{V}(s, t, u), \quad \widehat{V}_s = \widehat{V}(t \leftrightarrow s), \quad \widehat{V}_u = \widehat{V}(t \leftrightarrow u). \quad (5.27)$$

The color factor can be written as

$$\begin{aligned} \text{Tr}(T^{a_1} T^{a_2} T^{a_3} T^{a_4}) &= d^{a_1 a_2 a_3 a_4} + \frac{i}{2} (d^{a_1 a_4 n} f^{a_2 a_3 n} - d^{a_2 a_3 n} f^{a_1 a_4 n}) \\ &+ \frac{1}{12} (f^{a_1 a_4 n} f^{a_2 a_3 n} - f^{a_1 a_2 n} f^{a_3 a_4 n}) \end{aligned} \quad (5.28)$$

where the totally symmetric symbols

$$d^{a_1 a_2 a_3} = \text{STr}(T^{a_1} T^{a_2} T^{a_3}), \quad d^{a_1 a_2 a_3 a_4} = \text{STr}(T^{a_1} T^{a_2} T^{a_3} T^{a_4}) \quad (5.29)$$

are the symmetrized traces [50] while  $f^{a_1 a_2 a_3}$  is the totally antisymmetric structure constant.

The full MHV amplitude can be obtained [9,10] by summing the partial amplitudes (5.24) with the indices permuted in the following way:

$$\mathcal{M}(g_1^-, g_2^-, g_3^+, g_4^+) = 4g^2 \langle 12 \rangle^4 \sum_{\sigma \in S_4/Z_4} \frac{\text{Tr}(T^{a_{1\sigma}} T^{a_{2\sigma}} T^{a_{3\sigma}} T^{a_{4\sigma}}) \widehat{V}(k_{1\sigma}, k_{2\sigma}, k_{3\sigma}, k_{4\sigma})}{\langle 1_\sigma 2_\sigma \rangle \langle 2_\sigma 3_\sigma \rangle \langle 3_\sigma 4_\sigma \rangle \langle 4_\sigma 1_\sigma \rangle}. \quad (5.30)$$

where  $S_4$  is the set of all permutations of  $\{1, 2, 3, 4\}$  while  $Z_4$  is the subset of cyclic permutations. As a result, the imaginary part of the color factor (5.28) cancels and one obtains

$$\begin{aligned} \mathcal{M}(g_1^-, g_2^-, g_3^+, g_4^+) &= 8g^2 \langle 12 \rangle^4 \times \\ &\left\{ \frac{\widehat{V}_t}{\langle 12 \rangle \langle 23 \rangle \langle 34 \rangle \langle 41 \rangle} \left[ d^{a_1 a_2 a_3 a_4} + \frac{1}{12} (f^{a_1 a_4 n} f^{a_2 a_3 n} - f^{a_1 a_2 n} f^{a_3 a_4 n}) \right] \right. \\ &+ \frac{\widehat{V}_s}{\langle 14 \rangle \langle 42 \rangle \langle 23 \rangle \langle 31 \rangle} \left[ d^{a_1 a_2 a_3 a_4} + \frac{1}{12} (f^{a_2 a_4 n} f^{a_3 a_1 n} - f^{a_2 a_3 n} f^{a_1 a_4 n}) \right] \\ &\left. + \frac{\widehat{V}_u}{\langle 13 \rangle \langle 34 \rangle \langle 42 \rangle \langle 21 \rangle} \left[ d^{a_1 a_2 a_3 a_4} + \frac{1}{12} (f^{a_3 a_4 n} f^{a_1 a_2 n} - f^{a_3 a_1 n} f^{a_2 a_4 n}) \right] \right\}, \quad (5.31) \end{aligned}$$

All non-vanishing amplitudes can be obtained from the above expression by appropriate crossing operations.

#### 5.4. Two gauge bosons and two fermions

We consider the following correlation function:

$$\langle V_{Ax}^{(0)}(z_1, \xi_1, k_1) V_{Ay}^{(-1)}(z_2, \xi_2, k_2) V_{\psi_{\beta_3}}^{(-1/2)}(z_3, u_3, k_3) V_{\bar{\psi}_{\alpha_4}}^{(-1/2)}(z_4, \bar{u}_4, k_4) \rangle. \quad (5.32)$$

The fact that fermions originate from the same pair of stacks, say  $a$  and  $b$  is forced upon us by the conservation of twist charges, in a similar way as their opposite helicities are forced by the internal charge conservation. It follows that both gauge bosons must be associated either to one of these stacks, say  $(x, y) = (a_1, a_2)$ , or one of them is associated to  $a$  while the other to  $b$ , say  $(x, y) = (a, b)$ . The corresponding disk diagrams are shown in Figure 7.

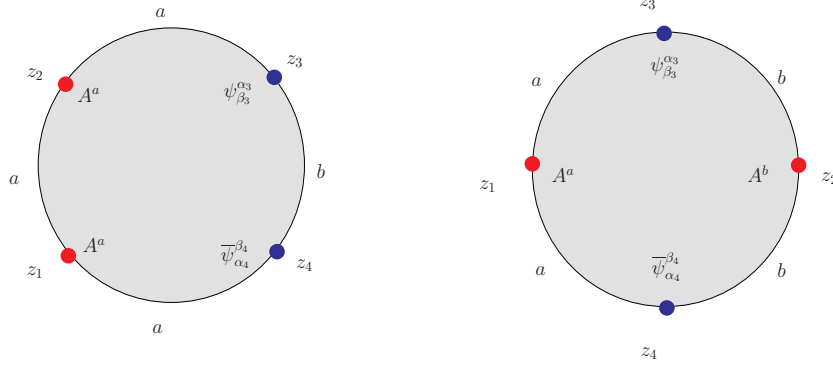


**Fig. 7** Ordering of gauge boson and fermion vertex operators, for  $(x, y) = (a_1, a_2)$  (left diagram) and  $(x, y) = (a, b)$  (right diagram).

With the position  $z_4 = \infty$  as in (5.4) and (5.5), the correlator (5.32) becomes

$$2\alpha' g_{Dp_x} g_{Dp_y} \left\{ \frac{1}{z_{12}} \left[ k_{1\rho} (\xi_1 \xi_2) - \xi_{1\rho} (\xi_2 k_1) + \xi_{2\rho} (\xi_1 k_2) + \xi_{2\rho} (\xi_1 k_3) \frac{z_{12}}{z_{13}} \right] (u_3 \sigma^\rho \bar{u}_4) \right. \\ \left. + \frac{1}{2} \frac{1}{z_{13}} k_{1\lambda} \xi_{1\mu} \xi_{2\rho} (u_3 \sigma^\lambda \bar{\sigma}^\mu \sigma^\rho \bar{u}_4) \right\} \frac{z_{13}}{z_{23}} |z_{12}|^s |z_{23}|^u \quad (5.33)$$

times the Chan Paton factor which is determined by the relative position of  $z_2$  with respect to  $z_1$  and  $z_3$ . If  $(x, y) = (a_1, a_2)$ , there are two allowed orderings of vertex positions: as in (5.4), with  $z_2 < 0$  or  $0 < z_2 < 1$ , see the left side of Figure 7. Then

$$\mathcal{M}[A^{a_1}(\xi_1, k_1) A^{a_2}(\xi_2, k_2) \psi_{\beta_3}^{\alpha_3}(k_3, u_3) \bar{\psi}_{\alpha_4}^{\beta_4}(k_4, \bar{u}_4)] = -2 \alpha' g_{Dp_a}^2 \mathcal{K} \\ \times \left[ \text{Tr}(T^{a_1} T^{a_2} T_{\beta_3}^{\alpha_3} T_{\alpha_4}^{\beta_4}) B(s, u) + \text{Tr}(T^{a_2} T^{a_1} T_{\beta_3}^{\alpha_3} T_{\alpha_4}^{\beta_4}) \frac{t}{u} B(s, t) \right], \quad (5.34)$$

where the kinematic factor:

$$\mathcal{K} = \left\{ \left[ k_{1\rho} (\xi_1 \xi_2) - \xi_{1\rho} (\xi_2 k_1) + \xi_{2\rho} (\xi_1 k_2) - \frac{s}{t} \xi_{2\rho} (\xi_1 k_3) \right] (u_3 \sigma^\rho \bar{u}_4) \right. \\ \left. - \frac{1}{2} \frac{s}{t} k_{1\lambda} \xi_{1\mu} \xi_{2\rho} (u_3 \sigma^\lambda \bar{\sigma}^\mu \sigma^\rho \bar{u}_4) \right\}. \quad (5.35)$$

On the other hand, if  $(x, y) = (a, b)$ , then there is only one allowed ordering, as in (5.4), with  $z_2 > 1$ , see the right side of Figure 7, and we obtain

$$\mathcal{M}[A^a(\xi_1, k_1) A^b(\xi_2, k_2) \psi_{\beta_3}^{\alpha_3}(k_3, u_3) \bar{\psi}_{\alpha_4}^{\beta_4}(k_4, \bar{u}_4)] = -2 \alpha' g_{Dp_a} g_{Dp_b} \mathcal{K} \\ \times \text{Tr}(T^a T_{\beta_3}^{\alpha_3} T^b T_{\alpha_4}^{\beta_4}) \frac{t}{s} B(t, u). \quad (5.36)$$

The amplitudes (5.34) and (5.36) may be written as sums over infinite many  $s$ -channel poles at the masses (2.7) in exactly the same way as (2.6). On the other hand, for the lowest string correction of Eqs. (5.34) and (5.36), which gives rise to a string contact interaction in lines of Subsection 2.3, we use the expansion of the Euler Beta function (5.6):

$$\begin{aligned} \mathcal{M}[A^{a_1}(\xi_1, k_1)A^{a_2}(\xi_2, k_2) \psi_{\beta_3}^{\alpha_3}(k_3, u_3)\bar{\psi}_{\alpha_4}^{\beta_4}(k_4, \bar{u}_4)] \Big|_{\alpha'2} &= -2 \alpha' g_{Dp_a}^2 \frac{\pi^2}{6} t \mathcal{K} \\ &\times \left[ \text{Tr}(T^{a_1}T^{a_2}T_{\beta_3}^{\alpha_3}T_{\alpha_4}^{\beta_4}) + \text{Tr}(T^{a_2}T^{a_1}T_{\beta_3}^{\alpha_3}T_{\alpha_4}^{\beta_4}) \right], \\ \mathcal{M}[A^a(\xi_1, k_1)A^b(\xi_2, k_2) \psi_{\beta_3}^{\alpha_3}(k_3, u_3)\bar{\psi}_{\alpha_4}^{\beta_4}(k_4, \bar{u}_4)] \Big|_{\alpha'2} &= -2 \alpha' g_{Dp_a} g_{Dp_b} \frac{\pi^2}{6} t \mathcal{K} \\ &\times \text{Tr}(T^aT_{\beta_3}^{\alpha_3}T^bT_{\alpha_4}^{\beta_4}). \end{aligned} \quad (5.37)$$

Hence, the first string contact interaction appears at the order  $M_{\text{string}}^{-4}$  as in the case of four-gluon scattering (cf. Figure 3).

In order to write the kinematic factor (5.35) more explicitly, we choose  $k_2$  as the reference momentum for the polarization vector  $\xi_1$  and  $k_1$  as the reference momentum for  $\xi_2$ . Then it is easy to see that the kinematic factor vanishes if both gauge bosons have the same helicity, while for the opposite helicities  $\xi_1^\pm \xi_2^\mp = 0$  and most of terms the r.h.s. of Eq. (5.35) vanish except for

$$\xi_{2\rho}^+(\xi_1^- k_3)(u_3 \sigma^\rho \bar{u}_4) = \frac{1}{\alpha' s} \langle 13 \rangle^2 [23][24], \quad \xi_{2\rho}^-(\xi_1^+ k_3)(u_3 \sigma^\rho \bar{u}_4) = \frac{1}{\alpha' s} \langle 23 \rangle^2 [13][14]. \quad (5.38)$$

After combining the kinematic and Chan-Paton factors, and renaming external fields, Eqs. (5.34) and (5.34) become

$$\mathcal{M}(g_1^-, g_2^+, q_3^-, \bar{q}_4^+) = 2 g^2 \delta_{\beta_3}^{\beta_4} \frac{\langle 13 \rangle^2}{\langle 23 \rangle \langle 24 \rangle} \left[ (T^{a_1} T^{a_2})_{\alpha_4}^{\alpha_3} \frac{t}{s} \widehat{V}_t + (T^{a_2} T^{a_1})_{\alpha_4}^{\alpha_3} \frac{u}{s} \widehat{V}_u \right], \quad (5.39)$$

$$\mathcal{M}(g_1^-, B_2^+, q_3^-, \bar{q}_4^+) = 2 g_{Dp_b} g \frac{\langle 13 \rangle^2}{\langle 23 \rangle \langle 24 \rangle} (T^a)_{\alpha_4}^{\alpha_3} (T^b)_{\beta_3}^{\beta_4} \widehat{V}_s. \quad (5.40)$$

All other helicity amplitudes can be obtained from the above expressions by appropriate crossing operations. The low energy expansions of the above amplitudes can be obtained by using Eq. (5.6). The leading term agrees with the well-known QCD result.

### 5.5. Four chiral fermions

Let us first discuss what are the possible four-point disk amplitudes among four fermion fields. Of course the amplitudes are constrained by the  $SU(3) \times SU(2) \times U(1)_Y$  gauge invariance of the SM. In addition, the allowed disk scattering amplitudes are constrained by the conservation of the additional  $U(1)$  charges of the matter fields. Recall

that the these  $U(1)$ 's are part of the original  $U(N)$  gauge symmetries of the different stack of D-branes, and are in general massive due to the generalized Green-Schwarz mechanism. Only the SM hypercharge stays as a massless, anomaly free linear combination. Nevertheless, the massive  $U(1)$ 's act as global symmetries and provide selection rules that constrain the allowed tree level couplings. Note that space-time instantons, i.e. wrapped Euclidean D-branes, may violate the conservation of the global  $U(1)$  symmetries, and can hence lead to new processes, which we do not discuss here.

There are two classes of fermion disk amplitudes. The first class contains the amplitudes describing the processes that occur in the SM by the exchange of massless particles. They have poles in the associated exchange channels. Exchange of heavy Regge excitations of mass  $M_{\text{string}}$  provide additional string corrections to this kind of amplitudes. Therefore the SM background must be subtracted in order to see the new signal from string theory. Second, there are four fermion disk amplitudes, which do not exhibit any massless poles. Hence there are only the string contact interactions due to the exchange of Regge like excitations. Therefore these amplitudes do not possess SM, tree-level background. In the following we discuss the possible amplitudes in the prototype model of Section 4, with particle content as given in Table 4. We indicate which amplitudes occur already in the SM due to the tree level exchange of SM gauge bosons, and which can occur only in the D-brane model under investigation. At this stage we would like to stress that the computations of the four fermion disk amplitudes are performed for intersecting D6-branes wrapped around flat 3-cycles of a six-dimensional torus. It follows that the explicit expressions, which we shall present in the following, may contain also contributions from exchange of massive states (scalar fields), whose masses depend on the intersection angles of the 3-cycles. In addition there are contributions from fields that are due to the extended supersymmetries on the D6-branes on the torus, e.g. moduli fields that describe the positions of the D6-branes on the tori. All these model dependent fields may in general appear in intermediate channels of the four fermion amplitudes.

(i) All four fermions at the same intersection point (one angle).

The simplest case is the scattering of two pairs of fermion/anti-fermion fields which are located at the same intersection point of two stacks,  $a$  and  $b$ , cf. Figure 8.



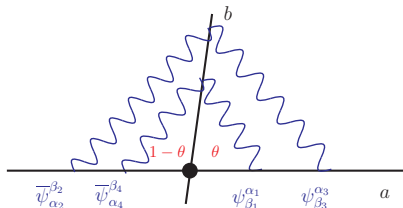


**Fig. 8** Two intersecting stacks  $a$  and  $b$  and two pairs of conjugate fermions.

The amplitude is

$$\langle \psi_{\beta_1}^{\alpha_1} \bar{\psi}_{\alpha_2}^{\beta_2} \psi_{\beta_3}^{\alpha_3} \bar{\psi}_{\alpha_4}^{\beta_4} \rangle \quad (5.41)$$

and exhibits poles due to the exchange of massless gauge bosons from the stack  $a$  and stack  $b$ . In addition, Regge excitations, KK and winding states are exchanged. An example for this amplitude is the process

$$q^- \bar{q}^+ \rightarrow q^- \bar{q}^+ \quad (q_L q_R^c \rightarrow q_L q_R^c) \quad (5.42)$$

which receives contributions from the exchange of gluons, photons,  $W, Z$ -bosons, as well as the Regge and KK excitations.

(ii) Two pairs of conjugate fermions at two different intersection points (two angles)

Now we are considering three stacks of D-branes,  $a, b$  and  $c$  with two intersection angles  $\theta := \theta_b - \theta_a$  and  $\nu := \theta_c - \theta_a$ , cf. Figure 9.

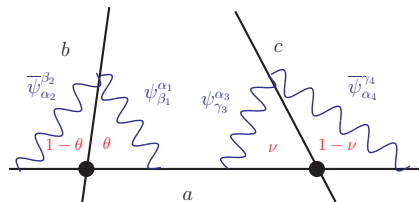


**Fig. 9** Three intersecting stacks  $a, b$  and  $c$  and two pairs of conjugate fermions.

We have open strings spanned between  $a$  and  $b$ , as well as open strings stretched between  $a$  and  $c$ <sup>14</sup>. Hence we consider the following amplitude:

$$\langle \psi_{\beta_1}^{\alpha_1} \bar{\psi}_{\alpha_2}^{\beta_2} \psi_{\gamma_3}^{\alpha_3} \bar{\psi}_{\alpha_4}^{\gamma_4} \rangle. \quad (5.43)$$

<sup>14</sup> In case of multiple intersections, namely considering different families, stack  $b$  and  $c$  can be the same, but the fermions may be associated to different intersections.

This amplitude exhibits massless poles due to the exchange of the common massless gauge boson from stack  $a$  as well from its Regge excitations, KK and windings states thereof. An example for this amplitude is the process

$$q^- \bar{q}^+ \rightarrow q^+ \bar{q}^- \quad (q_L q_R^c \rightarrow q_R q_L^c) . \quad (5.44)$$

(iii) Four different fermions at four intersection points (three angles):

Finally we are considering four stacks of D-branes,  $a, b, c$  and  $d$  with all four chiral fermions originating from different intersections, cf. Figure 10.

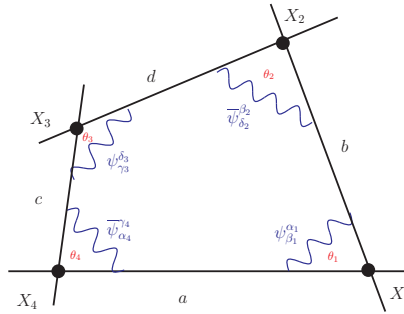


**Fig. 10** Four intersecting stacks  $a, b, c$  and  $d$  and fermions at four different intersections.

The corresponding amplitude is of the form

$$\langle \psi_{\beta_1}^{\alpha_1} \bar{\psi}_{\delta_2}^{\beta_2} \psi_{\gamma_3}^{\delta_3} \bar{\psi}_{\alpha_4}^{\gamma_4} \rangle . \quad (5.45)$$

No massless gauge bosons are exchanged in this amplitude. However, there may be the exchange of the SM Higgs field as well as some exotic states with masses of the order of the string scale. An example of this kind of amplitude is the following contribution to the Drell–Yan process:

$$q^- \bar{q}^- \rightarrow \mu^- \bar{\mu}^- \quad (q_L q_L^c \rightarrow \mu_L \mu_L^c) . \quad (5.46)$$

Note that purely hadronic  $2 \rightarrow 2$  parton scattering processes with quarks and antiquarks belonging to the same family involve no more than three stacks because all partons share the QCD D-brane stack.

In order to compute the four-fermion amplitudes, we evaluate Eq. (5.3) with the following correlator:

$$\langle V_{\psi_{\beta_1}^{\alpha_1}}^{(-1/2)}(z_1, u_1, k_1) V_{\bar{\psi}_{\delta_2}^{\beta_2}}^{(-1/2)}(z_2, \bar{u}_2, k_2) V_{\psi_{\gamma_3}^{\delta_3}}^{(-1/2)}(z_3, u_3, k_3) V_{\bar{\psi}_{\alpha_4}^{\gamma_4}}^{(-1/2)}(z_4, \bar{u}_4, k_4) \rangle \quad (5.47)$$

involving two chiral  $\psi_{\beta_1}^{\alpha_1}, \psi_{\gamma_3}^{\delta_3}$  and two anti-chiral  $\overline{\psi}_{\delta_2}^{\beta_2}, \overline{\psi}_{\alpha_4}^{\gamma_4}$  matter fermions. In the type IIA picture the latter are represented by open strings stretched between two intersecting stacks of branes with the vertex operator<sup>15</sup> (5.15). Although the following discussion is carried out for intersecting D6-branes it may be translated into other setups. We shall present the explicit expressions for the four-fermion string amplitudes in the case of the prototype four stack model introduced in Section 4.

The most general case may involve four different  $D$ -branes  $a, b, c$  and  $d$ , which intersect at the four points  $X_i$  with the angles  $\theta_i, i = 1, \dots, 4$ , respectively, cf. Figure 11. In addition we have the relation  $\theta_1 + \theta_2 + \theta_3 + \theta_4 = 2$ .

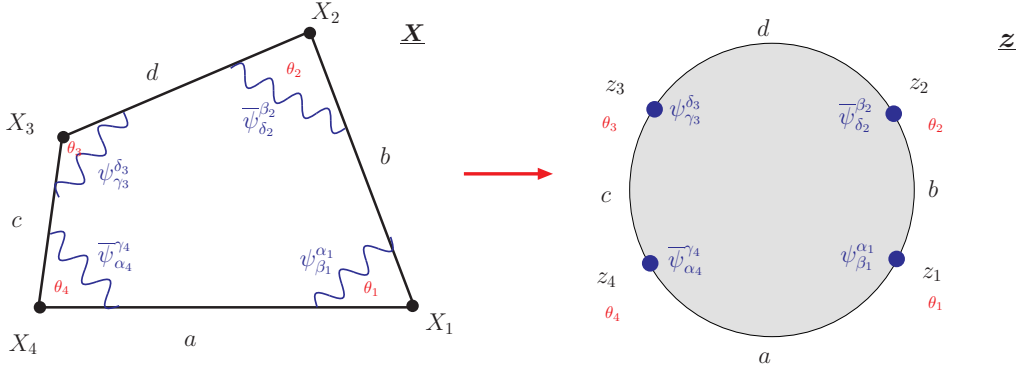


**Fig. 11** Four D-brane stacks and chiral fermions in the target space and on the disk world-sheet.

The explicit expression of (5.47) depends on the number of different branes  $a, \dots, d$  involved and the location of the four intersection points  $X_1, \dots, X_4$ . On the world-sheet of the disk the ordering  $X_i$  of adjacent D6-branes is translated into a related ordering of vertex operator positions  $z_i$  through the map  $z_i \rightarrow X_i := X(z_i)$ . Due to the chirality and twist properties of the four fermions the dual resonance channels of the full amplitude are very restricted. Further details depend on the specific configuration of intersections and will be discussed below.

In what follows we need to define the straight line distance between two different brane intersection points:

$$\delta_a^j := X_1^j - X_4^j, \quad \delta_b^j = X_2^j - X_1^j, \quad \delta_c^j = X_4^j - X_3^j, \quad \delta_d^j = X_3^j - X_2^j. \quad (5.48)$$

For a given brane  $a$  the latter are decomposed into

$$\delta_a^j = \epsilon_a^j L_a^j + d_a^j, \quad \epsilon_a^j \in \mathbf{R} \quad (5.49)$$

with the longitudinal direction  $L_a^j$  along the brane  $a$  and transverse component  $d_a^j$ , cf. Figure 12.

---

<sup>15</sup> Vertex operators for the case if one brane is on top of an orientifold plane have been constructed in [19].

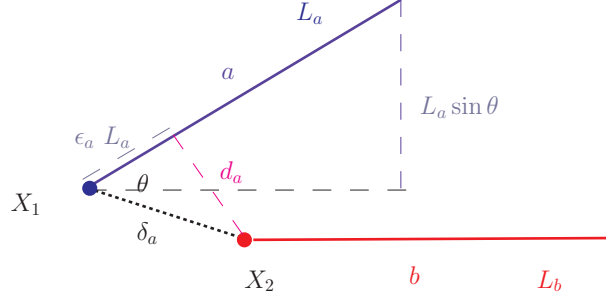


**Fig. 12** Two branes  $a$  and  $b$  and the distance  $\delta_a$ .

The distance of two equivalent intersections from one pair  $(a, b)$  of intersecting branes is given by a multiple of the lattice vectors  $L_a^j$  or  $L_b^j$ , i.e.  $d_a^j = 0$  and  $\epsilon_a^j \in \mathbf{Z}$ .

Depending on the angles  $\theta_i$  for particular brane configurations the amplitude (5.47) may furnish massless gauge boson exchange. In those cases massless gauge bosons, internal KK states w.r.t. the longitudinal brane directions and winding states w.r.t. their orthogonal directions are exchanged. The masses of internal KK states w.r.t. the compact direction  $L_b^j$  of brane  $b$  and winding states w.r.t the direction between brane  $b$  and  $a$  related to the gauge boson from stack  $b$  are given by:

$$\alpha' (m_{ab}^j)^2 = \frac{\sin^2(\pi\theta^j)}{\alpha'} |p_a^j L_a^j + \delta_a^j|^2 + \frac{\alpha' (\tilde{p}_b^j)^2}{|L_b^j|^2}, \quad p_a, \tilde{p}_b \in \mathbf{Z}. \quad (5.50)$$

In the following we discuss the three cases introduced before

$$\begin{aligned} (i) \quad & \theta_1 = \theta_3 = \theta, \quad \theta_2 = \theta_4 = 1 - \theta, \\ (ii) \quad & \theta_1 = \theta, \quad \theta_2 = 1 - \theta, \quad \theta_3 = \nu, \quad \theta_4 = 1 - \nu, \\ (iii) \quad & \theta_1, \theta_2, \theta_3, \theta_4 = 2 - \theta_1 - \theta_2 - \theta_3, \end{aligned} \quad (5.51)$$

separately. Furthermore we must specify the intersections classes  $f_i$  the four intersection points  $X_i$  are related to. In the following let us describe these cases in more detail.

(i) One angle  $\theta$  :

In case (i) we may either have (1) chiral fermions stemming from intersections  $f_i$  of a single pair of branes  $a, b$ . For this case we have  $d^j = 0$ , i.e.  $c \simeq b$ ,  $d \simeq a$ . In the second case (2) we consider chiral fermions stemming from intersections  $f_i, \tilde{f}_j$  of two pairs of branes  $a, b$  and  $c, d$ , which are mutually shifted by some distance  $d^j$  orthogonal to the brane directions  $L^j$ .

(i.1) The pair of two intersecting branes  $a$  and  $b$  has  $I_{ab}$  intersection points  $f_i$  and all four points  $X_i$  are assumed to be elements thereof. A generic case with  $I_{ab} = 3$  is depicted in Figure 13 with the three different intersection points drawn in black, red and blue, respectively. We must further specify the class of intersection points  $f_i$  involved, which yields to the subcases (i.1a) and (i.1b).

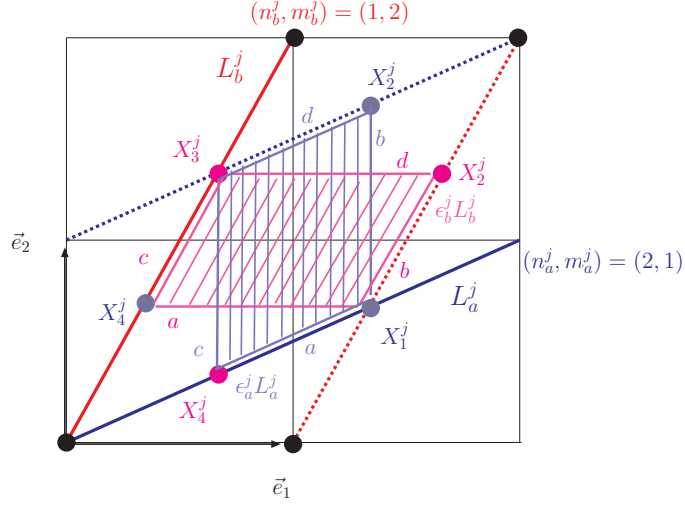


**Fig. 13** Two possible polygons between two pairs of conjugate intersection points of an intersecting brane pair  $(a, b)$  with intersection number  $I_{ab} = 3$ .

(i.1a) All four chiral fermions all located at the same intersection  $f$ . In that case all four intersection points  $X_i$  differ a by an integer lattice shift, i.e.  $X_i = f + \mathbf{Z} L$  and hence  $\epsilon^j \in \mathbf{Z}$ ,  $d^j = 0$ . In Figure 13 the class  $f$  may be e.g. the set of four black dots, which span one polygon.

(i.1b) A pair of two chiral fermions from the same intersection  $f_i$  and an other pair from an other intersection  $f_j$ . In Figure 13 the intersections  $f_i, f_j$  may be e.g. the two blue and two red dots, respectively. Obviously, the points from the same set of intersections are separated by are lattice vector, i.e.  $\epsilon^j \in \mathbf{Z}$ ,  $d^j = 0$ . However, the length between points from different intersections is smaller. It is given by the intersection number  $I_{ab}$ , i.e.  $\epsilon^j \in \frac{\mathbf{Z}}{I_{ab}}$ ,  $d^j = 0$ . Generically, there are two different configurations for the polygon spanned by the four points  $X_i$ . In Figure 13, these two polygons are drawn in red and blue, respectively:  $\epsilon_a^j, \epsilon_d^j \in \mathbf{Z}$ ,  $\epsilon_b^j, \epsilon_c^j \in \mathbf{Q}$  or  $\epsilon_b^j, \epsilon_c^j \in \mathbf{Z}$ ,  $\epsilon_a^j, \epsilon_d^j \in \mathbf{Q}$  and  $d^j = 0$ .

(i.2) The case  $d^j \neq 0$  describes two intersecting D-brane pairs  $(a, b)$  and  $(c, d)$  with the intersection angle  $\theta$ . This situation is similar as in (i.1) except, that intersection points  $\tilde{f}_i$  of one D-brane pair are mutually shifted by some distance  $d^j$  orthogonal to the brane directions  $L_a^j, L_b^j$ . The intersection numbers do not change, i.e.  $I_{ab} = I_{cd}$ .

(ii) Two angles  $\theta, \nu$ :

For this case we consider two different intersecting D-brane pairs  $(a, b)$  and  $(c, d)$  with the intersection angles  $\theta, \nu$  respectively, cf. Figure 11. In this case, there is no relation between

the set of intersections of  $(a, b)$  and  $(c, d)$  as in the previous case (i.2). All four chiral fermions may originate from different intersections  $f_i$ , cf. Figure 11. One pair of fermions is related to the twist–antitwist pair  $(\theta, 1 - \theta)$  at the intersections  $(X_1, X_2)$  and the second pair of fermions is related to the twist–antitwist pair  $(\nu, 1 - \nu)$  from the intersections  $(X_3, X_4)$ . Hence only one polygon configuration is possible.

(iii) Three angles  $\theta_1, \theta_2, \theta_3$  :

The most general case of (5.47) involves four fermions from four different intersections  $X_i$ . For that case we have three arbitrary angles  $\theta_1, \theta_2, \theta_3$  and  $\theta_4 = 2 - \theta_1 - \theta_2 - \theta_3$ . This is the situation depicted in Figure 10.

(i) *Four-fermion amplitudes involving two twist–antitwist pairs  $(\theta, 1 - \theta)$*

We consider the case of two pairs  $(a, b)$  and  $(c, d) \simeq (b', a')$  of D–branes intersecting at the angle  $\theta$ . In (5.47) we have two pairs of twist–antitwist fields  $(\theta, 1 - \theta)$  from intersections  $f_i$  and  $f_j$ , respectively. One pair of fermions is related to a twist–antitwist pair  $(\theta, 1 - \theta)$  at the points  $X_1, X_2$  related to the intersection  $f_i$  (or  $X_2, X_3$  related to the intersection  $f_j$ ) and a second fermion pair to an other twist–antitwist pair  $(\theta, 1 - \theta)$  at the points  $X_3, X_4$  related to the intersection  $f_j$  (or  $X_1, X_4$  related to the intersection  $f_i$ ).

The explicit expression of (5.47) for the case (i) has been computed<sup>16</sup> in [13,15,12] and extended in [20]

$$\begin{aligned} \mathcal{M}[\psi_{\beta_1}^{\alpha_1}(u_1, k_1) \bar{\psi}_{\alpha'_2}^{\beta_2}(\bar{u}_2, k_2) \psi_{\beta'_3}^{\alpha'_3}(u_3, k_3) \bar{\psi}_{\alpha_4}^{\beta'_4}(\bar{u}_4, k_4)] &= 4\pi \alpha' e^{\phi_{10}} (u_{1L} u_{3L}) (\bar{u}_{2R} \bar{u}_{4R}) \\ &\times \int_0^1 dx x^{s-1} (1-x)^{u-1} \left( \prod_{i=1}^3 I_i(x)^{-1/2} \right) \\ &\times \left\{ \text{Tr}(T_{\beta_1}^{\alpha_1} T_{\alpha'_2}^{\beta_2} T_{\beta'_3}^{\alpha'_3} T_{\alpha_4}^{\beta_4}) \sum_{p_b^j, p_d^j \in \mathbf{Z}} e^{-S_{\text{inst.}}^{bd}(x)} + \text{Tr}(T_{\beta_1}^{\alpha_1} T_{\alpha_4}^{\beta_4} T_{\beta'_3}^{\alpha'_3} T_{\alpha'_2}^{\beta_2}) \sum_{p_a^j, p_c^j \in \mathbf{Z}} e^{-S_{\text{inst.}}^{ac}(x)} \right\}, \end{aligned} \quad (5.52)$$

with the disk instanton action

$$S_{\text{inst.}}^{bd}(x) = \frac{\pi}{\alpha'} \sum_{j=1}^3 \sin(\pi\theta^j) \left[ \left| p_b^j L_b^j + \delta_b^j \right|^2 \tau_j(x) + \left| p_d^j L_d^j + \delta_d^j \right|^2 \tau_j(1-x) \right], \quad (5.53)$$

---

<sup>16</sup> Four–fermion interactions in D–brane models have also been discussed in [51,52].

and the combinations of hypergeometric functions:

$$\tau_j(x) = \frac{F_j(1-x)}{F_j(x)} \quad , \quad I_j(x) = \frac{F_j(x) F_j(1-x)}{\sin(\pi\theta^j)} \quad , \quad F_j(x) = {}_2F_1[\theta^j, 1-\theta^j, 1; x] \quad . \quad (5.54)$$

The first term of (5.52) accounts for the polygon with the twist–antitwist pairs at  $X_1, X_2$  and  $X_3, X_4$ , while the second term describes the polygon with the twist–antitwist pairs at  $X_1, X_4$  and  $X_2, X_3$ . In (5.52) the spinor products  $(u_{1L}u_{3L}) (\bar{u}_{2R}\bar{u}_{4R})$  arise from contracting the space–time spin fields of the fermion vertex operators (5.15). The following identity is useful for extracting the gauge boson exchange channels:

$$(u_{1L}u_{3L}) (\bar{u}_{2R}\bar{u}_{4R}) = \frac{1}{2} (u_{1L}\sigma^\mu\bar{u}_{2R}) (u_{3L}\sigma_\mu\bar{u}_{4R}) = -\frac{1}{2} (u_{1L}\sigma^\mu\bar{u}_{4R}) (u_{3L}\sigma_\mu\bar{u}_{2R}) \quad . \quad (5.55)$$

The normalization of (5.52) simply arises from our convention (5.21) and (5.22), i.e.  $g_\psi^4 \tilde{C}_{D_2} = 4\alpha' e^{\phi_{10}} g_{10}^2 \equiv 4\alpha' e^{\phi_{10}}$ .

With the limits

$$F(x) \rightarrow 1 \quad , \quad F(1-x) \rightarrow \frac{\sin(\pi\theta)}{\pi} \ln\left(\frac{\delta}{x}\right) \quad , \quad \ln \delta(\theta) = 2\psi(1) - \psi(\theta) - \psi(1-\theta) \quad (5.56)$$

as  $x \rightarrow 0$  we may extract from (5.52) the  $s$ -channel pole contribution

$$\begin{aligned} \mathcal{M} \longrightarrow & \alpha' (u_{1L}\sigma^\mu\bar{u}_{2R}) (u_{3L}\sigma_\mu\bar{u}_{4R}) \\ & \times \left\{ \text{Tr}(T_{\beta_1}^{\alpha_1} T_{\alpha'_2}^{\beta_2} T_{\beta'_3}^{\alpha'_3} T_{\alpha_4}^{\beta'_4}) g_{D6_{a'}}^2 \sum_{p_b^j, \tilde{p}_d^j \in \mathbf{Z}} \frac{\prod_{j=1}^3 \delta(\theta^j)^{-\alpha' (m_{bd}^j)^2} e^{2\pi i \tilde{p}_d^j \frac{\delta_d^j}{|L_d^j|}}}{s + \alpha' \sum_{j=1}^3 (m_{bd}^j)^2} \right. \\ & \left. + \text{Tr}(T_{\beta_1}^{\alpha_1} T_{\alpha_4}^{\beta'_4} T_{\beta'_3}^{\alpha'_3} T_{\alpha'_2}^{\beta_2}) g_{D6_{b'}}^2 \sum_{p_a^j, \tilde{p}_c^j \in \mathbf{Z}} \frac{\prod_{j=1}^3 \delta(\theta^j)^{-\alpha' (m_{ac}^j)^2} e^{2\pi i \tilde{p}_c^j \frac{\delta_c^j}{|L_c^j|}}}{s + \alpha' \sum_{j=1}^3 (m_{ac}^j)^2} \right\} \quad , \quad (5.57) \end{aligned}$$

with the gauge couplings

$$g_{D6_a}^{-2} = (2\pi)^{-1} \alpha'^{-3/2} e^{-\phi_{10}} \prod_{j=1}^3 |L_a^j| \quad (5.58)$$

introduced in (4.18) and the masses (5.50) of internal KK and winding states. In deriving (5.57) a Poisson resummation on the integers  $p_d$  and  $p_c$  is involved. On the other hand,

the  $u$ -channel of (5.52) gives rise to:

$$\begin{aligned}
\mathcal{M} \longrightarrow & -\alpha' (u_{1L}\sigma^\mu \bar{u}_{4R}) (u_{3L}\sigma_\mu \bar{u}_{2R}) \\
& \times \left\{ \text{Tr}(T_{\beta_1}^{\alpha_1} T_{\alpha_2}^{\beta_2} T_{\beta_3}^{\alpha_3} T_{\alpha_4}^{\beta_4}) g_{D6_b}^2 \sum_{p_a^j, \tilde{p}_b^j \in \mathbf{Z}} \frac{\prod_{j=1}^3 \delta(\theta^j)^{-\alpha'} (m_{db}^j)^2 e^{2\pi i \tilde{p}_b^j \frac{\delta_b^j}{|L_b^j|}}}{u + \alpha' \sum_{j=1}^3 (m_{db}^j)^2} \right. \\
& \left. + \text{Tr}(T_{\beta_1}^{\alpha_1} T_{\alpha_4}^{\beta_4} T_{\beta_3}^{\alpha_3} T_{\alpha_2}^{\beta_2}) g_{D6_a}^2 \sum_{p_c^j, \tilde{p}_a^j \in \mathbf{Z}} \frac{\prod_{j=1}^3 \delta(\theta^j)^{-\alpha'} (m_{ca}^j)^2 e^{2\pi i \tilde{p}_a^j \frac{\delta_a^j}{|L_a^j|}}}{u + \alpha' \sum_{j=1}^3 (m_{ca}^j)^2} \right\}. \tag{5.59}
\end{aligned}$$

In deriving (5.57) a Poisson resummation on the integers  $p_b$  and  $p_c$  is involved. In the case of  $d^j = 0$  with the identifications  $b' = c \simeq b$  and  $a' = d \simeq a$ , we have  $m_{ca}^j, m_{bd}^j \equiv m_{ba}^j$  and  $m_{ac}^j, m_{db}^j \equiv m_{ab}^j$ .

Finally let us discuss the special subcases of (i), introduced above:

(i.1) The pairs of two branes  $a, b$  and  $d, c$  are identical, i.e.  $d \simeq a$ ,  $c \simeq b$ , cf. Figure 14.

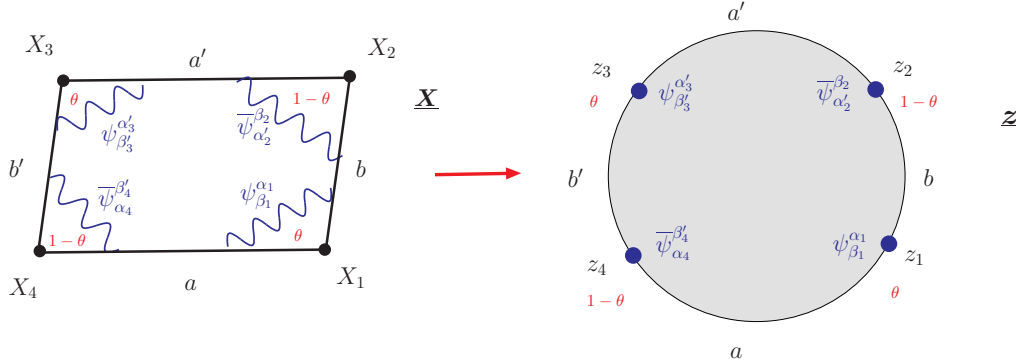


**Fig. 14** Four D-brane stacks and chiral fermions in the target space and on the disk world-sheet.

(i.1a) For all intersections  $X_i$  related to *one* intersection  $f$  we have  $\delta^j = 0$ . From (5.50) we see, that massless gauge boson exchange from stack  $a$  or stack  $b$  appears both in the  $s$ - and  $u$ -channel. The case under consideration corresponds e.g. to a scattering process of four quarks from one family, e.g. the scattering of  $u, \bar{u}$ -quarks (cf. Figure 8). For this case we introduce the function

$$V_{abab}(s, u) = 2\pi \alpha' e^{\phi_{10}} \int_0^1 dx x^{s-1} (1-x)^{u-1} \left( \prod_{i=1}^3 I_i(x)^{-1/2} \right) \sum_{p_a^j, p_b^j \in \mathbf{Z}} e^{-S_{\text{inst.}}^{ba}(x)}, \tag{5.60}$$



which will become relevant in the next Section. The instanton action becomes in that case:

$$S_{\text{inst.}}^{ba}(x) = \frac{\pi}{\alpha'} \sum_{j=1}^3 \sin(\pi\theta^j) \left[ |p_b^j L_b^j|^2 \tau_j(x) + |p_a^j L_a^j|^2 \tau_j(1-x) \right]. \quad (5.61)$$

According to (5.57) and (5.59) in the limit  $s, t, u \rightarrow 0$  the function  $V_{abab}(s, u)$  exhibits the behaviour:

$$V_{abab}(s, u) = \alpha' \left( \frac{g_{D6a}^2}{s} + \frac{g_{D6b}^2}{u} \right) + \dots. \quad (5.62)$$

(i.1b) In the case of two distinct intersections  $f_i, f_j$  we have:  $\delta_b^j \equiv 0$ ,  $\delta_d^j \sim \frac{L_d^j}{I_{db}^j} \simeq \frac{L_a^j}{I_{ab}^j}$  and  $\delta_a^j \equiv 0$ ,  $\delta_c^j \sim \frac{L_c^j}{I_{ac}^j} \simeq \frac{L_b^j}{I_{ab}^j}$ . Hence, there are massless gauge boson exchanges from stack  $a$  or stack  $b$  only in the  $s$ -channel (5.57). However, no massless gauge boson contribution stems from the  $u$ -channel (5.59). The case under consideration corresponds e.g. to a scattering process of a pair of quarks associated to two different families, e.g. the scattering of  $u, \bar{u}$ -quarks with  $c, \bar{c}$ -quarks.

(i.2) In the case of  $d^j \neq 0$  the two polygon contributions are parameterized by:  $\delta_a^j = d_a^j$ ,  $\delta_c^j \sim \frac{L_c^j}{I_{ac}^j}$  and  $\delta_b^j = d_b^j$ ,  $\delta_d^j \sim \frac{L_d^j}{I_{db}^j}$ . For this case the mass (5.50) is always non-zero and no massless gauge bosons are exchanged neither in the  $s$ -channel (5.57) nor in the  $u$ -channel (5.59).

(ii) *Four-fermion amplitudes involving two twist-antitwist pairs  $(\theta, 1-\theta)$  and  $(\nu, 1-\nu)$*

Here we consider the generic case of four different stacks of D6-branes  $a, b, c$  and  $d$  with two pairs of twist-antitwist fields,  $(\theta, 1-\theta)$  and  $(\nu, 1-\nu)$ . We have two intersection angles  $\theta$  and  $\nu$  referring to the pairs  $(a, b)$  and  $(c, d)$ , respectively, cf. Figure 15.

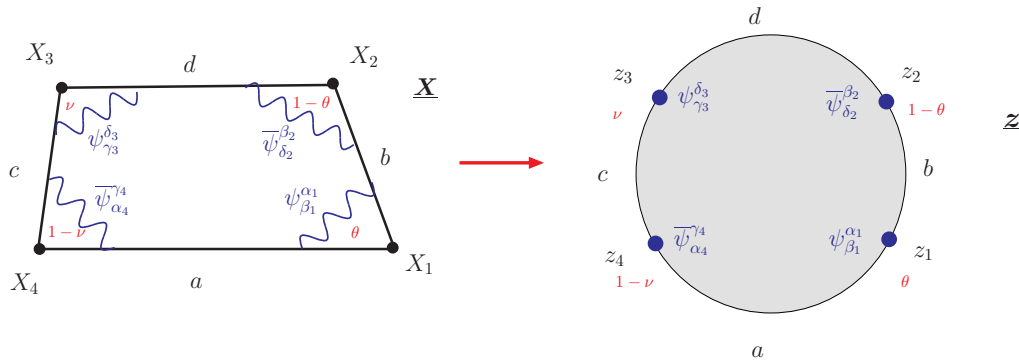


**Fig. 15** Four D-brane stacks and chiral fermions in the target space and on the disk world-sheet.

In the previous case  $\theta = \nu$  we have encountered two possible polygon contributions as a matter of how the two twist–antitwist pairs are paired:  $(X_1, X_2)$  and  $(X_3, X_4)$  or  $(X_1, X_4)$  and  $(X_2, X_3)$ , respectively. Obviously, for  $\theta \neq \nu$  we have only one polygon from the twist–antitwist pairs  $(X_1, X_2)$  and  $(X_3, X_4)$ .

The explicit expression of (5.47) for  $\theta \neq \nu$  has been computed in [13,16]

$$\begin{aligned} \mathcal{M}[\psi_{\beta_1}^{\alpha_1}(u_1, k_1) \bar{\psi}_{\delta_2}^{\beta_2}(\bar{u}_2, k_2) \psi_{\gamma_3}^{\delta_3}(u_3, k_3) \bar{\psi}_{\alpha_4}^{\gamma_4}(\bar{u}_4, k_4)] &= 4\pi \alpha' e^{\phi_{10}} \\ &\times \left[ \text{Tr}(T_{\beta_1}^{\alpha_1} T_{\delta_2}^{\beta_2} T_{\gamma_3}^{\delta_3} T_{\alpha_4}^{\gamma_4}) + \text{Tr}(T_{\beta_1}^{\alpha_1} T_{\alpha_4}^{\gamma_4} T_{\gamma_3}^{\delta_3} T_{\delta_2}^{\beta_2}) \right] (u_{1L} u_{3L}) (\bar{u}_{2R} \bar{u}_{4R}) \\ &\times \int_0^1 dx x^{s-1} (1-x)^{u-1} \left( \prod_{i=1}^3 I_i(x)^{-1/2} \right) \sum_{p_b^j, p_d^j \in \mathbf{Z}} e^{-S_{\text{inst.}}(x)}, \end{aligned} \quad (5.63)$$

with the disk instanton action

$$S_{\text{inst.}}(x) = \frac{\pi}{\alpha'} \sum_{j=1}^3 \sin(\pi\theta^j) \left\{ |v_b^j|^2 \left( \tau_j(x) + \frac{\beta^j}{2} \right) + \left| v_d^j + \frac{\beta^j}{2} v_b^j \right|^2 \frac{1}{\tau_j(x) + \frac{\beta^j}{2}} \right\}, \quad (5.64)$$

with  $v_r = p_r L_r + \delta_r$ ,  $\beta^j = -\frac{\sin[\pi(\theta^j - \nu^j)]}{\sin(\pi\nu^j)}$  and the function:

$$2\pi I_j(x) = B(1 - \theta^j, \nu^j) F_{1;j}(1-x) K_{2;j}(x) + B(\theta^j, 1 - \nu^j) F_{2;j}(1-x) K_{1;j}(x). \quad (5.65)$$

Above we have introduced the hypergeometric functions  $K_{1;j}(x) = {}_2F_1[1 - \theta^j, \nu^j, 1; x]$ ,  $K_{2;j}(x) = {}_2F_1[\theta^j, 1 - \nu^j, 1; x]$ ,  $F_{1;j}(x) = {}_2F_1[1 - \theta^j, \nu^j; 1 - \theta^j + \nu^j; x]$ , and  $F_{2;j}(x) = {}_2F_1[1 - \nu^j, \theta^j, 1 + \theta - \nu^j; x]$ , and the Euler Beta function (5.6). Finally, we have

$$\tau_j(x) = \frac{1}{\pi} B(1 - \theta^j, \nu^j) \sin(\pi\theta^j) \frac{F_{1;j}(1-x)}{K_{1;j}(x)}, \quad (5.66)$$

and the relation:

$$I_j(x) = \frac{1}{\sin(\pi\theta^j)} \left( \tau_j(x) + \frac{\beta^j}{2} \right) K_{1;j}(x) K_{2;j}(x). \quad (5.67)$$

As result of respecting the global monodromy conditions we have the relations:  $\beta^j v_b^j = v_a^j - v_d^j$ , i.e.  $v_d^j + \frac{\beta^j}{2} v_b^j = \frac{1}{2}(v_a^j + v_d^j)$  and  $\sin(\pi\nu^j) |v_c^j| = \sin(\pi\lambda^j) |v_b^j|$ . The function (5.65), which determines the quantum part of the amplitude (5.63), is the square root of the relevant closed string piece [53,54]. For  $\theta^j = \nu^j$  we have  $\beta^j = 0$  and the functions  $\tau_j(x)$  and  $I_j(x)$  reduce to the expressions (5.54). With this information it is straightforward to show, that (5.63) boils down to the first term of (5.52) as  $\nu^j \rightarrow \theta^j$ .

Due to the chirality and twist properties of the four fermions the amplitude (5.63) furnishes massless gauge boson exchange through the  $s$ -channel only. On the other hand,

for  $\theta^j \neq \nu^j$  the limit  $x \rightarrow 1$  does not imply massless gauge boson exchange and factorizes onto Yukawa couplings. This property is discussed in more detail for case (iii).

In the following let us consider the case  $d = a$ ,  $\delta = \alpha$  and  $\delta_c^j, \delta_b^j = 0$ , which corresponds to Figure 9. Only in the  $s$ -channel a massless gauge boson exchange occurs. To extract from (5.63) the  $s$ -channel pole contribution we need the limit

$$\tau_j(x) \rightarrow \frac{1}{\pi} \sin(\pi\theta^j) \ln \left( \frac{\delta(1 - \theta^j, \nu^j)}{x} \right), \quad (5.68)$$

as  $x \rightarrow 0$ , with  $\ln \delta(\theta^j, \nu^j) = 2\psi(1) - \psi(\theta^j) - \psi(\nu^j)$ . For the limit  $x \rightarrow 0$  we obtain

$$\begin{aligned} \mathcal{M} \longrightarrow & \alpha' \left\{ \text{Tr}(T_{\beta_1}^{\alpha_1} T_{\alpha_2}^{\beta_2} T_{\gamma_3}^{\alpha_3} T_{\alpha_4}^{\gamma_4}) + \text{Tr}(T_{\alpha_2}^{\beta_2} T_{\beta_1}^{\alpha_1} T_{\alpha_4}^{\gamma_4} T_{\gamma_3}^{\alpha_3}) \right\} (u_{1L} \gamma_\mu \bar{u}_{2R}) (u_{3L} \gamma^\mu \bar{u}_{4R}) \\ & \times g_{D6_a}^2 \sum_{p_b^j, \tilde{p}_a^j \in \mathbf{Z}} \frac{\prod_{j=1}^3 \delta(1 - \theta^j, \nu^j)^{-\alpha' (m_{ba}^j)^2} e^{2\pi i \tilde{p}_a^j \frac{\delta_a^j}{L_a^j}} e^{\pi i \left( \frac{1}{1 - e^{2\pi i \theta^j}} - \frac{1}{1 - e^{2\pi i \nu^j}} \right)} \alpha' (m_{ba}^j)^2}{s + \alpha' \sum_{j=1}^3 (m_{ba}^j)^2}, \end{aligned} \quad (5.69)$$

with the gauge coupling (5.58) and the mass  $m_{ba}^j$  of KK and winding states given in Eq. (5.50). In deriving (5.57) a Poisson resummation on the integer  $p_a$  is involved. Again, for  $\nu^j = \theta^j$  the limit (5.69) reduces to the corresponding expression of (5.57). The case under consideration describes e.g. the process  $q^- \bar{q}^+ \rightarrow q^+ \bar{q}^-$  ( $q_L q_R^c \rightarrow q_R q_L^c$ ), cf. (5.44). To accommodate the different choices of helicities of the four fermions we introduce the function

$$V_{abac}^{(n_1, n_2)}(s, u) = 2\pi \alpha' e^{\phi_{10}} \int_0^1 dx x^{s-1-\frac{n_1}{2}} (1-x)^{u-1-\frac{n_2}{2}} \left( \prod_{i=1}^3 I_i(x)^{-1/2} \right) \sum_{p_a^j, p_b^j \in \mathbf{Z}} e^{-S_{\text{inst.}}^{ba}(x)}, \quad (5.70)$$

with the following assignment of helicity configurations

$$\begin{aligned} V_{abac}(s, u) & := V_{abac}^{(0,0)}(s, u) \quad \text{for } (13)_L(24)_R \quad \text{and } (24)_L(13)_R, \\ V'_{abac}(s, u) & := V_{abac}^{(0,1)}(s, u) \quad \text{for } (14)_L(23)_R \quad \text{and } (23)_L(14)_R, \\ V''_{abac}(s, u) & := V_{abac}^{(1,0)}(s, u) \quad \text{for } (12)_L(34)_R \quad \text{and } (34)_L(12)_R, \end{aligned} \quad (5.71)$$

and the common instanton part:

$$S_{\text{inst.}}^{ba}(x) = \frac{\pi}{\alpha'} \sum_{j=1}^3 \sin(\pi\theta^j) \left\{ |p_b^j L_b^j|^2 \left( \tau_j(x) + \frac{\beta^j}{2} \right) + |p_a^j L_a^j + \delta_a^j|^2 \frac{1}{\tau_j(x) + \frac{\beta^j}{2}} \right\}. \quad (5.72)$$

According to (5.69) in the limit  $s, t, u \rightarrow 0$  the functions  $V_{abac}(s, u)$  and  $V'_{abac}(s, u)$  furnish massless gauge boson exchange:

$$V_{abac}(s, u) = \alpha' \frac{g_{D6_a}^2}{s} + \dots \quad , \quad V'_{abac}(s, u) = \alpha' \frac{g_{D6_a}^2}{s} + \dots \quad . \quad (5.73)$$

On the other hand, the function  $V''_{abac}(s, u)$  does not imply massless gauge boson exchange and behaves as:

$$V''_{abac}(s, u) = \alpha' \frac{g_{D6_a}^2}{s - \frac{1}{2}} + \dots \quad . \quad (5.74)$$

This case is discussed in more detail for case (iii).

(iii) *Four-fermion amplitudes involving fermions from four different intersections*

The most general case, depicted in Figure 11, involves four fermions from four different intersections  $X_i$  with the four angles  $\theta_i$  and  $\theta_4 = 2 - \theta_1 - \theta_2 - \theta_3$ . The explicit expression of (5.47) for this case has been computed in [16]

$$\begin{aligned} \mathcal{M}[\psi_{\beta_1}^{\alpha_1}(u_1, k_1) \bar{\psi}_{\delta_2}^{\beta_2}(\bar{u}_2, k_2) \psi_{\gamma_3}^{\delta_3}(u_3, k_3) \bar{\psi}_{\alpha_4}^{\gamma_4}(\bar{u}_4, k_4)] &= 4\pi \alpha' e^{\phi_{10}} \left( \prod_{i=1}^3 \frac{\sin(\pi\theta_2^i) \sin(\pi\theta_4^i)}{\sin(\pi\theta_1^i) \sin(\pi\theta_3^i)} \right)^{1/4} \\ &\times \left[ \text{Tr}(T_{\beta_1}^{\alpha_1} T_{\delta_2}^{\beta_2} T_{\gamma_3}^{\delta_3} T_{\alpha_4}^{\gamma_4}) + \text{Tr}(T_{\beta_1}^{\alpha_1} T_{\alpha_4}^{\gamma_4} T_{\gamma_3}^{\delta_3} T_{\delta_2}^{\beta_2}) \right] (u_{1L} u_{3L}) (\bar{u}_{2R} \bar{u}_{4R}) \\ &\times \int_0^1 dx x^{s-1} (1-x)^{u-1} \left( \prod_{i=1}^3 I_i(x)^{-1/2} \right) \sum_{p_b^j, p_d^j \in \mathbf{Z}} e^{-S_{\text{inst.}}(x)} \quad , \end{aligned} \quad (5.75)$$

with the disk instanton action

$$S_{\text{inst.}}(x) = \frac{\pi}{\alpha'} \sum_{j=1}^3 \sin(\pi\theta_2^j) \frac{\left| v_b^j \tau_j - v_d^j \right|^2 + \gamma^j \tilde{\gamma}^j \left| v_b^j (\beta^j + \tau_j) + v_d^j (1 + \alpha^j \tau_j) \right|^2}{\beta^j + 2 \tau_j + \alpha^j \tau_j^2} \quad , \quad (5.76)$$

with  $v_r = p_r L_r + \delta_r$  and the quantum contribution:

$$\begin{aligned} 2\pi I_j(x) &= \frac{\Gamma(1 - \theta_1^j) \Gamma(\theta_3^j)}{\Gamma(\theta_2^j + \theta_3^j) \Gamma(\theta_3^j + \theta_4^j)} F_{1;j}(1-x) K_{2;j}(x) \\ &+ \frac{\Gamma(\theta_1^j) \Gamma(1 - \theta_3^j)}{\Gamma(\theta_1^j + \theta_2^j) \Gamma(\theta_1^j + \theta_4^j)} F_{2;j}(1-x) K_{1;j}(x) \quad . \end{aligned} \quad (5.77)$$

Above we have introduced the hypergeometric functions  $K_{1;j}(x) = {}_2F_1[\theta_2^j, 1 - \theta_4^j, \theta_1^j + \theta_2^j; x]$ ,  $K_{2;j}(x) = {}_2F_1[\theta_4^j, 1 - \theta_2^j, \theta_3^j + \theta_4^j; x]$ ,  $F_{1;j}(x) = {}_2F_1[\theta_2^j, 1 - \theta_4^j, \theta_2^j + \theta_3^j; x]$ , and

$F_{2;j}(x) = {}_2F_1[\theta_4^j, 1 - \theta_2^j, \theta_1^j + \theta_4^j; x]$ ,  $\beta^j = -\frac{\sin[\pi(\theta_2^j + \theta_3^j)]}{\sin(\pi\theta_3^j)}$ ,  $\alpha^j = -\frac{\sin[\pi(\theta_1^j + \theta_2^j)]}{\sin(\pi\theta_1^j)}$  and  $\gamma^j = \frac{\Gamma(1-\theta_2^j) \Gamma(1-\theta_4^j)}{\Gamma(\theta_1^j) \Gamma(\theta_3^j)}$ ,  $\tilde{\gamma}^j = \frac{\Gamma(\theta_2^j) \Gamma(\theta_4^j)}{\Gamma(1-\theta_1^j) \Gamma(1-\theta_3^j)}$ . Finally, we have

$$\tau_j(x) = \frac{B(\theta_2^j, \theta_3^j)}{B(\theta_1^j, \theta_2^j)} \frac{F_{1;j}(1-x)}{K_{1;j}(x)}. \quad (5.78)$$

Note, that the function (5.77) and the classical action (5.76) have crossing symmetry under the combined manipulations  $x \leftrightarrow 1-x$  and  $\theta_1^j \leftrightarrow \theta_3^j$ . For  $\theta_1^j = \theta^j, \theta_2^j = 1 - \theta^j, \theta_3^j = \nu^j$  and  $\theta_4^j = 1 - \nu^j$  we have  $\alpha^j = 0$ ,  $\gamma^j, \tilde{\gamma}^j = 1$  and the functions  $I_j(x)$  and  $\tau_j(x)$  reduce to the expressions (5.65) and (5.66), respectively. With this information it is straightforward to show, that (5.75) boils down to (5.63) in this limit. Furthermore, for  $\theta_1^j = \theta_3^j = \theta^j$  and  $\theta_2^j = \theta_4^j = 1 - \theta^j$  we have  $\alpha^j, \beta^j = 0$ ,  $\gamma^j, \tilde{\gamma}^j = 1$  and the functions  $I_j(x)$  and  $\tau_j(x)$  reduce to the expressions (5.54).

The amplitude (5.75) does not furnish massless gauge boson exchange limits. On the other hand, it factorizes onto Yukawa couplings. In the following we investigate the helicity configuration  $(12)_L(34)_R$  and  $(34)_L(12)_R$ , which corresponds to the function

$$V_{abcd}(s, u) = 2\pi \alpha' e^{\phi_{10}} \left( \prod_{i=1}^3 \frac{\sin(\pi\theta_2^i) \sin(\pi\theta_4^i)}{\sin(\pi\theta_1^i) \sin(\pi\theta_3^i)} \right)^{1/4} \times \int_0^1 dx x^{s-3/2} (1-x)^{u-1} \left( \prod_{i=1}^3 I_i(x)^{-1/2} \right) \sum_{p_b^j, p_d^j \in \mathbf{Z}} e^{-S_{\text{inst.}}(x)}, \quad (5.79)$$

with the instanton action (5.76). For  $x \rightarrow 0$  and  $0 < \theta_1^j + \theta_2^j < 1$  the integral (5.79) gives rise to the  $s$ -channel limit

$$V_{abcd}(s, u) \longrightarrow \alpha' e^{\phi_{10}} Y(\theta_1, \theta_2) Y(1 - \theta_3, 1 - \theta_4) \frac{1}{s + \alpha' m_H^2}, \quad (5.80)$$

with the intermediate mass

$$\alpha' m_H^2 = 1 - \frac{1}{2} \sum_{j=1}^3 (\theta_1^j + \theta_2^j), \quad (5.81)$$

and the Yukawa couplings [13,18]:

$$Y(\theta_a, \theta_b) = (4\pi)^{1/2} \prod_{j=1}^3 \left( 2\pi \frac{\Gamma(1-\theta_a^j) \Gamma(1-\theta_b^j) \Gamma(\theta_a^j + \theta_b^j)}{\Gamma(\theta_a^j) \Gamma(\theta_b^j) \Gamma(1-\theta_a^j - \theta_b^j)} \right)^{1/4} \sum_{v_{ba}^j} e^{-\frac{\pi}{\alpha'}} \frac{\sin(\pi\theta_a^j) \sin(\pi\theta_b^j)}{\sin[\pi(\theta_a^j + \theta_b^j)]} |v_{ba}^j|^2. \quad (5.82)$$

Hence, in the limit  $x \rightarrow 0$  (heavy) string states with mass (5.81) are exchanged. These states may represent the SM Higgs field as well as some exotic states. The latter may give possible stringy signatures at the LHC [55].

The (relevant) four–point fermion amplitudes  $V(s, u)$ , whose explicit form is given in Eqs. (5.60), (5.70) and (5.79), receive world–sheet disk instanton corrections from holomorphic mappings of the string world–sheet into the polygon spanned by the four intersection points  $X_i$ , respectively. The three–point couplings (5.82) are derived from the latter by appropriate factorization and the relevant polygon splits into two triangles, cf. Eq. (5.80).

The amplitudes (5.60), (5.70) and (5.79) give rise to string corrections to the contact four fermion interaction. The first correction appears at the order  $\alpha'$ . For  $(n_1, n_2) = (0, 0)$  corresponding to the helicity configurations  $(13)_L(24)_R$  or  $(24)_L(13)_R$  the latter are extracted by setting  $s, u = 0$  and may be summarized in the expression:

$$V_{abcd}^{(0,0)}(s, u) \Big|_{\alpha'} = 2\pi \alpha' e^{\phi_{10}} \left( \prod_{i=1}^3 \frac{\sin(\pi\theta_2^i) \sin(\pi\theta_4^i)}{\sin(\pi\theta_1^i) \sin(\pi\theta_3^i)} \right)^{\frac{1}{4}} \int_0^1 dx \frac{\prod_{i=1}^3 I_i(x)^{-\frac{1}{2}}}{x(1-x)} \sum_{p_b^j, p_d^j \in \mathbf{Z}} e^{-S_{\text{inst.}}(x)}. \quad (5.83)$$

The three cases  $V_{abab}$ ,  $V_{abac}^{(0,0)}$  and  $V_{abcd}^{(0,0)}$ , which follow the classification (5.51), may be obtained from (5.83) by inserting the corresponding instanton actions (5.61), (5.72) and (5.76), respectively. Note, that in (5.83) the contributions of the poles  $x \rightarrow 0, 1$  cancel due to the relation  $\frac{1}{x(1-x)} = \frac{1}{x} + \frac{1}{1-x}$ . To conclude, in contrast to gluon scattering, the first string contact interaction appears already at the order  $\alpha'$ .

There is yet an other way of writing the expressions (5.60) and (5.70) following after a Poisson resummation on  $p_a$

$$V_{abac}^{(n_1, n_2)}(s, u) = \alpha' g_{D6_a}^2 \int_0^1 dx x^{s-1-\frac{n_1}{2}} (1-x)^{u-1-\frac{n_2}{2}} \left( \prod_{i=1}^3 K_{1;i}(x) K_{2;i}(x) \right)^{-1/2} \\ \times \sum_{p_b^j, \tilde{p}_a^j \in \mathbf{Z}} \prod_{j=1}^3 e^{2\pi i \tilde{p}_a^j \frac{\delta_a^j}{|L_a^j|}} e^{\pi i \left( \frac{1}{1-e^{2\pi i \theta^j}} - \frac{1}{1-e^{2\pi i \nu^j}} \right)} \alpha' (m_{ba}^j)^2 e^{-\pi \frac{\tau_j(x)}{\sin(\pi \theta^j)}} \alpha' (m_{ba}^j)^2, \quad (5.84)$$

with the mass  $m_{ba}$  of KK and winding modes, given in Eq. (5.50). If the longitudinal brane directions are somewhat greater than the string scale  $M_{\text{string}}$  the world–sheet instanton corrections are suppressed and the exponential sum in (5.84) may be ignored. In that case the four–fermion couplings are insensitive to how the D6–branes are wrapped around the compact space and they depend only on the local structure of the brane intersections encoded in the intersection angles  $\theta_i^j$ . In other words, the quantum part of (5.60), (5.70) and (5.79), given by the function  $I_j(x)$ , depends only on the angles  $\theta_i^j$  and the string scale  $M_{\text{string}}$  and is not sensitive to the scales of the internal space. In that case the four–fermion couplings may be written as sum over  $s$ –channel poles in lines of (2.6). The massive intermediate states exchanged are twisted states with masses of the order of  $M_{\text{string}}$ .

## 6. From Amplitudes to Parton Cross Sections

The purpose of this Section is to present the squared moduli of disk amplitudes derived in the previous Section, averaged over helicities and colors of the incident partons and summed over helicities and colors of the outgoing particles. In order to respect the notation and conventions used in experimental literature, which are rooted in the classic exposition of Björken and Drell, several steps have to be accomplished. The first one is to revert to the  $(+ - - -)$  metric signature. Furthermore, appropriate crossing operations have to be performed on the amplitudes, to ensure that the incident particles are always number 1 and 2 while the outgoing are number 3 and 4. They carry the initial four-momenta  $k_1, k_2$  and final four-momenta  $k_3, k_4$ , respectively, that satisfy the conservation law

$$k_1 + k_2 = k_3 + k_4 . \quad (6.1)$$

A generic process written as  $ef \rightarrow gh$  has the momenta assigned as  $e(k_1)f(k_2) \rightarrow g(k_3)h(k_4)$ . The kinematic invariants (Mandelstam variables) are defined in the standard way:

$$s = (k_1 + k_2)^2 = 2k_1k_2 , \quad t = (k_1 - k_3)^2 = -2k_1k_3 , \quad u = (k_1 - k_4)^2 = -2k_1k_4 . \quad (6.2)$$

They are constrained by

$$s + t + u = 0 , \quad (s > 0, t < 0, u < 0) . \quad (6.3)$$

Since in the previous Section, we implicitly used string mass units  $M_{\text{string}} \equiv M$  for the Mandelstam variables  $\hat{s}, \hat{t}, \hat{u}$ , and a metric of opposite signature, we need to redefine the universal string formfactor:

$$\hat{V} \rightarrow V(s, t, u) = \frac{su}{tM^2} B(-s/M^2, -u/M^2) = \frac{\Gamma(1 - s/M^2)\Gamma(1 - u/M^2)}{\Gamma(1 + t/M^2)} \quad (6.4)$$

and similarly

$$V_t = V(s, t, u) , \quad V_s = V(t \leftrightarrow s) , \quad V_u = V(t \leftrightarrow u) . \quad (6.5)$$

Now the low-energy expansions read

$$V(s, t, u) \approx 1 - \frac{\pi^2}{6} M^{-4} s u - \zeta(3) M^{-6} s t u + \dots \quad (6.6)$$

Similarly, we introduce the following functions describing the four-fermion amplitudes:

$$F(s, u) = \frac{s}{g_a^2} V_{abab}(-s/M^2, -u/M^2) \equiv F_{su} \quad (6.7)$$

$$G(s, u) = \frac{s}{g_a^2} V_{abac}(-s/M^2, -u/M^2) \equiv G_{su} \quad (6.8)$$

$$G'(s, u) = \frac{s}{g_a^2} V'_{abac}(-s/M^2, -u/M^2) \equiv G'_{su} \quad (6.9)$$

where  $V_{abab}$ ,  $V_{abac}$  and  $V'_{abac}$  are defined in Eqs. (5.60) and (5.71). The above functions depend on details of compactifications, therefore they are model-dependent. Note that the above redefinitions single out the QCD coupling  $g_a$  because it is the strongest coupling. Thus the results presented below coincide with the QCD predictions in the limit  $M \rightarrow \infty$ , *i.e.*  $V = F = G = G' = 1$ . The effects due to electro-weak forces can also be extracted, although with more care in taking this limit.

There are two basic operations performed when squaring the amplitudes and summing over colors and polarizations. First, the moduli squared of helicity amplitudes containing some spinor products (twistors) are expressed in terms of Mandelstam variables. This involves a repeated use of the following identities:<sup>17</sup>

$$\langle ij \rangle^* = [ji], \quad \langle ij \rangle [ji] = 2k_i k_j \quad (6.10)$$

$$\sum_{n \neq i, j} \langle in \rangle [nj] = 0 \quad (\text{momentum conservation}), \quad (6.11)$$

$$\langle ij \rangle \langle mn \rangle = \langle im \rangle \langle jn \rangle - \langle in \rangle \langle jm \rangle \quad (\text{Schouten's identity}). \quad (6.12)$$

The second operation is the summation over color indices. It depends on the representations of external particles, therefore we include it case by case in the following discussion of all parton scattering processes.

### 6.1. $gg \rightarrow gg$ , $gg \rightarrow gA$ , $gg \rightarrow AA$

The starting expression is Eq. (5.31) that holds for  $SU(N)$  gluons and  $U(1)$  vector bosons  $A$  coupled to the baryon number. In order to obtain the cross section for the (unpolarized) partonic subprocess  $gg \rightarrow gg$ , we take the squared moduli of individual amplitudes, sum over final polarizations and colors, and average over initial polarizations and colors. The following formulae are useful for summing over  $SU(N)$  colors:

$$\begin{aligned} \sum_{a_1, a_2, a_3} d^{a_1 a_2 a_3} d^{a_1 a_2 a_3} &= \frac{(N^2 - 1)(N^2 - 4)}{16N} \\ \sum_{a_1, a_2, a_3, a_4} d^{a_1 a_2 a_3 a_4} d^{a_1 a_2 a_3 a_4} &= \frac{(N^2 - 1)(N^4 - 6N^2 + 18)}{96N^2} \\ \sum_{a_1, a_2} f^{i_1 a_1 a_2} f^{i_2 a_1 a_2} &= N \delta^{i_1 i_2} \\ \sum_{a_1, a_2, a_3} f^{i_1 a_1 a_2} f^{i_2 a_2 a_3} f^{i_3 a_3 a_1} &= \frac{N}{2} f^{i_1 i_2 i_3} \end{aligned} \quad (6.13)$$

---

<sup>17</sup> It is worth mentioning that in the step of inverting the momenta from incoming to outgoing ones,  $k_3 \rightarrow -k_3$ ,  $k_4 \rightarrow -k_4 \implies 2k_1 k_3 \rightarrow -2k_1 k_3 = t$ ,  $2k_1 k_4 \rightarrow -2k_1 k_4 = u$ .



As an example, the modulus square of the amplitude (5.30), *summed* over initial and final colors, is:

$$|\mathcal{M}(g_1^-, g_2^-, g_3^+, g_4^+)|^2 = g^4(N^2 - 1) s^4 \times \left[ 2N^2 \left( \frac{V_t^2}{s^2 u^2} + \frac{V_s^2}{t^2 u^2} + \frac{V_u^2}{s^2 t^2} \right) + \frac{4(-N^2 + 3)}{N^2} \left( \frac{V_t}{s u} + \frac{V_s}{t u} + \frac{V_u}{s t} \right)^2 \right] \quad (6.14)$$

The modulus squared of the  $gg \rightarrow gg$  amplitude, summed over final polarizations and colors, and averaged over all  $4(N^2 - 1)^2$  possible initial polarization/color configurations, reads

$$|\mathcal{M}(gg \rightarrow gg)|^2 = g^4 \left( \frac{1}{s^2} + \frac{1}{t^2} + \frac{1}{u^2} \right) \times \left[ C(N)(s^2 V_s^2 + t^2 V_t^2 + u^2 V_u^2) + D(N)(s V_s + t V_t + u V_u)^2 \right], \quad (6.15)$$

where

$$C(N) = \frac{2N^2}{N^2 - 1}, \quad D(N) = \frac{4(-N^2 + 3)}{N^2(N^2 - 1)}. \quad (6.16)$$

Note that  $D(N)$  is of order  $\mathcal{O}(1/N^2)$  with respect to  $C(N)$ . Furthermore, the corresponding kinematic factor is suppressed in the low-energy limit at the rate  $\mathcal{O}(M^{-8})$  with respect to the leading QCD contribution which emerges from the first term (with  $C(N)$  factor), *c.f.* Eqs. (6.3) and (6.6). Thus the second term in Eq. (6.15) is suppressed in both large  $N$  and in low-energy limits.

The  $U(1)$  gauge bosons  $A$  can be produced by gluon fusion,  $gg \rightarrow gA$  and  $gg \rightarrow AA$ , the processes that appear at the disk level as a result of tree level couplings of gauge bosons to massive Regge excitations [21,22]. It is convenient to relax the normalization constraint on the  $U(1)$  generator:

$$T^{a_4} = Q_A \mathbb{I}_N \quad (6.17)$$

where  $\mathbb{I}_N$  is the  $N \times N$  identity matrix and  $Q_A$  is an arbitrary charge. In our conventions, the standard normalization corresponds to  $Q_A = 1/\sqrt{2N}$ . Then

$$d^{a_1 a_2 a_3 a_4} = Q_A d^{a_1 a_2 a_3} \quad (6.18)$$

and all non-Abelian structure constants drop out from Eq. (5.31). The corresponding helicity amplitudes can be obtained from the four-gluon amplitudes by the respective replacement of the color factors in Eqs. (5.31) *etc.* In this way, the averaged squared amplitudes become

$$|\mathcal{M}(gg \rightarrow gA)|^2 = 4g^4 \frac{(N^2 - 4)Q_A^2}{N(N^2 - 1)} \left( \frac{1}{s^2} + \frac{1}{t^2} + \frac{1}{u^2} \right) (s V_s + t V_t + u V_u)^2 \quad (6.19)$$

$$|\mathcal{M}(gg \rightarrow AA)|^2 = 16g^4 \frac{Q_A^4}{N^2 - 1} \left( \frac{1}{s^2} + \frac{1}{t^2} + \frac{1}{u^2} \right) (s V_s + t V_t + u V_u)^2. \quad (6.20)$$

In the low-energy limit, the Abelian gauge boson production rates (6.19) and (6.20) are of order  $\mathcal{O}(M^{-8})$  compared to the gluon production. However, they can be larger than QCD rates in the string resonance region [21,22].

6.2.  $gg \rightarrow q\bar{q}$ ,  $gq \rightarrow gq$ ,  $gq \rightarrow qA$ ,  $gq \rightarrow qB$ ,  $q\bar{q} \rightarrow gg$ ,  $q\bar{q} \rightarrow gA$ ,  $q\bar{q} \rightarrow gB$

All non-vanishing helicity amplitudes involving two quarks and two gauge bosons can be obtained by appropriate crossing operations from Eqs. (5.39) and (5.40). The squared moduli of these amplitudes, *summed* over initial and final gauge indices, read:

$$|\mathcal{M}(g_1^-, g_2^+, q_3^-, \bar{q}_4^+)|^2 = 4g_a^4 N_b \left[ \sum_{a_1, a_2} \text{Tr}(T^{a_1} T^{a_1} T^{a_2} T^{a_2}) \frac{t}{us^2} (tV_t + uV_u)^2 - \frac{1}{2} \sum_{a_1, a_2, i} f^{a_1 a_2 i} f^{a_1 a_2 i} \frac{t^2}{s^2} V_t V_u \right], \quad (6.21)$$

$$|\mathcal{M}(g_1^-, B_2^+, q_3^-, \bar{q}_4^+)|^2 = 4g_a^2 g_b^2 \sum_{a, b} \text{Tr}(T^a T^a) \text{Tr}(T^b T^b) \frac{t}{u} V_s^2. \quad (6.22)$$

The above expressions are written in a form suitable for non-Abelian as well as Abelian gauge bosons. In the latter case, the second term drops out from Eq. (6.21).

As an example, consider the gluon fusion  $gg \rightarrow q\bar{q}$ . In this case, the following identity is used for summing over the color indices:

$$\sum_a T^a T^a = \frac{N^2 - 1}{2N} \mathbb{I}_N. \quad (6.23)$$

This process takes place entirely on the QCD stack  $a$  while stack  $b$  is a spectator and its only effect is to supply the overall factor  $N_b$  in Eq. (6.21). Note that summing over quark helicities requires some attention because left- and right-handed quarks originate from different stacks. We will handle this by adding contributions from both stacks, with the net result of doubling the square of the chiral amplitude (6.21) and replacing  $N_b$  by the number of flavors  $N_f$ .<sup>18</sup> We will also apply this procedure to other channels of the same reaction. The squared modulus of the corresponding amplitude, summed over final polarizations and colors, and averaged over all  $4(N^2 - 1)^2$  initial polarization/color configurations, is

$$|\mathcal{M}(gg \rightarrow q\bar{q})|^2 = g^4 \frac{N_f}{2N} \left[ \frac{t^2 + u^2}{uts^2} (tV_t + uV_u)^2 - \frac{2N^2}{(N^2 - 1)} \frac{t^2 + u^2}{s^2} V_t V_u \right], \quad (6.24)$$

The hadroproduction of  $B$  vector bosons from a non-QCD stack  $b$  involves at least one incoming quark or antiquark. We average over  $N_b$  species of each of them. We also sum over all  $N_b^2 - 1$   $SU(N_b)$   $B$ -bosons; depending on the model, we can always add the  $U(1)_b$  boson by hand. Since  $B$ -bosons couple to chiral quarks, we do *not* add initial quarks of opposite helicity because they are coupled to other stacks. Thus in order to average the  $B$  production rates over incident helicities, we simply divide by the number of available initial helicity configurations. All amplitudes obtained by using Eqs. (6.21) and (6.22) are collected in Tables 5-8.

---

<sup>18</sup> Note that summing over vector boson helicities amounts to adding ( $t \leftrightarrow u$ ) terms to the r.h.s. of Eqs. (6.21) and (6.22).

### 6.3. $qq \rightarrow qq$ , $q\bar{q} \rightarrow q\bar{q}$

These amplitudes are more complicated for several reasons. Their computations are sensitive to left-right asymmetry of the SM, *i.e.* to the fact that different helicity states come in different gauge group representations, originating from strings stretching between distinct stacks of D-branes. Furthermore, by construction, the intermediate channels of quark scattering processes include all  $N^2$  gauge bosons of each  $U(N)$ , therefore  $SU(N)$  gauge bosons, as well as their string and KK excitations, must be separated “by hand” from their  $U(1)$  counterparts. Whenever this problem is encountered, we will implement the following identity on the group factors:

$$\delta_{\alpha_2}^{\alpha_1} \delta_{\alpha_4}^{\alpha_3} = 2 \sum_a (T^a)_{\alpha_4}^{\alpha_1} (T^a)_{\alpha_2}^{\alpha_3} + 2 Q_A^2 \delta_{\alpha_4}^{\alpha_1} \delta_{\alpha_2}^{\alpha_3}, \quad (6.25)$$

where the sum is over all  $SU(N)$  generators of  $N$ -color QCD and  $Q_A = 1/\sqrt{2N}$ . Note that due to Fierz identity,

$$\langle 13 \rangle [24] = \frac{1}{2} \sum_{\mu} (u_1 \sigma_{\mu} \bar{u}_2) (\bar{u}_4 \bar{\sigma}^{\mu} u_3) = -\frac{1}{2} \sum_{\mu} (u_1 \sigma_{\mu} \bar{u}_4) (\bar{u}_2 \bar{\sigma}^{\mu} u_3), \quad (6.26)$$

the factor  $\langle 13 \rangle [24]$  can be interpreted as arising from the exchange of intermediate vector bosons in either  $s$  or  $u$  channels, depending on the nature of accompanying kinematic singularity.

If the amplitude involves left-handed quarks and right-handed antiquarks only,  $q^-$  and  $\bar{q}^+$ , respectively, then all fermions come from one intersection, say of stack  $a$  and stack  $b$ . The corresponding amplitude reads:

$$\begin{aligned} \mathcal{M}[q_{\beta_1}^{\alpha_1}(1-) \bar{q}_{\alpha_2}^{\beta_2}(2+) q_{\beta_3}^{\alpha_3}(3-) \bar{q}_{\alpha_4}^{\beta_4}(4+)] &= 4 g_a^2 \langle 13 \rangle [24] \\ &\times \left( \frac{F_{su}}{s} \sum_{a,b} \left[ (T^a)_{\alpha_2}^{\alpha_1} (T^a)_{\alpha_4}^{\alpha_3} + Q_A^2 \delta_{\alpha_2}^{\alpha_1} \delta_{\alpha_4}^{\alpha_3} \right] \times \left[ (T^b)_{\beta_1}^{\beta_4} (T^b)_{\beta_3}^{\beta_2} + Q_B^2 \delta_{\beta_1}^{\beta_4} \delta_{\beta_3}^{\beta_2} \right] \right. \\ &\left. + \frac{F_{us}}{u} \sum_{a,b} \left[ (T^a)_{\alpha_4}^{\alpha_1} (T^a)_{\alpha_2}^{\alpha_3} + Q_A^2 \delta_{\alpha_4}^{\alpha_1} \delta_{\alpha_2}^{\alpha_3} \right] \times \left[ (T^b)_{\beta_1}^{\beta_2} (T^b)_{\beta_3}^{\beta_4} + Q_B^2 \delta_{\beta_1}^{\beta_2} \delta_{\beta_3}^{\beta_4} \right] \right), \end{aligned} \quad (6.27)$$

where the functions  $F_{su} = F(s, u)$  and  $F_{us} = F(u, s)$  are defined in Eq. (6.7). The most important difference between the above amplitude and the amplitudes involving gauge bosons is that its intermediate channels include not only massless particles and their string (Regge) excitations, but also KK excitations and winding modes associated to the extra dimensions spanned by intersecting D-branes. Even in the limit  $M \rightarrow \infty$ , the function  $F(s, u)$  contains, in addition to the poles due to intermediate gauge bosons, an infinite number of poles associated to such massive particles. In fact,  $F(s, u)$  encompasses

the effects of gauge bosons from both stacks  $a$  and  $b$ , as reflected by the residues of its massless poles,

$$(s \rightarrow 0, u \rightarrow 0, t \rightarrow 0) : F(s, u) \approx 1 + \frac{g_b^2 s}{g_a^2 u}, \quad (6.28)$$

and of all their excitations.

In order to explain how Eqs. (6.25) and (6.26) are useful for the interpretation of kinematic poles, let us extract from the amplitude (6.27) the singularities associated to intermediate gluons, coming from the limit  $g_b \rightarrow 0$  in Eq. (6.28), in which the strength of other interactions is negligible:

$$(s \rightarrow 0, u \rightarrow 0, t \rightarrow 0) : F_{su} \approx F_{us} \approx 1. \quad (6.29)$$

To be precise, it is the  $M \rightarrow \infty$  (string zero slope) limit, with the additional assumption that  $g_b \ll g_a = g$ . Then stack  $b$  is a spectator, therefore we should use Eq. (6.25) to revert the factors involving  $G_b$  generators back to their original form. Furthermore, we rewrite the kinematic factor by using Eq. (6.26) in order to exhibit a  $s$ -channel vector exchange in the first term of Eq. (6.27) and a  $u$ -channel vector boson exchange in the second term. As a result, the amplitude becomes

$$\begin{aligned} \mathcal{M}[q_{\beta_1}^{\alpha_1}(1-) \bar{q}_{\alpha_2}^{\beta_2}(2+) q_{\beta_3}^{\alpha_3}(3-) \bar{q}_{\alpha_4}^{\beta_4}(4+)] \rightarrow \\ \frac{g^2}{s} \sum_{\mu, a} (u_1 \sigma_\mu \bar{u}_2) (\bar{u}_4 \bar{\sigma}^\mu u_3) \left[ (T^a)_{\alpha_2}^{\alpha_1} (T^a)_{\alpha_4}^{\alpha_3} + Q_A^2 \delta_{\alpha_2}^{\alpha_1} \delta_{\alpha_4}^{\alpha_3} \right] \delta_{\beta_1}^{\beta_2} \delta_{\beta_3}^{\beta_4} \\ - \frac{g^2}{u} \sum_{\mu, a} (u_1 \sigma_\mu \bar{u}_4) (\bar{u}_2 \bar{\sigma}^\mu u_3) \left[ (T^a)_{\alpha_4}^{\alpha_1} (T^a)_{\alpha_2}^{\alpha_3} + Q_A^2 \delta_{\alpha_4}^{\alpha_1} \delta_{\alpha_2}^{\alpha_3} \right] \delta_{\beta_1}^{\beta_4} \delta_{\beta_3}^{\beta_2} \end{aligned} \quad (6.30)$$

which does indeed reproduce the well-known QCD result after setting  $Q_A = 0$ , *i.e.* subtracting the unwanted contribution of the  $U(1)$  gauge boson  $A$ .

The squared modulus of the amplitude (6.27), *summed* over initial and final gauge indices, is

$$\begin{aligned} |\mathcal{M}(q_1^-, \bar{q}_2^+, q_3^-, \bar{q}_4^+)|^2 = g^4 K(N_a) K(N_b) \left( \frac{t^2 F_{su}^2}{s^2} + \frac{t^2 F_{us}^2}{u^2} \right) \\ + 2 g^4 L(N_a) L(N_b) \frac{t^2}{su} F_{su} F_{us} \end{aligned} \quad (6.31)$$

where

$$\begin{aligned} K(N) &= N^2 - 1 + 4Q^4 N^2 \\ L(N) &= \frac{(1 - N^2)}{N} + 4Q^2(N^2 - 1) + 4Q^4 N \end{aligned} \quad (6.32)$$

The charges  $Q$  should be adjusted in certain regions of parameter space and/or kinematic limits. For instance, in the QCD limit (6.29), with  $g_b \ll g$ , the appropriate choice is  $Q_A = 0$

[ $U(1)$  component eliminated] and  $Q_B = 1/\sqrt{2N_b}$  (stack  $b$  treated as spectator). Note that  $N_a = N$  for  $N$ -color QCD and  $N_b = 2$  for one [electroweak  $SU(2)$ ] quark doublet. Thus

$$K(N_a)K(N_b) = (N^2 - 1)N_b^2, \quad L(N_a)L(N_b) = -\frac{(N^2 - 1)}{N}N_b, \quad (6.33)$$

and Eq. (6.31) becomes

$$|\mathcal{M}(q_1^-, \bar{q}_2^+, q_3^-, \bar{q}_4^+)|^2 \xrightarrow{\text{QCD}} g^4 \left[ (N^2 - 1)N_b^2 \left( \frac{t^2}{s^2} + \frac{t^2}{u^2} \right) - 2\frac{(N^2 - 1)}{N}N_b \frac{t^2}{su} \right], \quad (6.34)$$

which could be obtained directly from Eq. (6.30). In some cases however, it is more appropriate to consider the cases of identical and different flavors [ $SU(2)$  doublet components] separately, instead of summing over them. Then Eqs. (6.27) and (6.31) can be easily disentangled into the contributions describing  $(u\bar{u}u\bar{u})$ ,  $(d\bar{d}d\bar{d})$ ,  $(u\bar{u}u\bar{u})$  and  $(d\bar{d}d\bar{d})$ .

There are five more helicity configuration that remain to be included in unpolarized cross sections. The amplitude with the helicity assignments reversed with respect to (6.27) ( $+ \leftrightarrow -$ ) is very similar because it involves right-handed quarks and left-handed antiquarks originating from one intersection (of the QCD stack  $a$  with one of  $U(1)$  stacks,  $c$  or  $d$ ), provided that all quarks are of the same flavor. For each flavor, one obtains the same result as on the r.h.s. of Eq. (6.31), with  $N_a = N$  and  $N_b = 1$ , although the function  $F$  is associated now to a different intersection<sup>19</sup>. If the flavors are different, then the amplitude falls into the category discussed below, because it couples the QCD stack to two other stacks and the disk boundary connects three different stacks. Then the function  $F$  has to be replaced by  $G$  defined in Eq. (6.8).

The four remaining helicity configurations fall into one class. They involve  $SU(2)$  doublets and singlets at the same time, therefore they mix the QCD stack with two other stacks:  $SU(2)$  stack  $b$  and one of  $U(1)$  stacks, say  $c$ . The corresponding helicity amplitudes contain massless poles in only one channel, due to intermediate gluons and the  $A$ -boson. They are:

$$\begin{aligned} \mathcal{M}[q_{\beta_1}^{\alpha_1}(1-) \bar{q}_{\alpha_2}^{\beta_2}(2+) q_{\gamma_3}^{\alpha_3}(3+) \bar{q}_{\alpha_4}^{\gamma_4}(4-)] &= 2 g_a^2 \delta_{\beta_1}^{\beta_2} \delta_{\gamma_3}^{\gamma_4} \langle 14 \rangle [23] \\ &\times \frac{G'_{su}}{s} \sum_a \left[ (T^a)_{\alpha_2}^{\alpha_1} (T^a)_{\alpha_4}^{\alpha_3} + Q_A^2 \delta_{\alpha_2}^{\alpha_1} \delta_{\alpha_4}^{\alpha_3} \right] \end{aligned} \quad (6.35)$$

$$\begin{aligned} \mathcal{M}[q_{\beta_1}^{\alpha_1}(1-) \bar{q}_{\alpha_2}^{\gamma_2}(2-) q_{\gamma_3}^{\alpha_3}(3+) \bar{q}_{\alpha_4}^{\beta_4}(4+)] &= 2 g_a^2 \delta_{\beta_1}^{\beta_4} \delta_{\gamma_3}^{\gamma_2} \langle 12 \rangle [34] \\ &\times \frac{G'_{us}}{u} \sum_a \left[ (T^a)_{\alpha_4}^{\alpha_1} (T^a)_{\alpha_2}^{\alpha_3} + Q_A^2 \delta_{\alpha_4}^{\alpha_1} \delta_{\alpha_2}^{\alpha_3} \right], \end{aligned} \quad (6.36)$$

---

<sup>19</sup> It is defined as in Eq. (6.7), but starting from  $V_{acac}$  or  $V_{adad}$ .

and the two amplitudes describing the helicity configurations reversed by  $(+ \leftrightarrow -)$ . These can be obtained from the above by the permutation  $(1 \leftrightarrow 3, 2 \leftrightarrow 4)$ , with the net effect of complex conjugation. The functions  $G'_{su} = G'(s, u)$  and  $G'_{us} = G'(u, s)$  are defined in Eq. (6.9). Recall that their low-energy expansions have the form  $G(s, u) \approx G'(s, u) \approx 1 + \mathcal{O}(M^{-2})$ .

The squared moduli of the amplitudes (6.35) and (6.36), *summed* over initial and final gauge indices are, respectively:

$$|\mathcal{M}(q_1^-, \bar{q}_2^+, q_3^+, \bar{q}_4^-)|^2 = g^4 K(N_a) N_b \frac{u^2}{s^2} G'^2_{su}, \quad (6.37)$$

$$|\mathcal{M}(q_1^-, \bar{q}_2^-, q_3^+, \bar{q}_4^+)|^2 = g^4 K(N_a) N_b \frac{s^2}{u^2} G'^2_{us}. \quad (6.38)$$

where we set  $g_a = g$  and  $N_c = 1$ . The factor  $N_b = 2$  takes combines the cases of same and different components (flavors) of the  $SU(2)$  doublet which can be easily disentangled if flavor summation or averaging is not desirable. We should also set

$$K(N_a) = N^2 - 1 \quad (6.39)$$

in order to eliminate the contributions of intermediate color singlets.

At this point, we have all ingredients at hand, ready for writing down the squared amplitudes for quark-quark scattering and quark-antiquark annihilation, averaged over the polarizations, colors of the incident particles, and summed over the polarizations, colors of the outgoing quarks and antiquarks. We will consider the cases of identical and different flavors separately. The sum over helicity configurations combines disk diagrams with various stack configurations along the boundary, with the QCD stack  $a$  repeating two times and the two other being either  $b$  [electroweak  $SU(2)$ ],  $c$  (right-handed  $u$  quark) or  $c'$  (right-handed  $d$  quark). We distinguish functions  $F$  associated to disk diagram with two  $b$  stacks, two  $c$  stacks or two  $c'$  stacks as  $F^{bb}$ ,  $F^{cc}$  and  $F^{c'c'}$ , respectively, see Eq. (6.7). Similarly,  $G$  and  $G'$  need indication of two non-QCD stacks. Thus we define  $G^{cc'}$ , by Eq. (6.8) with  $V_{acac'}$  etc.

By adding all helicity configurations contributing to unpolarized quark-quark scattering, we obtain the following squared amplitudes:

$$\begin{aligned} |\mathcal{M}(qq \rightarrow qq)|^2 &= g^4 \left( \frac{N^2 - 1}{4N^2} \right) \frac{1}{t^2} \left[ (sF_{tu}^{bb})^2 + (sF_{tu}^{cc})^2 + (uG_{tu}^{'bc})^2 + (uG_{tu}^{'cb})^2 \right] \\ &+ g^4 \left( \frac{N^2 - 1}{4N^2} \right) \frac{1}{u^2} \left[ (sF_{ut}^{bb})^2 + (sF_{ut}^{cc})^2 + (tG_{ut}^{'bc})^2 + (tG_{ut}^{'cb})^2 \right] \\ &- g^4 \left( \frac{N^2 - 1}{2N^3} \right) \frac{s^2}{tu} (F_{tu}^{bb} F_{ut}^{bb} + F_{tu}^{cc} F_{ut}^{cc}) \end{aligned} \quad (6.40)$$

for identical flavors and

$$|\mathcal{M}(qq' \rightarrow qq')|^2 = g^4 \left( \frac{N^2 - 1}{4N^2} \right) \frac{1}{t^2} \left[ (s F_{tu}^{bb})^2 + (s G_{tu}^{cc'})^2 + (u G_{tu}^{'bc})^2 + (u G_{tu}^{'bc'})^2 \right] \quad (6.41)$$

for different flavors. Similarly, for quark-antiquark annihilation:

$$|\mathcal{M}(q\bar{q} \rightarrow q\bar{q})|^2 = |\mathcal{M}(qq \rightarrow qq)|^2 (s \rightarrow u, u \rightarrow t, t \rightarrow s) \quad (6.42)$$

$$|\mathcal{M}(q\bar{q}' \rightarrow q\bar{q}')|^2 = |\mathcal{M}(qq' \rightarrow qq')|^2 (s \leftrightarrow u) \quad (6.43)$$

$$|\mathcal{M}(q\bar{q} \rightarrow q'\bar{q}')|^2 = |\mathcal{M}(qq' \rightarrow qq')|^2 (s \rightarrow u, u \rightarrow t, t \rightarrow s). \quad (6.44)$$

#### 6.4. $q\bar{q} \rightarrow l\bar{l}$

The disk amplitudes involving four D-brane stacks do not contribute to  $2 \rightarrow 2$  parton scattering processes, at least in the simplest realizations of intersecting D-brane scenarios. They are relevant though to the Drell-Yan process  $q\bar{q} \rightarrow l\bar{l}$ . The relevant amplitude is

$$\mathcal{M}[q_{\beta_1}^{\alpha_1}(1-) \bar{q}_{\alpha_2}^{\gamma_2}(2-) l_{\gamma_3}^{\delta_3}(3+) \bar{l}_{\delta_4}^{\beta_4}(4+)] = \delta_{\alpha_2}^{\alpha_1} \delta_{\beta_1}^{\beta_4} \delta_{\gamma_3}^{\gamma_2} \delta_{\delta_4}^{\delta_3} \langle 12 \rangle [34] V_{abcd}(s, u), \quad (6.45)$$

with the function  $V_{abcd}(s, u)$  is defined in Eq. (5.79). The low-energy expansion of this amplitude is free of kinematic singularities and begins at the order  $\mathcal{O}(M^{-2})$ . For this process, there are also helicity amplitudes receiving contributions from three stacks, as already discussed in the context of quark-quark scattering:

$$\begin{aligned} \mathcal{M}[q_{\beta_1}^{\alpha_1}(1-) \bar{q}_{\alpha_2}^{\beta_2}(2+) l_{\beta_3}^{\gamma_3}(3-) \bar{l}_{\gamma_4}^{\beta_4}(4+)] &= 2\delta_{\alpha_2}^{\alpha_1} \delta_{\gamma_4}^{\gamma_3} \langle 13 \rangle [24] \\ &\times V_{babc}(s, u) \sum_b \left[ (T^b)_{\beta_2}^{\beta_1} (T^b)_{\beta_4}^{\beta_3} + Q_B^2 \delta_{\beta_2}^{\beta_1} \delta_{\beta_4}^{\beta_3} \right]. \end{aligned} \quad (6.46)$$

It is clear from the above expressions, especially from Eq. (6.46) which includes all gauge bosons exchanged in the  $s$ -channel, that the amplitudes involving leptons are sensitive to the implementation of electro-weak symmetry breaking mechanism in string theory. Since it is a model-dependent problem, we stop short from computing the production rates (averaged squared moduli) for such processes.

### 6.5. Tables

In the Tables below, we collect the squared amplitudes for all parton subprocesses discussed in this Section, summed over the polarizations and colors of final particles and averaged over the polarizations and colors of incident partons. The number of colors has been set to  $N = 3$ . Recall that  $A$  denotes the  $U(1)$  gauge boson from the QCD stack, *i.e.* the “quiver neighbor” of  $SU(3)$  gluons. The corresponding coupling  $Q_A = 1/\sqrt{6}$  is displayed explicitly. Furthermore,  $B$  is a generic (massless) gauge boson from another stack, for example a  $SU(2)$  boson. We assumed that  $B$  couples to left-handed quarks only; the generalization to a left-right symmetric vector coupling is straightforward. We factored out the QCD coupling factor  $g^4$ . Thus in the amplitudes involving  $B$  vector bosons, marked with (\*), this factor should be corrected to  $g^2 g_B^2$ , where  $g_B$  denotes the coupling of  $B$  gauge group. In these amplitudes,  $T_{q\bar{q}'}^B$  denotes the  $(q\bar{q}')$  matrix element of the corresponding group generator. The  $SU(3) \times SU(2) \times U(1)$  SM limit of the amplitudes, with  $V = F = G = G' = 1$  as  $s \ll M^2$ , is in agreement with Table 9.1 of [56].

**Table 5:** *Gluon fusion processes.*

subprocess	$ \mathcal{M} ^2/g^4$
$gg \rightarrow gg$	$\left(\frac{1}{s^2} + \frac{1}{t^2} + \frac{1}{u^2}\right) \left[ \frac{9}{4}(s^2 V_s^2 + t^2 V_t^2 + u^2 V_u^2) - \frac{1}{3}(sV_s + tV_t + uV_u)^2 \right]$
$gg \rightarrow gA$	$\frac{5}{6} Q_A^2 \left(\frac{1}{s^2} + \frac{1}{t^2} + \frac{1}{u^2}\right) (sV_s + tV_t + uV_u)^2$
$gg \rightarrow AA$	$2 Q_A^4 \left(\frac{1}{s^2} + \frac{1}{t^2} + \frac{1}{u^2}\right) (sV_s + tV_t + uV_u)^2$
$gg \rightarrow q\bar{q}$	$\frac{t^2 + u^2}{s^2} \left[ \frac{1}{6} \frac{1}{ut} (tV_t + uV_u)^2 - \frac{3}{8} V_t V_u \right]$



**Table 6:** *Gluon-quark scattering.*

subprocess	$ \mathcal{M} ^2/g^4$
$gq \rightarrow gq$	$\frac{s^2 + u^2}{t^2} \left[ V_s V_u - \frac{4}{9} \frac{1}{su} (sV_s + uV_u)^2 \right]$
$gq \rightarrow Aq$	$-\frac{1}{3} Q_A^2 \frac{s^2 + u^2}{sut^2} (sV_s + uV_u)^2$
$gq \rightarrow Bq'$	$-\frac{1}{6}  T_{q\bar{q}'}^B ^2 \frac{s^2 + u^2}{su} V_t^2 \quad (*)$

**Table 7:** *Quark-quark scattering.*

subprocess	$ \mathcal{M} ^2/g^4$
$qq \rightarrow qq$	$\frac{2}{9} \frac{1}{t^2} \left[ (sF_{tu}^{bb})^2 + (sF_{tu}^{cc})^2 + (uG_{tu}^{bc})^2 + (uG_{tu}^{cb})^2 \right]$ $+ \frac{2}{9} \frac{1}{u^2} \left[ (sF_{ut}^{bb})^2 + (sF_{ut}^{cc})^2 + (tG_{ut}^{bc})^2 + (tG_{ut}^{cb})^2 \right] - \frac{4}{27} \frac{s^2}{tu} (F_{tu}^{bb} F_{ut}^{bb} + F_{tu}^{cc} F_{ut}^{cc})$
$qq' \rightarrow qq'$	$\frac{2}{9} \frac{1}{t^2} \left[ (sF_{tu}^{bb})^2 + (sG_{tu}^{cc'})^2 + (uG_{tu}^{bc})^2 + (uG_{tu}^{bc'})^2 \right]$

**Table 8:** *Quark-antiquark annihilation.*

subprocess	$ \mathcal{M} ^2/g^4$
$q\bar{q} \rightarrow gg$	$\frac{8}{3} \frac{t^2 + u^2}{s^2} \left[ \frac{4}{9} \frac{1}{ut} (tV_t + uV_u)^2 - V_t V_u \right]$
$q\bar{q} \rightarrow gA$	$\frac{8}{9} Q_A^2 \frac{t^2 + u^2}{tus^2} (tV_t + uV_u)^2$
$q\bar{q} \rightarrow AA$	$\frac{2}{3} Q_A^4 \frac{t^2 + u^2}{tus^2} (tV_t + uV_u)^2$
$q\bar{q}' \rightarrow gB$	$\frac{4}{9}  T_{q\bar{q}'}^B ^2 \frac{t^2 + u^2}{tu} V_s^2 \quad (*)$
$q\bar{q}' \rightarrow BA$	$\frac{1}{3}  T_{q\bar{q}'}^B ^2 Q_A^2 \frac{t^2 + u^2}{tu} V_s^2 \quad (*)$
$q\bar{q} \rightarrow q\bar{q}$	$ \mathcal{M}(q\bar{q} \rightarrow q\bar{q}) ^2 =  \mathcal{M}(qq \rightarrow qq) ^2 (s \rightarrow u, u \rightarrow t, t \rightarrow s)$
$q\bar{q}' \rightarrow q\bar{q}'$	$ \mathcal{M}(q\bar{q}' \rightarrow q\bar{q}') ^2 =  \mathcal{M}(qq' \rightarrow qq') ^2 (s \leftrightarrow u)$
$q\bar{q} \rightarrow q'\bar{q}'$	$ \mathcal{M}(q\bar{q} \rightarrow q'\bar{q}') ^2 =  \mathcal{M}(qq' \rightarrow qq') ^2 (s \rightarrow u, u \rightarrow t, t \rightarrow s)$

## 7. Summary

This article is intended to provide some information useful in the upcoming searches for the signals of string physics at the LHC, assuming that the fundamental scale determining the masses of string excitations is of order few TeVs. While on the theoretical side, low mass scenarios face many challenges, it is an experimental question whether string theory describes the physics beyond the SM. Needless to say, since low mass strings require the existence of large extra dimensions, the discovery of fundamental strings at the LHC would revolutionize our understanding of space and time.

The search for string signals should focus on Regge excitations i.e. the resonances created by vibrating strings. The main message of this work is that string theory provides very clear, model-independent, universal predictions not only for the masses and spins of these particles<sup>20</sup>, but also for their couplings to gluons and quarks. These predictions do not depend on details of compactification, D-brane configurations and hold even if supersymmetry is broken in four dimensions. The reason why certain amplitudes are universal, independent of the spectrum of Kaluza–Klein excitations is very simple. At the disk level, the gluon scattering amplitudes involve only one stack of D-branes, thus the momentum components along the compactified D-brane directions are conserved and as a consequence, Kaluza–Klein states carrying such momenta cannot appear as intermediate states. From all  $2 \rightarrow 2$  parton scattering amplitudes, only four-fermion processes are model-dependent, but these are suppressed by group-theoretical factors and usually occur at luminosities lower than gluon collisions. The model-dependence of these amplitudes, and also the necessity to avoid FCNC’s or proton decay via four-fermion amplitudes, could be useful for some “precision tests” that would distinguish between various compactification scenarios.

The resonant character of parton cross sections should not be difficult to observe. In Refs. [21] and [22], the process  $gg \rightarrow g\gamma$ , which is absent in the SM at the tree-level, but appears in string theory as a QCD process involving strongly interacting resonances, has been examined to that effect. It turns out that a string mass as high as 3 TeV is observable in this process. More recently [24], we examined the dijet invariant mass spectrum which is sensitive to even higher mass scales. The resonant behavior of stringy cross section at the parton center of mass energies equal to the masses of Regge states is a signal that cannot be missed at the LHC, unless the string scale is too high or the theory does not describe the physics beyond the SM correctly.

We have computed the full-fledged string four-particle scattering amplitudes for the SM fields, as they occur at the (leading) disk level in a large class of orientifold compactifications on an internal manifold with large volume and low string scale. The SM fields

---

<sup>20</sup> The decay widths of lowest Regge recurrences have been recently computed in Ref. [57].

arise in these models as open strings ending on a set of intersecting D-branes. Here are the basic characteristics of these amplitudes:

(i) *Two gluon/two SM gauge boson processes:*

These amplitudes are given in terms of one kinematic function  $V(s, t, u)$ , given in (6.5), and can be computed in a completely model independent way. The poles of  $V(s, t, u)$  are due to the exchange of massless SM gauge bosons and heavy string Regge excitations. In some particular processes, like  $gg \rightarrow gY$  or  $gg \rightarrow YY$  ( $Y = \gamma, Z_0$ ), the poles due to massless gauge bosons are absent, and the leading contribution originates from heavy string states.

(ii) *Two SM gauge boson/two SM fermion processes:*

As before these processes can be computed in a completely model independent way and are given in terms of the same function  $V(s, t, u)$ . Hence they receive contributions from the exchange of SM gauge bosons and heavy string excitations. We find that low scale string theory at the LHC leads to model independent string contributions to processes such as  $q\bar{q} \rightarrow gW^\pm$  or  $q\bar{q} \rightarrow gZ$ , which should be a clear signal for new physics. Likewise, exchanges of Regge excitations contribute to processes like  $gq \rightarrow qW^\pm$  and  $gq \rightarrow qZ$  in a model independent way.

(iii) *Four SM fermion processes:*

The four quark or two quark/two lepton amplitudes like the Drell–Yan process  $q\bar{q} \rightarrow l\bar{l}$  are model-dependent and can be expressed in terms of three functions,  $V_{abab}(s, u)$ ,  $V_{abac}(s, u)$  and  $V_{abcd}(s, u)$ , given in (5.60), (5.71) and (5.79), respectively. In general, the latter depend on the string scale and on the parameters describing the internal manifold and the cycles around which D-branes are wrapped. Here one finds poles not only due to exchanges of SM gauge bosons and Regge excitations thereof, but also poles due to internal Kaluza–Klein and winding modes, and open string states with masses depending on the intersection angles.

All parton subprocesses receive string contributions which should be separable from the SM background if the string scale is not too high.

The squared amplitudes, summed over the polarizations and colors of final particles and averaged over the polarizations and colors of incident partons, are collected in Tables 5–8. They are presented in a form suitable for the computations of the respective cross sections and are ready to be implemented in the LHC data analysis.

## Acknowledgments

We wish to thank Michael Peskin and Andreas Ringwald for inspiring discussions. We are grateful to Luis Anchordoqui, Haim Goldberg and Satoshi Nawata for their collaboration on Ref. [24]. We also thank Ignatios Antoniadis for his permission to use Figure 1. Most of other diagrams have been created by the program JaxoDraw [58]. This work is supported in part by the European Commission under Project MRTN-CT-2004-005104. St.St. thanks the Theory Division of CERN for hospitality and financial support during preparation of this work. The research of T.R.T. is supported in part by the U.S. National Science Foundation Grants PHY-0600304 and PHY-0757959, and by the Cluster of Excellence “Origin and Structure of the Universe” in München, Germany. He is grateful to Arnold Sommerfeld Center for Theoretical Physics at Ludwig–Maximilians–Universität, and to Max–Planck–Institut für Physik in München, for their kind hospitality. Any opinions, findings, and conclusions or recommendations expressed in this material are those of the authors and do not necessarily reflect the views of the National Science Foundation.

## References

- [1] N. Arkani-Hamed, S. Dimopoulos and G.R. Dvali, “The hierarchy problem and new dimensions at a millimeter,” *Phys. Lett. B* **429**, 263 (1998) [arXiv:hep-ph/9803315].
- [2] I. Antoniadis, N. Arkani-Hamed, S. Dimopoulos and G.R. Dvali, “New dimensions at a millimeter to a Fermi and superstrings at a TeV,” *Phys. Lett. B* **436**, 257 (1998) [arXiv:hep-ph/9804398].
- [3] D.M. Ghilencea, L.E. Ibanez, N. Irges and F. Quevedo, “TeV-scale Z’ bosons from D-branes,” *JHEP* **0208**, 016 (2002) [arXiv:hep-ph/0205083].
- [4] S.A. Abel, M.D. Goodsell, J. Jaeckel, V.V. Khoze and A. Ringwald, “Kinetic Mixing of the Photon with Hidden U(1)s in String Phenomenology,” arXiv:0803.1449 [hep-ph].
- [5] G.T. Horowitz and J. Polchinski, “A correspondence principle for black holes and strings,” *Phys. Rev. D* **55** 6189 (1997) [arXiv:hep-th/9612146].
- [6] P. Meade and L. Randall, “Black Holes and Quantum Gravity at the LHC,” *JHEP* **0805**, 003 (2008) [arXiv:0708.3017 [hep-ph]].
- [7] S. Cullen, M. Perelstein and M.E. Peskin, “TeV strings and collider probes of large extra dimensions,” *Phys. Rev. D* **62**, 055012 (2000) [arXiv:hep-ph/0001166].
- [8] D. Oprisa and S. Stieberger, “Six gluon open superstring disk amplitude, multiple hypergeometric series and Euler-Zagier sums,” arXiv:hep-th/0509042.
- [9] S. Stieberger and T.R. Taylor, “Amplitude for N-gluon superstring scattering,” *Phys. Rev. Lett.* **97**, 211601 (2006) [arXiv:hep-th/0607184].
- [10] S. Stieberger and T.R. Taylor, “Multi-gluon scattering in open superstring theory,” *Phys. Rev. D* **74**, 126007 (2006) [arXiv:hep-th/0609175].
- [11] S. Stieberger and T.R. Taylor, “Complete Six-Gluon Disk Amplitude in Superstring Theory,” *Nucl. Phys. B* **801**, 128 (2008) [arXiv:0711.4354 [hep-th]].
- [12] I.R. Klebanov and E. Witten, “Proton decay in intersecting D-brane models,” *Nucl. Phys. B* **664**, 3 (2003) [arXiv:hep-th/0304079].
- [13] M. Cvetič and I. Papadimitriou, “Conformal field theory couplings for intersecting D-branes on orientifolds,” *Phys. Rev. D* **68**, 046001 (2003) [Erratum-ibid. *D* **70**, 029903 (2004)] [arXiv:hep-th/0303083].
- [14] S.A. Abel, M. Masip and J. Santiago, “Flavour changing neutral currents in intersecting brane models,” *JHEP* **0304**, 057 (2003) [arXiv:hep-ph/0303087];  
S.A. Abel, O. Lebedev and J. Santiago, “Flavour in intersecting brane models and bounds on the string scale,” *Nucl. Phys. B* **696**, 141 (2004) [arXiv:hep-ph/0312157].
- [15] S.A. Abel and A.W. Owen, “Interactions in intersecting brane models,” *Nucl. Phys. B* **663**, 197 (2003) [arXiv:hep-th/0303124].
- [16] S.A. Abel and A.W. Owen, “N-point amplitudes in intersecting brane models,” *Nucl. Phys. B* **682**, 183 (2004) [arXiv:hep-th/0310257].

- [17] D. Lüst, P. Mayr, R. Richter and S. Stieberger, “Scattering of gauge, matter, and moduli fields from intersecting branes,” Nucl. Phys. B **696**, 205 (2004) [arXiv:hep-th/0404134].
- [18] D. Cremades, L.E. Ibanez and F. Marchesano, “Yukawa couplings in intersecting D-brane models,” JHEP **0307**, 038 (2003) [arXiv:hep-th/0302105]; “Computing Yukawa couplings from magnetized extra dimensions,” JHEP **0405**, 079 (2004) [arXiv:hep-th/0404229].
- [19] M. Cvetič and R. Richter, “Proton decay via dimension-six operators in intersecting D6-brane models,” Nucl. Phys. B **762**, 112 (2007) [arXiv:hep-th/0606001].
- [20] M. Chemtob, “Nucleon decay in gauge unified models with intersecting D6-branes,” Phys. Rev. D **76**, 025002 (2007) [arXiv:hep-ph/0702065].
- [21] L.A. Anchordoqui, H. Goldberg, S. Nawata and T.R. Taylor, “Jet signals for low mass strings at the LHC,” Phys. Rev. Lett. **100**, 171603 (2008) [arXiv:0712.0386 [hep-ph]].
- [22] L.A. Anchordoqui, H. Goldberg, S. Nawata and T.R. Taylor, “Direct photons as probes of low mass strings at the LHC,” arXiv:0804.2013 [hep-ph].
- [23] V. Balasubramanian, P. Berglund, J.P. Conlon and F. Quevedo, “Systematics of moduli stabilisation in Calabi-Yau flux compactifications,” JHEP **0503**, 007 (2005) [arXiv:hep-th/0502058].
- [24] L. Anchordoqui, H. Goldberg, D. Lüst, S. Nawata, S. Stieberger, T.R. Taylor, “Dijet signals for low mass strings at the LHC,” MPP–2008–86, LMU–ASC 42/08, to appear.
- [25] I. Antoniadis, “The physics of extra dimensions,” Lect. Notes Phys. **720**, 293 (2007) [arXiv:hep-ph/0512182].
- [26] J. Polchinski, “String Theory”, Sections 6 & 12, Cambridge University Press 1998.
- [27] J.P. Conlon, F. Quevedo and K. Suruliz, “Large-volume flux compactifications: Moduli spectrum and D3/D7 soft supersymmetry breaking,” JHEP **0508**, 007 (2005) [arXiv:hep-th/0505076].
- [28] J.P. Conlon, C.H. Kom, K. Suruliz, B.C. Allanach and F. Quevedo, “Sparticle Spectra and LHC Signatures for Large Volume String Compactifications,” JHEP **0708**, 061 (2007) [arXiv:0704.3403 [hep-ph]].
- [29] S. Dimopoulos and G.L. Landsberg, “Black holes at the LHC,” Phys. Rev. Lett. **87**, 161602 (2001) [arXiv:hep-ph/0106295].
- [30] S.B. Giddings and S.D. Thomas, “High energy colliders as black hole factories: The end of short distance physics,” Phys. Rev. D **65**, 056010 (2002) [arXiv:hep-ph/0106219].
- [31] C. Beasley, J.J. Heckman and C. Vafa, “GUTs and Exceptional Branes in F-theory - I,” arXiv:0802.3391 [hep-th]; “GUTs and Exceptional Branes in F-theory - II: Experimental Predictions,” arXiv:0806.0102 [hep-th].
- [32] P. Anastasopoulos, T.P.T. Dijkstra, E. Kiritsis and A.N. Schellekens, “Orientifolds, hypercharge embeddings and the standard model,” Nucl. Phys. B **759**, 83 (2006) [arXiv:hep-th/0605226].

- [33] D. Berenstein, V. Jejjala and R.G. Leigh, “The standard model on a D-brane,” *Phys. Rev. Lett.* **88**, 071602 (2002) [arXiv:hep-ph/0105042].
- [34] H. Verlinde and M. Wijnholt, “Building the standard model on a D3-brane,” *JHEP* **0701**, 106 (2007) [arXiv:hep-th/0508089].
- [35] D. Malyshev and H. Verlinde, “D-branes at Singularities and String Phenomenology,” *Nucl. Phys. Proc. Suppl.* **171**, 139 (2007) [arXiv:0711.2451 [hep-th]].
- [36] R. Blumenhagen, B. Körs, D. Lüst and S. Stieberger, “Four-dimensional String Compactifications with D-Branes, Orientifolds and Fluxes,” *Phys. Rept.* **445**, 1 (2007) [arXiv:hep-th/0610327].
- [37] M. Berg, M. Haack and E. Pajer, “Jumping Through Loops: On Soft Terms from Large Volume Compactifications,” *JHEP* **0709**, 031 (2007) [arXiv:0704.0737 [hep-th]].
- [38] R. Blumenhagen, S. Moster and E. Plauschinn, “Moduli Stabilisation versus Chirality for MSSM like Type IIB Orientifolds,” *JHEP* **0801**, 058 (2008) [arXiv:0711.3389 [hep-th]].
- [39] D. Cremades, L.E. Ibanez and F. Marchesano, “Standard model at intersecting D5-branes: Lowering the string scale,” *Nucl. Phys. B* **643**, 93 (2002) [arXiv:hep-th/0205074].
- [40] R. Blumenhagen, M. Cvetič, F. Marchesano and G. Shiu, “Chiral D-brane models with frozen open string moduli,” *JHEP* **0503**, 050 (2005) [arXiv:hep-th/0502095].
- [41] M. Cvetič, P. Langacker and G. Shiu, “Phenomenology of a three-family standard-like string model,” *Phys. Rev. D* **66**, 066004 (2002) [arXiv:hep-ph/0205252].
- [42] G. Shiu and S.H. Tye, “TeV scale superstring and extra dimensions,” *Phys. Rev. D* **58**, 106007 (1998) [arXiv:hep-th/9805157].
- [43] D. Cremades, L.E. Ibanez and F. Marchesano, “SUSY quivers, intersecting branes and the modest hierarchy problem,” *JHEP* **0207**, 009 (2002) [arXiv:hep-th/0201205].
- [44] D. Lüst, S. Reffert and S. Stieberger, “Flux-induced soft supersymmetry breaking in chiral type IIB orientifolds with D3/D7-branes,” *Nucl. Phys. B* **706**, 3 (2005) [arXiv:hep-th/0406092].
- [45] S. Stieberger and T.R. Taylor, “Supersymmetry Relations and MHV Amplitudes in Superstring Theory,” *Nucl. Phys. B* **793**, 83 (2008) [arXiv:0708.0574 [hep-th]].
- [46] T. Banks, L.J. Dixon, D. Friedan and E.J. Martinec, “Phenomenology and Conformal Field Theory Or Can String Theory Predict the Weak Mixing Angle?,” *Nucl. Phys. B* **299**, 613 (1988)
- [47] T. Banks and L.J. Dixon, “Constraints on String Vacua with Space-Time Supersymmetry,” *Nucl. Phys. B* **307**, 93 (1988).
- [48] S. Ferrara, D. Lüst and S. Theisen, “World Sheet Versus Spectrum Symmetries In Heterotic And Type II Superstrings,” *Nucl. Phys. B* **325**, 501 (1989).



- [49] M.B. Green and J.H. Schwarz, “Supersymmetrical Dual String Theory. 2. Vertices And Trees,” Nucl. Phys. B **198**, 252 (1982);  
J.H. Schwarz, “Superstring Theory,” Phys. Rept. **89**, 223 (1982).
- [50] T. van Ritbergen, A.N. Schellekens and J.A.M. Vermaseren, “Group theory factors for Feynman diagrams,” Int. J. Mod. Phys. A **14**, 41 (1999) [arXiv:hep-ph/9802376].
- [51] E. Gava, K.S. Narain and M.H. Sarmadi, “On the bound states of p- and (p+2)-branes,” Nucl. Phys. B **504**, 214 (1997) [arXiv:hep-th/9704006].
- [52] I. Antoniadis, K. Benakli and A. Laugier, “Contact interactions in D-brane models,” JHEP **0105**, 044 (2001) [arXiv:hep-th/0011281].
- [53] T.T. Burwick, R.K. Kaiser and H.F. Müller, ”General Yukawa Couplings Of Strings On  $\mathbf{Z}_N$  Orbifolds,” Nucl. Phys. B **355**, 689 (1991).
- [54] S. Stieberger, D. Jungnickel, J. Lauer and M. Spalinski, ”Yukawa couplings for bosonic  $\mathbf{Z}_N$  orbifolds: Their moduli and twisted sector dependence,” Mod. Phys. Lett. A **7**, 3059 (1992) [arXiv:hep-th/9204037];  
J. Erler, D. Jungnickel, M. Spalinski and S. Stieberger, ”Higher twisted sector couplings of  $\mathbf{Z}_N$  orbifolds,” Nucl. Phys. B **397**, 379 (1993) [arXiv:hep-th/9207049].
- [55] D. Berenstein, “Possible exotic stringy signatures at the LHC,” arXiv:0803.2545 [hep-th].
- [56] V.D. Barger and R.J.N. Phillips, *Collider Physics*, Westview Press (1996).
- [57] L.A. Anchordoqui, H. Goldberg and T.R. Taylor, “Decay widths of lowest massive Regge excitations of open strings,” arXiv:0806.3420 [hep-ph].
- [58] D. Binosi and L. Theussl, “JaxoDraw: A graphical user interface for drawing Feynman diagrams,” Comput. Phys. Commun. **161**, 76 (2004) [arXiv:hep-ph/0309015].